



UNIVERSITAT DE
BARCELONA

Evaluation of immunebiomarkers in Lung Cancer

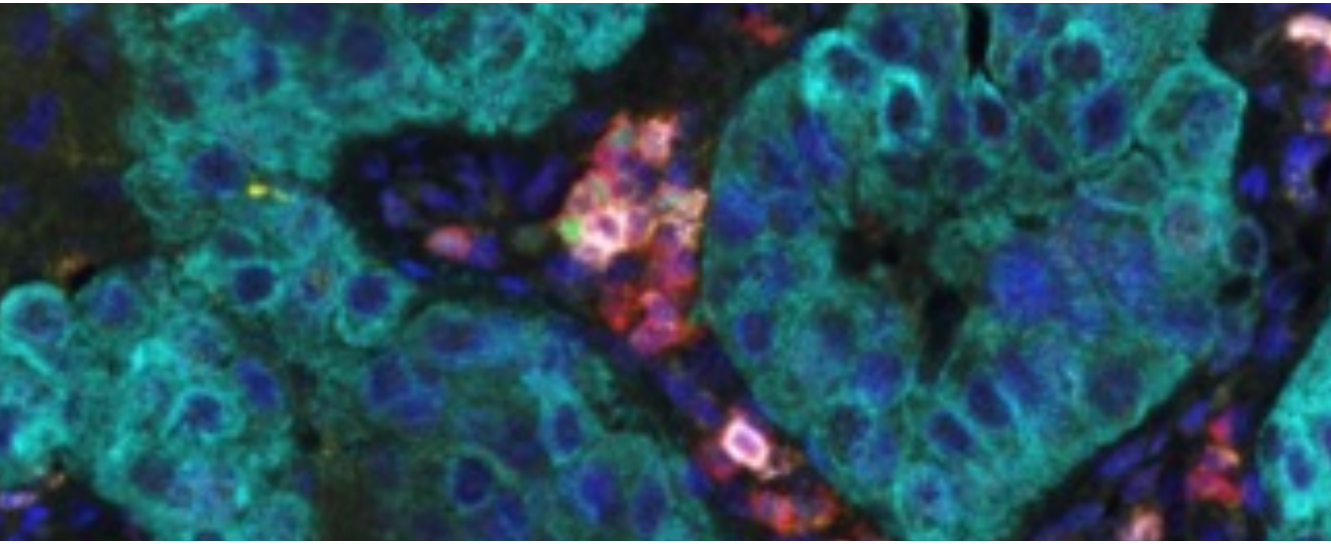
Pedro Filipe Simões da Rocha

ADVERTIMENT. La consulta d'aquesta tesi queda condicionada a l'acceptació de les següents condicions d'ús: La difusió d'aquesta tesi per mitjà del servei TDX (www.tdx.cat) i a través del Dipòsit Digital de la UB (diposit.ub.edu) ha estat autoritzada pels titulars dels drets de propietat intel·lectual únicament per a usos privats emmarcats en activitats d'investigació i docència. No s'autoritza la seva reproducció amb finalitats de lucre ni la seva difusió i posada a disposició des d'un lloc aliè al servei TDX ni al Dipòsit Digital de la UB. No s'autoritza la presentació del seu contingut en una finestra o marc aliè a TDX o al Dipòsit Digital de la UB (framing). Aquesta reserva de drets afecta tant al resum de presentació de la tesi com als seus continguts. En la utilització o cita de parts de la tesi és obligat indicar el nom de la persona autora.

ADVERTENCIA. La consulta de esta tesis queda condicionada a la aceptación de las siguientes condiciones de uso: La difusión de esta tesis por medio del servicio TDR (www.tdx.cat) y a través del Repositorio Digital de la UB (diposit.ub.edu) ha sido autorizada por los titulares de los derechos de propiedad intelectual únicamente para usos privados enmarcados en actividades de investigación y docencia. No se autoriza su reproducción con finalidades de lucro ni su difusión y puesta a disposición desde un sitio ajeno al servicio TDR o al Repositorio Digital de la UB. No se autoriza la presentación de su contenido en una ventana o marco ajeno a TDR o al Repositorio Digital de la UB (framing). Esta reserva de derechos afecta tanto al resumen de presentación de la tesis como a sus contenidos. En la utilización o cita de partes de la tesis es obligado indicar el nombre de la persona autora.

WARNING. On having consulted this thesis you're accepting the following use conditions: Spreading this thesis by the TDX (www.tdx.cat) service and by the UB Digital Repository (diposit.ub.edu) has been authorized by the titular of the intellectual property rights only for private uses placed in investigation and teaching activities. Reproduction with lucrative aims is not authorized nor its spreading and availability from a site foreign to the TDX service or to the UB Digital Repository. Introducing its content in a window or frame foreign to the TDX service or to the UB Digital Repository is not authorized (framing). Those rights affect to the presentation summary of the thesis as well as to its contents. In the using or citation of parts of the thesis it's obliged to indicate the name of the author.

TESIS DOCTORAL



Evaluation of Immunebiomarkers in Lung Cancer

Pedro Filipe Simões da Rocha

Doctoral Programme in Biomedicine University of Barcelona. Biology School
Barcelona, 2022



UNIVERSITAT DE
BARCELONA



Evaluation of Immunebiomarkers in Lung Cancer



Author

Pedro Filipe Simões da Rocha



Thesis Supervisor

Dr. Edurne Arriola Aperribay



Thesis Tutor

Dr. Montserrat Jaumot Pijoan

IMIM: Institut Hospital del Mar d'Investigacions Mèdiques
Carrer del Dr. Aiguader, 88, 08003, Barcelona, Spain



UNIVERSITAT DE
BARCELONA



Dr. Edurne Arriola Aperribay, Doctor in Medicine, Head of Thoracic and GU tumors and Principal Investigator at Institut Hospital del Mar d'Investigacions Mèdiques.

CERTIFY:

That, **Pedro Filipe Simões da Rocha**, doctoral student at University of Barcelona. Biology School, has performed under her supervision the work corresponding to his thesis entitled:

Evaluation of Immunebiomarkers in Lung Cancer

After careful review, it is considered that the current work meets all the conditions - quality, content, and form - required and its presentation is authorized to be evaluated by the corresponding evaluation committee.

For the appropriate purposes, this certificate is signed in Barcelona on September 4th, 2022.

Signature

Edurne Arriola

Approval and Funding sources

The work presented here entitled '*Evaluation of Immunebiomarkers in Lung Cancer*' was developed at IMIM - Institut Hospital del Mar d'Investigacions Mèdiques, Barcelona, Spain, and at The University of Texas, MDAnderson Cancer Center, Houston, Texas, USA. This work was partially supported by an unrestricted grant by Roche.

The Doctoral Student, Pedro Filipe Simões da Rocha, was partially supported by SEOM (Sociedad Española de Oncología Médica) and ESMO (European Society of Medical Oncology).

Patient's sample collection, analysis and results communication included in this work were approved by the relevant institutional review boards and were conducted according to the principles of the Helsinki Declaration.

Acknowledgments

Uma semana antes de escrever a parte mais importante da minha tese, e enquanto jantava, entre quatro adultos jogávamos a um jogo de crianças. Era um jogo que tínhamos de responder a perguntas como *‘O que preferias comer: uma minhoca com sabor a chocolate o um chocolate com sabor a minhoca?’* (só para que tenham uma ideia do nível de jogo que estamos a falar). No meio destas perguntas uma delas realmente chamou-me á atenção – *‘Se tivesses que escrever um livro, em que idioma o escreverias?’* – *‘Português disse eu’*, e acrescentei *‘A final é o idioma em que melhor posso expressar os meus sentimentos e verdadeiramente transmitir o que o que me vai na alma’*. Assim que, como chegou o momento de poder escrever o que me vai *‘na alma’*, vou fazê-lo em bom português.

Primeiro, está claro que tenho de agradecer á minha mentora durante os últimos 7 anos, Edurne Arriola. Contigo aprendi, medicina, oncologia, cancro de pulmão, como escrever um artigo científico (como não escrever um artigo científico também), como pedir uma bolsa e mais importante que tudo o resto, aprender que realmente o importante é disfrutar do que fazemos e sempre a pensar nos nossos doentes. Por tudo isto e por muitas mais coisas que agora não me lembro muito, muito obrigado.

Ao Dr. Albanell, pela sua visão e por acreditar na importância da investigação clínica e translacional. Por confiar em mim, e dar-me a oportunidade de voltar ao melhor serviço de Oncologia do mundo.

A todos os oncólogos do serviço de Oncologia do Hospital del Mar, que antes eram os meus referentes e que agora são os meus referentes e companheiros.

A todos os meus colegas 'Resistentes', dos maiores aos mais pequenos: Joana, Ana, David, Miriam, Maria, Anna, Tamara, Noélia, Alex y Laura muito muito obrigado. E claro que não me esqueço da Mayrita, mas não seria justo que estivesse no meio dos 'Resistentes', porque além de ser a mais 'Resistente' sempre me motivou para fazer '*as minhas coisas*' porque sabia que eu era feliz com '*as minhas coisas da imunoterapia*'. Mayrita, sabes que tens e terás sempre um lugar muito especial no meu coração (e aqui na tese também).

Ao Dr. Wistuba, á Luisa Solis, e ao Humam Kadara. Que durante a minha estadia no MDAnderson, longe no meu país natal (e também do meu país emprestado) fizeram que me sentisse em casa, por todas as oportunidades que me deram e a confiança que depositaram num oncologista que no era patologista e que estava num laboratório de patologia molecular. Muito obrigado pelo apoio incondicional que sempre me deram (e continuam a dar). A todos os meus colegas de laboratório em Houston: Debbie, Hitoshi, Alex, Mario, Frank, Cibelle, Sharia, Auriole, Rossana, Daniela, Lorena, Harsh, Sakshi, Wei, Mei, Lakshmi, Auriole, Ansam, Warapen, Hiro, Jiexin e muitos mais, com vocês aprendi tudo o que sei de laboratório e de patologia, muito obrigado pela paciência que sempre tiveram para ensinar-me e para responder a todas as perguntas (muitas delas sem muito sentido provavelmente).

À minha família em Portugal, que apesar de só quererem que volte para Portugal sempre me apoiam de forma incondicional. Pai e Mãe nunca vos poderei agradecer todas as oportunidades que vocês me deram, o esforço que fizeram para que estudasse o que eu queria e que nunca eu tivesse de perguntar se podia, porque para vocês eu era o mais importante. Espero que durante este caminho os tenha deixado orgulhosos em algum momento. Agora que já vou entregar a tese já tenho uma desculpa menos para não voltar a Portugal, assim que só um bocadinho mais de paciência que está quase. Mano e agora o melhor de voltar a Portugal, Leonor e Beatriz obrigado por sempre ver um ponto positivo em todo o meu caminho, por ser tão bom voltar a casa para vos ver, por ter tantas saudades de casa e por me lembrar cada vez que Portugal é o melhor país do mundo para viver.

Laurita, obrigado por toda a compreensão, paciência, apoio em presença e á distancia, por todas as horas de conversa científica e sobretudo não científica que tão importante foram para que isto fosse possível.

Muito muito obrigado a todas as pessoas que durante estes anos se cruzaram no meu caminho. Infelizmente, tudo o que aprendi com vocês, apesar de ser o mais importante, seria impossível de pôr em tão poucas páginas.

Muito muito obrigado.

Pedro Rocha

Abstract

Treatment landscape in early-stage NSCLC is rapidly changing after approval of anti-PD-1/PD-L1 in the neoadjuvant and adjuvant settings, respectively. However, biomarkers for patient selection, to predict response and to inform immunotherapeutic resistance are not available. Here we interrogate the expression patterns of CD73 in malignant cells and examined host anti-tumor immune response in order to describe and elucidate potential tumor mechanisms that promote immune evasion. We also assess immune biomarkers in early stage NSCLC surgical specimens. Finally, we evaluate immune features that promote response after chemotherapy or chemoimmunotherapy treatment, with the aim to uncover immune predictive and prognostic biomarkers in early-stage lung cancer.

Our results pointed to the potential role of CD73, and other members of the adenosine signaling pathway, as potential mechanisms of tumor immune evasion and resistance to ICI, thus providing additional rationale for propagating anti-CD73 antibodies in new combinatorial immunotherapeutic regimens. We found that CD73 expression was significantly and progressively increased across normal-appearing lung tissue, adenomatous atypical hyperplasia, adenocarcinoma in situ, minimally invasive adenocarcinoma, and lung adenocarcinoma (LUAD). We observed that differential CD73 localization was associated with distinct clinicopathological and molecular features in LUAD. CD73 expression was positively associated with an increase in PD-L1 expression in tumor cells and increase of tumor-associated

immune cells. Additionally, and using targeted gene sequencing analysis and immunohistochemistry, we characterized immune programs across patients that underwent upfront surgery, neoadjuvant chemotherapy, or neoadjuvant chemoimmunotherapy. We identified immune gene programs that are unique to PD-L1 positive and PD-L1 negative NSCLCs as well as those that are shared between both groups. Using IHC, we observed that PD-L1 positive ($\geq 1\%$) LUADs exhibited an augmented infiltration of T cells (CD3⁺, CD4⁺, CD8⁺ cells) along with increase of FOXP3⁺ cells, resident memory cells (CD103⁺) and macrophages (CD68⁺). Spatial distribution of CD8⁺ T cells unveiled distinctive TIME phenotypes whose frequencies differed based on TNM stage, PD-L1 expression, and mutational burden. Inflamed and PD-L1⁺/TILs⁺ NSCLCs displayed significantly amplified levels of immune signatures, with the excluded group representing an intermediate immune state. Subgroup analysis based on the expression of tumor PD-L1, and resident memory immune cells (CD103⁺ cells) showed an enrichment of immune cell infiltrates (CD3⁺, CD4⁺, CD8⁺, CD68⁺ cells) in tumors harboring higher levels of CD103⁺ immune cells along with an increase of CD80⁺ cells, essential for T cell activation. Longitudinal analysis of patients following neoadjuvant chemoimmunotherapy showed strong upregulation of immune cells signatures within the TIME. In this cohort, pathologic response to chemoimmunotherapy was positively associated with higher expression of genes involved in immune activation, chemotaxis, as well as T and natural killer cells. Comparative analysis between the three cohorts, underscored immune programs and signatures that overall were progressively modulated along the spectrum of treatment-naïve, neoadjuvant chemotherapy-treated, up to those treated with chemoimmunotherapy, pointing to an association between perturbation of an expanded repertoire of immune gene sets with neoadjuvant chemoimmunotherapy.

In conclusion, our findings suggest that higher CD73 expression is associated with an overall augmented host immune response, suggesting potential implications in the immune pathobiology of early-stage lung adenocarcinoma. Additionally, our results highlight immune gene programs and IHC markers that may underlie host tumor immunity and response to neoadjuvant chemotherapy and chemoimmunotherapy in resectable NSCLC.

Resumen

El escenario del tratamiento del cáncer de pulmón en estadios localizados está cambiando rápidamente después de la aprobación de anti-PD-1/PD-L1 como tratamiento neoadyuvante o adyuvante, respectivamente. Sin embargo, no disponemos de biomarcadores para la selección de pacientes que ayuden a predecir la respuesta y para informar la resistencia a la inmunoterapia. En este trabajo, evaluamos los patrones de expresión de CD73 en las células malignas, así como la respuesta inmunitaria antitumoral del huésped con el objetivo de describir y dilucidar algunos de los mecanismos tumorales que promueven la evasión inmunitaria, así como las características inmunitarias que desencadenan la respuesta después del tratamiento con quimioterapia o quimioinmunoterapia, con el objetivo de revelar biomarcadores inmunes en el cáncer de pulmón en etapa temprana.

Nuestros resultados señalan el papel de CD73 y otros miembros de la vía de señalización de la adenosina como mecanismos potenciales de evasión inmune por parte de los tumores y de resistencia a la inmunoterapia, proporcionando una justificación adicional para el desarrollo de anticuerpos anti-CD73 en combinación con inmunoterapia. Además, encontramos que la expresión de CD73 aumenta significativa y progresivamente a lo largo de tejido pulmonar de apariencia normal, hiperplasia atípica adenomatosa, adenocarcinoma *in situ*, adenocarcinoma mínimamente invasivo y, finalmente, adenocarcinoma de pulmón. Observamos también que la localización diferencial de CD73 se asocia con distintas características clinicopatológicas y moleculares en adenocarcinomas de pulmón. La expresión de CD73 se asocia positivamente con un aumento en la expresión de PD-L1 en células tumorales y un aumento de células inmunitarias intratumorales.

Además, mediante el uso de análisis de secuenciación de genes específicos y por inmunohistoquímica (IHC), caracterizamos los perfiles inmunes en pacientes que se sometieron a cirugía, quimioterapia neoadyuvante o quimioinmunoterapia neoadyuvante. Identificamos perfiles de genes inmunitarios que son exclusivos de tumores PD-L1 positivos y PD-L1 negativos, así como los que comparten ambos grupos. Usando IHC, observamos que los adenocarcinomas de pulmón positivos para PD-L1 ($\geq 1\%$) exhiben una infiltración aumentada de células T (células CD3⁺, CD4⁺, CD8⁺) junto con un aumento de células FOXP3⁺, células de memoria residentes (CD103⁺) y macrófagos (CD68⁺). La distribución espacial de las células T CD8⁺ revela distintos fenotipos de microambientes tumorales cuyas frecuencias difieren según el estadio TNM, la expresión de PD-L1 y la carga mutacional. Los tumores inflamados y PD-L1⁺/TILs⁺ muestran niveles significativamente aumentados de marcadores inmunes, mientras que el fenotipo excluido representa un estado inmunitario intermedio. El análisis de subgrupos basado en la expresión tumoral de PD-L1 y la presencia de células inmunitarias de memoria residentes (células CD103⁺) muestra un enriquecimiento de infiltrados de células inmunitarias (células CD3⁺, CD4⁺, CD8⁺, CD68⁺) en tumores que albergan niveles elevados de células inmunitarias CD103⁺ junto con un aumento de células CD80⁺, esenciales para la activación de los linfocitos T. El análisis longitudinal de los pacientes después de quimioinmunoterapia neoadyuvante muestra un aumento de los marcadores inmunes intratumorales. En esta cohorte, la respuesta patológica a la quimioinmunoterapia se asocia positivamente con una mayor expresión de genes implicados en la activación inmune, la quimiotaxis, así como genes característicos de células T y células natural killer. El análisis comparativo entre las tres cohortes subraya los perfiles inmunes que, en general, se modulan progresivamente a lo largo del espectro de los pacientes tratados con cirugía de entrada, quimioterapia neoadyuvante, hasta los tratados con quimioinmunoterapia, lo que señala el papel de la quimioinmunoterapia neoadyuvante como desencadenante de una respuesta inmunitaria antitumoral.

En conclusión, nuestros hallazgos sugieren que una mayor expresión de CD73 se asocia con una respuesta inmune aumentada, con potenciales implicaciones en la patobiología inmune de los adenocarcinomas de pulmón en estadio iniciales. Además, nuestros resultados destacan perfiles de genes inmunitarios y marcadores por IHC que caracterizan la inmunidad anti-tumoral del huésped y de respuesta a tratamientos con quimioterapia o quimioinmunoterapia neoadyuvantes en el cáncer de pulmón resecable.

Outline

1. INTRODUCTION	22
1.1. Lung Cancer	22
1.1.1 Incidence and Epidemiology	22
1.1.2 Treatment landscape in early-stage NSCLC	23
1.1.3 Biomarkers in early-stage NSCLC	28
1.2. Immune system and Cancer	33
1.2.1 Tumor microenvironment	34
1.2.2 Antitumor host immunity	34
1.2.3 Adenosine pathway	36
2. AIMS	40
3. THESIS SUPERVISOR REPORT	42
4. ARTICLES	44
4.1. CD73 expression defines immune, molecular, and clinicopathological subgroups of lung adenocarcinoma	44
Pedro Rocha, Ruth Salazar, Jiexin Zhang, Debora Ledesma, Jose L. Solorzano, Barbara Mino, Pamela Villalobos, Hitoshi Dejima, Dzifa Y. Douse, Lixia Diao, Kyle Gregory Mitchell, Xiuning Le, Jianjun Zhang, Annikka Weissferdt, Edwin Parra-Cuentas, Tina Cascone, David C. Rice, Boris Sepesi, Neda Kalhor, Cesar Moran, Ara Vaporciyan, John Heymach, Don L. Gibbons, J. Jack Lee, Humam Kadara, Ignacio Wistuba, Carmen Behrens, Luisa M. Solis. Cancer Immunology, Immunotherapy, 2021.	

4.2. Distinct immune gene programs associated with host tumor immunity, neoadjuvant chemotherapy and chemoimmunotherapy in resectable NSCLC	57
<p>Pedro Rocha, Jiexin Zhang, Raquel Laza-Briviesca, Alberto Cruz-Bermúdez, Katsuhiko Yoshimura, Carmen Behrens, Apar Pataer, Edwin R Parra, Cara Haymaker, Junya Fujimoto, Stephen G Swisher, John V Heymach, Don L Gibbons, J. Jack Lee, Boris Sepesi, Tina Cascone, Luisa M Solis, Mariano Provencio, Ignacio I Wistuba, Humam Kadara. <i>Clinical Cancer Research</i>, 2022.</p>	
4.3. Pre-existing tumor host immunity characterization in resected Non-Small Cell Lung Cancer	71
<p>Pedro Rocha, Maite Rodrigo, Laura Moliner, Silvia Menendez, Nil Navarro, Laura Masfarré, Raúl Del Rey-Vergara, Miguel Galindo, Álvaro Taus, Mario Giner, Ignacio Sanchez, Lara Pijuan, Alberto Rodríguez, Rafael Aguiló, Roberto Chalela, Albert Font, Josep Belda, Víctor Curull, David Casadevall, Sergi Clavé, Beatriz Bellosillo, Júlia Perera, Laura Comerma, Edurne Arriola. <i>In preparation</i>.</p>	
5. GLOBAL DISCUSSION	90
6. CONCLUSIONS	101
7. REFERENCES	102
8. SUPPLEMENTARY MATERIAL	114
8.1 Supplementary material – Article 1	114
8.2 Supplementary material – Article 2	124
8.3 Supplementary material – Article 3	141

Abbreviations

AAH	Atypical adenomatous hyperplasia
AIS	Adenocarcinoma <i>in situ</i>
BL	Basolateral
cPR	Complete pathological response
ctDNA	Circulating tumor DNA
CTLA-4	Cytotoxic T lymphocyte-associated 4
CT scan	Computed tomography scan
CTLs	Cytotoxic T lymphocytes
DFS	Disease-free survival
ICI	Immune checkpoint inhibitors
IHC	Immunohistochemistry
mIF	Multiplex immunofluorescence
L	Luminal
LUAD	Lung adenocarcinoma
LUSC	Lung squamous carcinoma
MIA	Minimally invasive adenocarcinoma
MPR	Major pathological response
NK	Natural killer
NSCLC	Non-small cell lung cancer
OS	Overall survival
RNA	Ribonucleic acid
PD-1	Programmed Death 1
PD-L1	Programmed Death Ligand-1
T	Total
TAICs	Tumor-associated immune cells
TCGA	The Cancer Genome Atlas

TH	Total high group
TILs	Tumor infiltrate lymphocytes
TL	Total low group
TN	Total negative group
TIME	Tumor immune microenvironment
TMB	Tumor mutation burden
TME	Tumor microenvironment
TNM	Tumor, Nodes, Metastases

Chapter 1

1. INTRODUCTION

1.1. Lung Cancer

1.1.1. Incidence and Epidemiology

Despite remarkable improvements on diagnostic tools and treatment, lung cancer remains the first cause of cancer-related deaths worldwide¹. Particularly in Spain, the last numbers published by SEOM (Sociedad Española de Oncología Médica), show that lung cancer represents more than 20% of all cancer-related deaths². Globally, more than 2 million/year cases of lung cancer are diagnosed³. In Spain, approximately 30.000 lung cancer cases are diagnosed each year, accounting for more than 22.000 deaths every year³.

Of note, while in the last few years a clear reduction in the incidence of lung cancer in males has been observed, the same is not true in females, with an increased number of new diagnoses since 2015 in Spain and worldwide - Figure 1. These findings can be explained by the late introduction (approximately two decades compared with men) of smoking habit in late 70-80's, consequently we are now diagnosing patients born between 1950 and 1960^{1,3}.

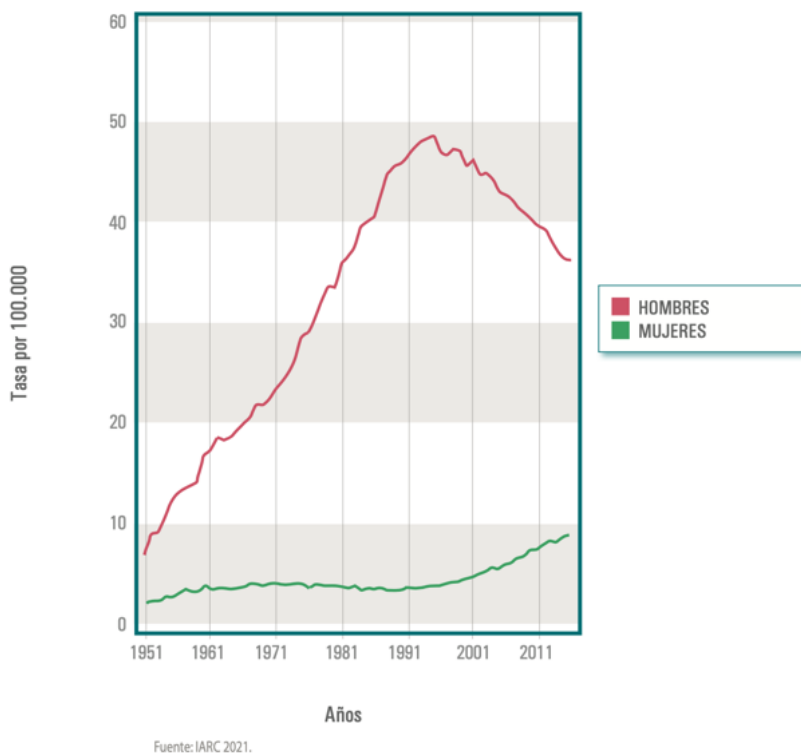


Figure 1. Lung cancer incidence across gender. Adapted from SEOM report (Las cifras del cancer en España – 2021).

With the aim to promote early diagnosis, lung cancer screening using low-dose CT scan has shown a significant reduction in lung cancer mortality in high-risk patients (more than 55 years and at least 30 pack-years)^{4,5}. These results led to recommendation of screening implementation from most scientific associations⁶. Therefore, an increase in the number of early-stage lung cancer is expected for the upcoming years^{1,3}, generating an urgent need to optimize and improve treatment strategies in this setting.

1.1.2. Treatment landscape in early-stage NSCLC.

Chemotherapy.

Early-stage lung cancers are potentially curable tumors, nevertheless, a significant proportion of patients will relapse and succumb to this disease⁷.

With the aim to improve clinical outcomes in this setting, several clinical trials exploring the addition of adjuvant chemotherapy to surgery revealed an overall benefit of this approach with an improvement of 5% in disease-free survival (DFS) and overall survival (OS)⁸, with a greater benefit of chemotherapy observed in patients with higher stage. Of note, granular analysis of the benefit of adjuvant chemotherapy exposed that this benefit is restricted to tumors larger than 4 cm and those with lymph node involvement – using the current 8th edition TNM staging, this corresponds to the tumors stage IIA or higher^{7,9}. Another strategy is to deliver systemic treatment before surgery – known as neoadjuvant therapy. This strategy is accepted in the lung cancer field as an interchangeable approach comparable with adjuvant strategies. A meta-analysis including 15 trials evaluating neoadjuvant chemotherapy compared to surgery alone found a benefit of 5% (similar benefit as adjuvant chemotherapy)¹⁰. Until the recent approval of immune checkpoint inhibitors^{11,12}, adjuvant or neoadjuvant chemotherapy remained as the standard of care for patients with resectable lung cancer for the last 15 years, highlighting the difficulty (considering number of patients need to include in these trials, as well as the long follow-up) to demonstrate a clinical significant benefit in this setting.

Targeted Therapy

In this scenario, trials had used a biomarker-matched drug approach and most of them focused on the use of targeted therapy. One example is the CTONG1104 trial comparing gefitinib (first generation TKI) for 24 months versus cisplatin-based chemotherapy in stage II-IIIa tumors. Initial results of this trial suggested promising results with an improvement on DFS but after a longer follow-up, this strategy was not able to demonstrate an overall survival benefit¹³. More recently, the use of Osimertinib (third generation TKI) up to three years after the standard-of-care adjuvant chemotherapy – ADAURA trial – has shown encouraging results with a clear reduction on DFS and a great impact on the incidence of central

nervous system recurrence, however, longer follow-up is needed with mature OS data¹⁴. Similar trials exploring the use of targeted therapies in the adjuvant setting are being explored in other oncogenic addicted lung cancers¹⁵.

Immunotherapy

In contrast to resectable NSCLC, in the advanced setting immunotherapy has consolidated as front-line therapy, alone or in combination with chemotherapy, in patients with metastatic lung cancer without driver mutations^{16–19}. The encouraging results from these trials prompted the initiation of new trials evaluating the role of immune checkpoint blockade in the perioperative setting.

In the adjuvant setting, a phase III trial (IMpower010) evaluating atezolizumab in patients with resected NSCLC (tumors ≥ 4 cm) that received cisplatin-based adjuvant chemotherapy showed a benefit on DFS for the subgroup of patients with stage II-III A (7th edition TNM), with marked benefit in tumors expressing PD-L1¹¹. The benefit of adjuvant immunotherapy was later confirmed by the PEARLS/KEYNOTE-091 trial²⁰. However, in this last trial the benefit in tumors with PD-L1 higher than 50% was not significantly different compared with the control arm. Nevertheless, it is worthy to mention that patients' characteristics differ between both trials (e.g., IMpower010 only includes patients that received adjuvant chemotherapy) and longer follow-up and overall survival results are needed to fully interpret these results.

Early in 2018, Forde et al, reported the first insights on the potential role of neoadjuvant anti-PD-1 (nivolumab) with 9 out of 20 patients (45%) showing a major pathological response (MPR – less than 10% of viable tumor cells in the surgical specimen) after only two doses of nivolumab²¹.

These results were used as the foundation for the following trials exploring the role of anti-PD-1/PD-L1 in early-stages as well as in combination with anti-CTLA4^{22,23} and chemotherapy^{12,24,25}. A phase II trial – LCMC3 trial – involving several institutions at the USA, investigated two doses of neoadjuvant atezolizumab and reported a 20% of MPR and 7% of tumors exhibiting pathological complete response (pCR – no viable tumor cells in the surgical resected specimen). Interestingly, the authors also reported a trend towards a greater pathological response in tumors with high PD-L1 and high tumor mutation burden (TMB)^{26,27}. In another phase II study (NEOSTAR), Cascone and colleagues explored nivolumab monotherapy or in combination with ipilimumab in the neoadjuvant setting for patients with resectable stage I-IIIa NSCLC. Of note, 8 out of 21 patients (38%) receiving nivolumab plus ipilimumab arm achieved a MPR, compared with 5 out of 21 patients (24%) in the nivolumab monotherapy arm²³.

More recently, three phase II trials (NCT02716038, NADIM I and NADIM II trial) have explored the combination of anti-PD-1/PD-L1 plus platinum-based chemotherapy as neoadjuvant treatment in resectable NSCLC stage IB-IIIa. Notably, MPRs were observed in 57%, 83% and 52% patients respectively, including up to 63% and 36.2% of the patients in the NADIM I and II trial achieving pCR – even though larger tumors were included (in the NADIM trial all tumors included were stage IIIa)^{24,25,28}. Initial results from the above-mentioned trials prompted the initiation of the corresponding phase III trials investigating the addition of ICI to standard platinum-based chemotherapy.

In this line, Forde et al reported the results from the first phase III trial comparing three cycles of neoadjuvant platinum-based chemotherapy plus nivolumab versus chemotherapy alone. In this trial, patients included in the experimental treatment arm presented significant longer event-free survival (EFS) (31.6 Vs 20.8 months) and higher rates of pCR with 24% and 2,2% of the cases respectively¹², leading to

the approval of this strategy by the FDA in March 2022. By the time of this work, there are several clinical trials evaluating different immune checkpoint inhibitors and adding the corresponding anti-PD-1/PD-L1 as adjuvant treatment.

Overall, adjuvant Osimertinib, adjuvant immunotherapy (anti-PD-1/PD-L1) and neoadjuvant chemo-immunotherapy are changing the treatment scenario of early-stage NSCLC, nevertheless longer follow-up, and overall survival data for all these studies are needed to definitively establish these new strategies as standard-of-care across Europe. Clinical trials investigating the role of adjuvant ICI after neoadjuvant chemoimmunotherapy are ongoing. However, questions such as the value of adjuvant ICI in patients who achieved pCR or had lower stage tumors will be difficult to answer.

It is worthy to highlight that neoadjuvant treatment offers several advantages compared with adjuvant therapy – 1) Systemic treatment is usually better tolerated before surgery; 2) Tumor downstaging that can help achieve better surgical results; 3) Opportunity to eradicate micrometastases earlier; 4) Rapid assessment of therapeutic efficacy either before surgery (using CT or PET scans) or at the time of resection; 5) in context of neoadjuvant ICI (alone or in combination with chemotherapy), administration of ICI before surgery will result in a stronger systemic anti-tumor immune response, suggested by preclinical data demonstrating a more efficient anti-tumor T cell response driven by the high antigen burden in the neoadjuvant setting²⁹⁻³¹.

Additionally, this approach provides a unique opportunity to evaluate surrogate markers of clinical efficacy that correlate with improved survival as well as the opportunity to develop translational work that could answer important questions to the scientific field. Indeed, preclinical studies suggest that ICIs would be more effective as neoadjuvant treatment. These results are mediated by an enhance of

T-cell priming, activation and expansion of antitumor T cells that result in higher anti-tumor activity, limited recurrence, and improved survival outcomes observed with neoadjuvant compared with adjuvant immunotherapy in murine models³².

1.1.3. Biomarkers in early-stage NSCLC.

The most relevant prognostic marker in early-stage NSCLC is the TNM stage, and specifically the pathological TNM⁷ – Figure 2. In this line, previous works evaluating neoadjuvant treatment have suggested that tumor downstaging and pathological response can be used as a surrogate endpoint of overall survival^{33–36}, similar to other tumor types such as breast cancer where pathological response is widely accepted as a valid survival outcome³⁷.

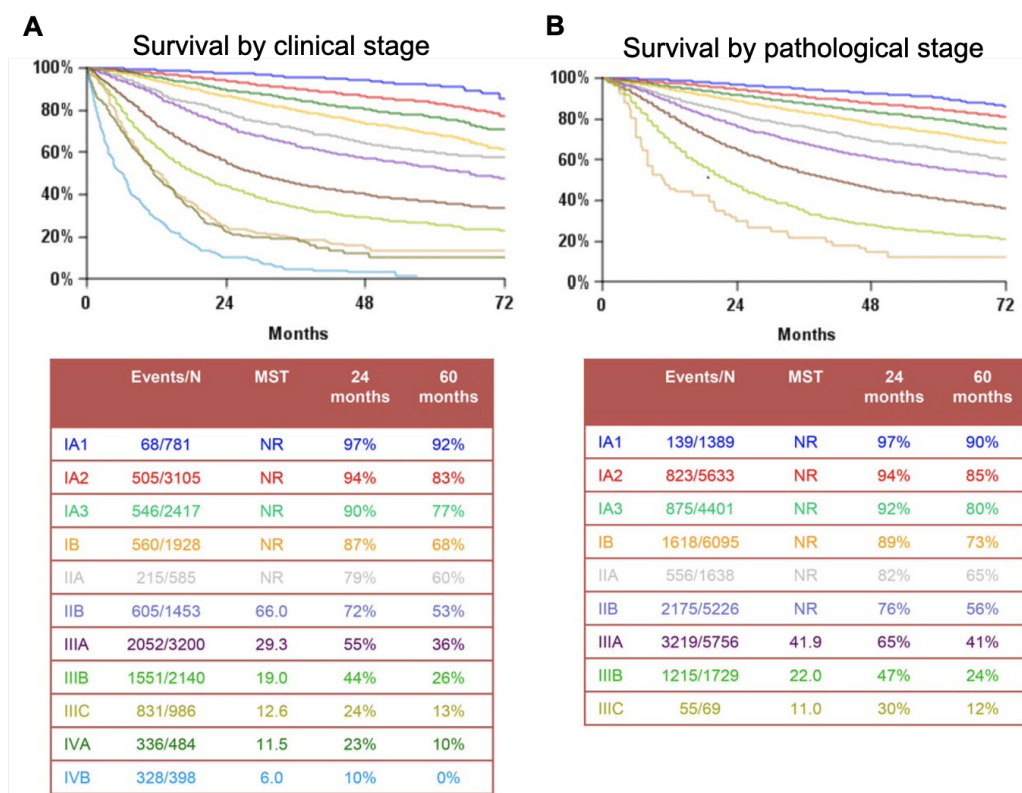


Figure 2. Survival by A) clinical and B) pathological stages. MST=median survival time in months. Adapted from Porta et al, CA Cancer 2017.

Pathological response

Pathological response evaluation consists of the histopathological examination of the extension of viable tumor cells in the tumor bed of a surgically resected primary tumor and lymph nodes that underwent neoadjuvant treatment. In lung cancer, and after neoadjuvant treatment, two concepts are important to retain: 1) Major complete response (MPR) and 2) Pathological complete response (pCR). The first one (MPR) is defined by less than or equal 10% of viable tumor cells in the resected tumor, and the second one is defined by the absence (0%) of viable tumor cells in the surgical specimen³⁸.

In 2012, Pataer and colleagues reported histopathologic response to neoadjuvant therapy as prognostic biomarker for survival in patients with resected lung cancer after receiving neoadjuvant chemotherapy. In this work, the authors compared two cohorts of patients with NSCLC, the first one comprising patients treated with neoadjuvant chemotherapy (n=192) and the second one including patients that underwent surgery alone. They observed a significantly higher rate of MPR in patients treated with neoadjuvant chemotherapy – 36 patients (19%). In addition, the percentage of viable tumor cells was a significant predictor of survival only in patients with NSCLC who received neoadjuvant chemotherapy (even when controlled for pathologic stage)³⁶.

Another provocative study suggested that the optimal cutoff for MPR after neoadjuvant chemotherapy in resected NSCLC could differ among histological subtypes. Specifically, the authors found that the optimal cutoff for lung squamous cell carcinoma was 10% and 65% viable tumor cells for lung adenocarcinomas. Both percentages were found to be independent factors on a multivariate analysis³⁹. Prospective studies report that around 22% of patients with stage I-IIIa NSCLC achieve a MPR after neoadjuvant chemotherapy^{34,40}.

A new approach to increase MPR rates is to add ICI to the platinum-based neoadjuvant chemotherapy. This approach was used in the CheckMate 816 trial, leading to an increase of MPR rate, from 8.9% (in the chemotherapy alone arm) versus 36.9% in the neoadjuvant nivolumab plus chemotherapy arm¹². Exploratory analysis showed that EFS for patients achieving pCR at 2 years was 93% compared with 58% of patients without pCR⁴¹. The abovementioned results led to nivolumab approval in combination with platinum-based chemotherapy as a new neoadjuvant treatment strategy in resectable NSCLC by the FDA.

Overall, pathological response (both MPR and cPR) as surrogates for survival in lung cancer have the potential to improve the cost-benefit of clinical trials in this setting and accelerate biomarker-driven questions that ultimately will bring new and better treatments to our patients.

Membrane PD-L1 expression

Immunohistochemical PD-L1 expression can be found on tumor and immune cells and is one of the few biomarkers used in advanced NSCLC (without driver mutations) to inform treatment decisions. After extensive debates on how to choose the correct antibody clone and pathologically evaluate tissue specimens, a harmonization study concluded that, with exception of SP142 clone, all the other antibodies tested provided similar results. Also important, pathologists showed excellent concordance when scoring malignant cells, nevertheless, this study also highlighted the difficulty to evaluate and get reproducible results when evaluating PD-L1 in immune cells⁴². Although imperfect, it is considered a predictive biomarker of response to anti-PD-1/PD-L1 in metastatic NSCLC, since patients with higher PD-L1 expression had higher chances to respond to anti-PD-L1 and better clinical outcomes^{43,44}.

In the neoadjuvant setting, the results of PD-L1 expression and their association with treatment response and/or clinical outcomes were not consistent across trials. The first trial evaluating immunotherapy alone, Forde and colleagues did not observe an association between pretreatment PD-L1 expression and MPR in a cohort of 21 NSCLC patients treated with neoadjuvant nivolumab⁴⁵. In the same line, in the NEOSTAR trial evaluating nivolumab or nivolumab plus ipilimumab, MPR achievement was independent of PD-L1 expression. In contrast, LCMC trial evaluating atezolizumab and a small trial conducted at Johns Hopkins University (JHU) and Memorial Sloan Kettering Cancer Center (MSKCC) evaluating nivolumab plus ipilimumab showed a correlation between levels of PD-L1 and MPR^{22,46}.

The NADIM I and NADIM II trials (neoadjuvant ICI-chemotherapy) the authors reported an association between tumor PD-L1 expression and MPR/cPR. These results are in line with a subgroup analysis from a more recent phase 3 trial – CheckMate 816 – where the magnitude of benefit was incremented in patients with a tumor PD-L1 expression $\geq 1\%$, compared with those with less than 1%¹². Conversely, a study reported by Shu et al evaluating the combination of atezolizumab plus platinum-based chemotherapy observed pathological responses regardless of PD-L1 expression – with tumors with less than 1% for PD-L1 displaying a reduction of 34% in tumor size – , while their counterparts (PD-L1 positive tumors) showed a median reduction of 40% in tumor size²⁵.

It is plausible to hypothesize that the variability in the results among several small-scale studies could be induced by different factors such as tumor histology, TNM stage, PD-L1 heterogeneous expression, tumor genomic features, tissue availability, neoadjuvant treatment scheme, and different methodologies to evaluate pathological response⁴⁷. Hopefully, translational work from ongoing phase 3 neoadjuvant clinical trials will bring light into the dark.

Tumor associated immune cells

Tumor-associated immune cells (TAIC) comprise different immune cell types within the tumor microenvironment, including tumor-infiltrating lymphocytes (TILs – T cells, B cells), macrophages, natural killer (NK) and dendritic cells, as well as their subpopulations and different functional states. TILs in quantity and composition can serve as a predictive biomarker of the response to therapy and prognosis^{48,49}.

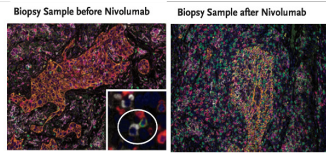
Early reports evaluating the immune contexture after ICI showed an influx of CD8⁺ T cells and higher PD-L1 expression of immune cells on the resected specimens⁴⁵. This increase of CD8⁺ T cells was consistently observed in following trials, as well as after treatment with anti-PD-1 plus anti-CTLA4^{22,23}. Forde and colleagues also observed an increased interaction of PD-L1⁺ macrophages and PD-1⁺CD8⁺ T cells, suggesting an increase of antigen presenting ongoing after treatment with ICI⁵⁰. Detailed analysis of specific immune cell subtypes using multiplex immunofluorescence showed an increase in post-treatment specimens of: T cells (CD3⁺); Cytotoxic T cells (CD3⁺ CD8⁺); Memory T cells (CD3⁺ CD45RO⁺); Antigen experienced T cells (CD3⁺PD-1⁺); Activated T cells (CD3⁺ Granzyme B⁺) and PD-L1⁺ Macrophages (CDD68⁺ PD-L1⁺)^{22–24,50}.

Of interest, a common pathological finding was observed across all studies; the appearance of lymphoid follicles in the post-treatment samples resembling tertiary lymphoid structures^{23,24,50}. In other tumors, such as melanoma, bladder cancer and sarcomas, neoadjuvant treatment with anti-PD-1 was associated with an increase of B cell density, TLSs and a notable increase of the ratio TLS/tumor area in the post-treatment sample^{51–55}. It has been described that those tumors exhibiting mature TLS within the tumor microenvironment also present a high density of B cells and plasma cells, as well as antibodies to tumor-associated antigens. Features that are frequently associated with favorable clinical outcomes as well as higher rates of response to immunotherapy⁵⁵ – Figure 3.

Forde et al., 2018, NEJM

- MPR: 9/20 (45%)
- cPR: 3/20 (15%)

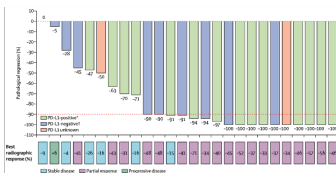
- MPR independently from PD-L1 expression.
- Interactions of PD-L1⁺ Macrophages with PD-1⁺CD8⁺T cells.
- Influx of CD8⁺T cells and higher PD-L1 on immune cells.



Shu et al., 2020, Lancet Oncology

- MPR: 17/30 (57%)
- cPR: 10/30 (33%)

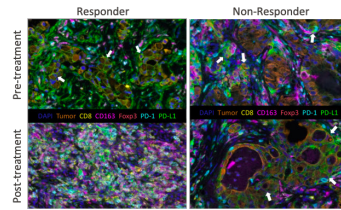
- Responses regardless of PD-L1 expression.
 - PD-L1<1%: -34%(Δin tumor size).
 - PD-L1≥1%: -40%(Δin tumor size).
- No mIF data available.



Reuss et al., 2020, JTC

- MPR: 2/9 (33%)
- cPR: 2/9 (33%)

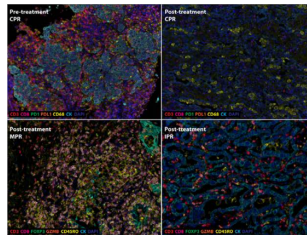
- Pathologic response associated with PD-L1 expression.
- Dense CD8⁺T cells infiltrates (Resp).
- Intact tumor cells plus Macrophage-predominant infiltrates (Non- resp).



Provencio et al., 2020, Lancet Oncology

- MPR: 34/41 (83%)
- cPR: 26/41 (63%)

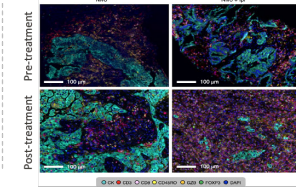
- Higher PD-L1 expression (TPS) in cPR.
- Decrease from pre- to post-treatment:
 - T cells (CD3⁺).
 - Cytotoxic T cells (CD3⁺CD8⁺).



Cascone et al., 2021, Nature Medicine

- Nivo arm – MPR: 5/23 (22%)
- Nivo-Ipi arm – MPR: 8/21 (38%)
- cPR: 2/23 (9%) Vs 6/21 (19%)

- MPR independently of PD-L1.
- Increase from pre- to post-therapy:
 - T cells (CD3⁺ and CD3⁺CD8⁺).
 - Memory T cells (CD45RO⁺).
 - Antigen-experienced T cells (PD-1⁺).
 - Activated T cells (GZB⁺).
 - Macrophages PD-L1 (CD68⁺PD-L1⁺).



Carbone et al., 2021, World Conference Lung Cancer

- MPR: 30/144 (21%)
- cPR: 10/144 (7%)

- PD-L1 ≥ 50% correlates with MPR.
- BS enrichment of Macrophages (CD68⁺) and 'Antigen experienced' T cells (CD3⁺PD-1⁺) in MPR patients.
- Increase in post-tx samples of T cells PD-1⁺ (CD3⁺PD-1⁺).

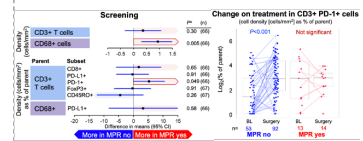


Figure 3. Summary of the most relevant translational results derived from initial clinical trials exploring immune checkpoint blockade in the neoadjuvant non-small cell lung cancer.

1.2. Immune system and cancer.

The ‘malignant’ intrinsic characteristic of cancers results from the abnormal regulation of cell proliferation, resistance of tumor cells to apoptotic death, and the ability of the tumor cells to invade and metastasize to other tissues⁵⁶. Another important hallmark in cancer development is the ability acquired by tumors to evade the host anti-tumor immune response⁵⁷. In this line, the concept of immune surveillance in cancer refers to a normal function of the immune system that

recognizes and eliminates transformed cells before they start to grow into tumors. Yet, immune response frequently fails to prevent tumor growth, through different mechanisms such as, increase of checkpoint blockade signaling, reduction of immunogenicity (selection of less immunogenic clones) and the rapid tumor cell replication that overcomes the capacity of the immune system to effectively control the tumor⁵⁸.

1.2.1 Tumor microenvironment

The tumor microenvironment is constituted by normal cells (immune cells, stromal cells such as fibroblasts, endothelial cells), molecules and blood vessels that surround and feed a tumor cell⁴⁸. The interactions between tumor cells and immune cells can activate or inhibit an anti-tumor immune response. In order to grow and invade tissues, tumors must evade and resist host anti-tumor immune response. Several mechanisms have been described that support this hypothesis and unveil potential therapeutic approaches. Tumor cells may evade host immune response by losing expression of antigens or major histocompatibility complex (MHC) molecules, by producing ligands for T cell inhibitory receptors (e.g., PD-1 and CTLA-4), immunosuppressive cytokines, and promoting the migration of immunosuppressive cells (Myeloid derived suppressor cells)²⁹.

1.2.2 Antitumor host immunity

Immune responses against tumor cells usually target several types of molecules that cancer cells express and may be recognized by the host immune system. Protein antigens that stimulate T cell responses are dominant proteins that trigger a protective antitumor immunity. Galon et al demonstrated that T cells within a resected tumor predict the likelihood of metastatic disease, and led to the development of an immune score that can assess prognosis and potentially inform therapeutic decisions⁵⁹. This has been developed initially in colon cancer, in which a score was given to tumors based on the number of CD45RO⁺ memory

T cells and CD8⁺ CTLs (cytotoxic T lymphocytes) present at the invasive margin of resected tumors. A low score was found to predict a higher chance for relapse, metastasis, and death within 5 years compared with tumors with high score, suggesting a protective role for intratumor immune cells⁶⁰.

In lung cancer, previous studies have demonstrated the potential implications of tumor infiltrating lymphocytes (TILs) and other markers such as PD-1 and PD-L1 on survival outcomes^{49,61–64}. Particularly, in stage I NSCLC, an increase in CD3⁺ and CD8⁺ T cells was correlated with better OS and RFS, while no association of FOXP3⁺ cells with survival was observed^{65,66}. Additional work interrogating for specific features related to a host anti-tumor immune response identify CD103 expression in T lymphocytes as a possible marker⁴⁹. In this work, the authors found that tumors highly infiltrated by TILs exhibited an increase expression of *ITGAE* (CD103). In this same work, transcriptomic profiling of purified TILs showed that expression of tissue resident memory markers such as CD69 was co-expressed with CD103 and at the same time with *KLRG1*, *CCR7*, *CD62L* along with an increase expression of granzyme B suggesting the potential immune effector activity of these cells. Lastly, in this study, patients with higher infiltration by CD103 TILs had significantly better overall survival⁴⁹.

Earlier work has shown that the extent and spatial pattern (intratumoral or peritumoral) of lymphocyte infiltration impact on host immunity and response to ICIs⁶⁷. In this sense, tumor immune microenvironment (TIME) patterns were described in order to summarize the complexity of TIME: tumors can be categorized on the tumor immunity continuum as having inflamed, desert, or excluded immune phenotypes based on the spatial localization of immune cells with respect to the tumor and stromal compartments⁶⁸. Inflamed tumors are associated with close proximity of immune cells with tumor cells, immune-excluded tumors associated with immune cells embedded in the surrounding

tumor stroma away from tumor cells, and immune desert phenotype is associated with tumors lacking tumor-infiltrating lymphocytes (TILs)^{69,70} Figure 4.

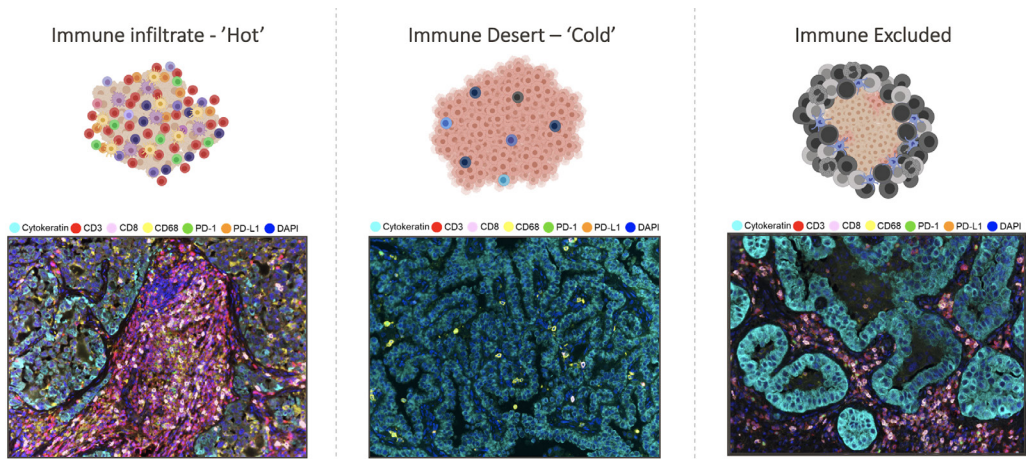


Figure 4. Tumor immune microenvironment patterns. Representative multiplex immunofluorescence images of immunologically inflamed, cold, and excluded TIME phenotype are shown.

1.2.3 The adenosine pathway

The canonical adenosine-generating pathway involves the hydrolysis of ATP by ectonucleotidases such as CD39 (also known as ectonucleoside triphosphate diphospho-hydrolase 1) and CD73 (also known as 5'-nucleotidase)¹⁹. CD39 is a transmembrane enzyme that hydrolyses eATP to produce extracellular ADP and AMP. Subsequently, extracellular AMP (eAMP) can be converted to eADO by CD73. In the second, or non-canonical, pathway leading to adenosine production, NAD⁺ is utilized as the substrate to generate eAMP via the activity of CD38 (an NAD⁺ ectohydrolase also known as ADP-ribosyl cyclase/cyclic ADP-ribose hydrolase 1) and CD203a (also known as ectonucleotide pyrophosphatase/phosphodiesterase family member 1 (ENPP1) or PC-1). The eAMP produced can then be hydrolyzed to adenosine by CD73⁷¹. It is worth emphasizing that, although the canonical CD39-CD73 pathway has a major role in the production of adenosine, other pathways involving alternative ectoenzymes, nucleoside

transporters (ENT1/2 and CNT1/2) and intracellular adenosine metabolism can also modulate adenosine concentrations⁷².

Using gene-targeted mouse models and selective pharmacological inhibitors, several independent groups have established that CD39/CD73-derived adenosine and A2A and/or A2B signaling suppress the anti-tumor activity of CD8⁺ T cells and NK cells^{73,74} and promote the production of tolerogenic factors (such as TGFβ and IL-10) by myeloid cells⁷⁵. Adenosine suppresses tumor immunity largely by restricting immune cell infiltration and attenuating the effect of in situ activated cytotoxic lymphocytes through the reduction of cytokines such as interferon-γ^{76,77}. One of the strongest inducers of the adenosine pathway is HIF1α, a central transcriptional regulator in hypoxia that constitutes a cancer hallmark; and hence, as expected, various tumors types present overexpression of key proteins in the adenosine pathway such as CD73 and CD39⁷⁸.

In human tumor samples, CD73 tumor expression correlates with a poor prognosis across different cancer types. In this line, two meta-analyses comprising more than 15.000 patients and 15 cancer types showed that CD73 expression was significantly associated with reduced OS and DFS as well as lymph node metastases, and, thus, rising as a prognostic factor in different types of cancers^{79,80}. Particularly, previous studies evaluating CD73 expression in early-stage NSCLC have shown that a higher expression of CD73 (by IHC) was independently associated with poor prognosis and worse OS and DFS. The same authors observed that TTF-1 positive lung adenocarcinomas harboring *EGFR* mutations displayed the highest expression of CD73 by IHC⁸¹.

The immunosuppressive adenosine pathway, in which CD73 plays a critical role, has been proposed as one of the possible mechanisms of primary and acquired resistance to ICI^{71,82}. A previous study defined a gene expression signature to infer

levels of the adenosine signaling in tumors and then was applied to The Cancer Genome Atlas (TCGA) and different cohorts of patients treated with ICI. Initial analysis from the TCGA confirmed the negative association between adenosine levels and clinical outcomes (OS, DFS). Subgroup analysis only including tumors with high abundance of *CD8A* expression (potential surrogate for cell density of CD8⁺ T cells) unveil striking decreased survival in patients with tumors exhibiting both CD8 and adenosine upregulation, suggesting a strong effect of adenosine on modulating the tumor microenvironment⁸³. Additional analysis in a small cohort of patients (different cancer types and treated with anti-PD-1) showed that responders to ICI displayed a lower baseline level of adenosine, compared to non-responders⁸³.

Pursuing this line, several anti-CD73 monoclonal antibodies are currently being tested. Oleclumab inhibits the enzymatic function of CD73 and prevents the conversion of AMP to adenosine by promoting the internalization of CD73.

Initial results in unresectable stage III NSCLC with oleclumab (anti-CD73 antibody) combined with durvalumab (anti-PD-L1) after completed chemo-radiotherapy showed an increased in ORR compared with durvalumab alone, 30% and 17.9% respectively. Improvement on ORR translated into an increase in PFS, with a 12-month PFS rate of 62.5% for the oleclumab arm compared with 33.9% in the durvalumab monotherapy arm⁸⁴. These findings prompted the initiation of a phase 3 clinical trial – the PACIFIC-9 (currently enrolling patients).

In the neoadjuvant setting, the NEOCOAST trial also explored the combination of Oleclumab plus durvalumab and chemotherapy for 4 cycles. MPR was observed in 22.2% of tumors included in the oleclumab arm, with these tumors expressing higher levels of CD73 (by IHC). Of note, differential expression between responders (MPR) and non-responders (no MPR) identified upregulation

of specific genes involved in B-cell activation, and T cell costimulatory pathways in the oleclumab arm⁸⁵.

Overall, adenosine is generated in the tumor microenvironment owing mainly to the degradation of extracellular ATP^{71,86,87} and NAD⁺⁸⁸. Several ectonucleotidases tightly control levels of ATP and Adenosine, such as CD38, CD39, and CD73; among them, CD73 irreversibly converts AMP to Adenosine and was suggested as the rate-limiting enzyme for adenosine formation⁸⁹. Increased adenosine levels permit an immune-tolerant tumor microenvironment by regulating the functions of immune and inflammatory cells such as macrophages, dendritic cells, myeloid-derived suppressor cells, T cells, and natural killer (NK) cells⁹⁰. Targeting the adenosine pathway is feasible, with promising results from the initial trials in lung cancer. Translational work originated from these trials showed that modulation of this pathway can induce immune cell activation, supporting the combination with ICI⁸⁵.

Chapter 2

AIM

To identify molecular and immune biomarkers in early-stage non-small cell lung cancer, their association with host antitumor immune response, and response to neoadjuvant chemotherapy and chemoimmunotherapy.

SPECIFIC AIMS:

1. To identify histological patterns and prevalence of CD73 expression in lung adenocarcinomas.
2. To investigate CD73 expression with PD-L1 expression and immune cell infiltrates.
3. To interrogate the association of CD73 expression with genomic mutations in lung adenocarcinoma.
4. To evaluate the canonical and non-canonical adenosinergic pathway in lung adenocarcinoma.
5. To characterize the tumor microenvironment in early-stage non-small cell lung cancer (NSCLC) by histology, PD-L1 tumor membrane expression and molecular subtype.
6. To classify NSCLC based on main immunological features and their spatial distribution.

7. To identify host antitumor immune responses and their corresponding dynamic changes upon treatment with chemotherapy and chemoimmunotherapy.
8. To evaluate the association of immune biomarkers and response to therapy.

Chapter 3

42 THESIS DIRECTOR REPORT.

Two articles already published, and an additional article currently in preparation are included in this Thesis.

The first article, entitled '*CD73 expression defines immune, molecular, and clinicopathological subgroups of lung adenocarcinoma*' published at *Cancer Immunology, Immunotherapy* in 2021, and reports by the first-time different implications of CD73 membrane localization and their association with the tumor microenvironment in early-stage lung adenocarcinoma. The journal has currently an impact-factor of 6.630 (first quartile in oncology journals).

The second article, entitled '*Distinct Immune Gene Programs Associated with Host Tumor Immunity, Neoadjuvant Chemotherapy, and Chemoimmunotherapy in Resectable NSCLC*' published at *Clinical Cancer Research* in 2022. Here for the first time a direct comparison of the tumor microenvironment using the same methodology/platform (RNAseq – HTG EdgeSeq Precision Immuno-Oncology panel) was applied to three different cohorts (treatment naïve, neoadjuvant chemotherapy and neoadjuvant chemo-immunotherapy). *Clinical Cancer Research* has presently an impact-factor of 13.801 (first quartile in oncology journals).

Finally, the third article entitled '*Pre-existing tumor host immunity characterization in resected Non-Small Cell Lung Cancer*', currently in preparation to be submitted to Lung Cancer journal, describe the immune contexture between histologic types, PD-L1 expression and oncogenic driver mutations in early-stage NSCLC.

Dr. Edurne Arriola Aperribay



Chapter 4

4. ARTICLES.

44

4.1 CD73 expression defines immune, molecular, and clinicopathological subgroups of lung adenocarcinoma.

Pedro Rocha, Ruth Salazar, Jiexin Zhang, Debora Ledesma, Jose L. Solorzano, Barbara Mino, Pamela Villalobos, Hitoshi Dejima, Dzifa Y. Douse, Lixia Diao, Kyle Gregory Mitchell, Xiuning Le, Jianjun Zhang, Annikka Weissferdt, Edwin Parra-Cuentas, Tina Cascone, David C. Rice, Boris Sepesi, Neda Kalhor, Cesar Moran, Ara Vaporciyan, John Heymach, Don L. Gibbons, J. Jack Lee, Humam Kadara, Ignacio Wistuba, Carmen Behrens, Luisa M. Solis. *Cancer Immunology, Immunotherapy*, 2021.



CD73 expression defines immune, molecular, and clinicopathological subgroups of lung adenocarcinoma

Pedro Rocha^{1,2} · Ruth Salazar¹ · Jiexin Zhang³ · Debora Ledesma¹ · Jose L. Solorzano¹ · Barbara Mino¹ · Pamela Villalobos¹ · Hitoshi Dejima¹ · Dzifa Y. Douse¹ · Lixia Diao³ · Kyle Gregory Mitchell⁴ · Xiuning Le⁴ · Jianjun Zhang⁴ · Annikka Weissferdt⁶ · Edwin Parra-Cuentas¹ · Tina Cascone⁴ · David C. Rice⁵ · Boris Sepesi⁴ · Neda Kalhor⁶ · Cesar Moran⁶ · Ara Vaporciyan⁵ · John Heymach⁴ · Don L. Gibbons⁴ · J. Jack Lee³ · Humam Kadara¹ · Ignacio Wistuba^{1,4} · Carmen Behrens⁴ · Luisa Maren Solis¹

Received: 15 June 2020 / Accepted: 6 December 2020 / Published online: 8 January 2021
© The Author(s) 2021, corrected publication 2021

Abstract

Introduction CD73 is a membrane-bound enzyme crucial in adenosine generation. The adenosinergic pathway plays a critical role in immunosuppression and in anti-tumor effects of immune checkpoint inhibitors (ICI). Here, we interrogated CD73 expression in a richly annotated cohort of human lung adenocarcinoma (LUAD) and its association with clinicopathological, immune, and molecular features to better understand the role of this immune marker in LUAD pathobiology.

Materials and methods Protein expression of CD73 was evaluated by immunohistochemistry in 106 archived LUADs from patients that underwent surgical treatment without neoadjuvant therapy. Total CD73 (T+) was calculated as the average of luminal (L+) and basolateral (BL+) percentage membrane expression scores for each LUAD and was used to classify tumors into three groups based on the extent of T CD73 expression (high, low, and negative).

Results CD73 expression was significantly and progressively increased across normal-appearing lung tissue, adenomatous atypical hyperplasia, adenocarcinoma in situ, minimally invasive adenocarcinoma, and LUAD. In LUAD, BL CD73 expression was associated with an increase in PD-L1 expression in tumor cells and increase of tumor-associated immune cells. Stratification of LUADs based on T CD73 extent also revealed that tumors with high expression of this enzyme overall exhibited significantly elevated immune infiltration and PD-L1 protein expression. Immune profiling demonstrated that T-cell inflammation and adenosine signatures were significantly higher in CD73-expressing lung adenocarcinomas relative to those lacking CD73.

Conclusion Our study suggests that higher CD73 expression is associated with an overall augmented host immune response, suggesting potential implications in the immune pathobiology of early stage lung adenocarcinoma. Our findings warrant further studies to explore the role of CD73 in immunotherapeutic response of LUAD.

Keywords CD73 · Lung adenocarcinoma · Immune profiling · Adenosinergic pathway · PD-L1

Abbreviations

NSCLC Non-small cell lung cancer
LUADs Lung adenocarcinomas
T Total

BL Basolateral
L Luminal
TH Total high group
TL Total low group
TN Total negative group
TAICs Tumor-associated immune cells.
ICI Immune checkpoint inhibitors
PD-1 Programmed death 1
PD-L1 Programmed death-Ligand 1
CTLA-4 Cytotoxic T lymphocyte-associated 4
NK Natural killer
TME Tumor microenvironment

Pedro Rocha and Ruth Salazar have contributed equally to this work.

✉ Luisa Maren Solis
lmsolis@mdanderson.org

Extended author information available on the last page of the article

FFPE Formalin-fixed paraffin-embedded
MCs Malignant cells

Introduction

Despite significant improvements in treatment, lung cancer remains the leading cause of cancer-related deaths worldwide [1]. Immune checkpoint inhibitors (ICI), as a single agent or in combination with chemotherapy, are increasingly becoming the standard treatment for non-small cell lung cancer (NSCLC), including advanced-stage lung adenocarcinoma (LUAD) [2–5]. Recent studies have shed light on the clinical value of immunotherapy for earlier stage lung tumors including in the neoadjuvant and adjuvant settings [6, 7]. Yet, a limited fraction of NSCLC patients respond to immune checkpoint blockade consisting of anti-PD-1/PD-L1 (Programmed death 1/Programmed death-ligand 1) and CTLA-4 (Cytotoxic T Lymphocyte-associated 4); perhaps warranting the need for other combinatorial immunotherapeutic regimens to potentiate anti-tumor effects of ICI.

Adenosine is generated in the tumor microenvironment owing mainly to the degradation of extracellular ATP [8–10] and NAD⁺ [11]. Several ectonucleotidases tightly control levels of ATP and Adenosine, such as CD38, CD39, and CD73; among them, CD73 irreversibly converts AMP to Adenosine and was suggested as the rate-limiting enzyme for adenosine formation [12]. Increased adenosine levels permit an immune-tolerant tumor microenvironment by regulating the functions of immune and inflammatory cells such as macrophages, dendritic cells, myeloid-derived suppressor cells, T cells, and natural killer (NK) cells [13]. Adenosine also regulates cancer growth and dissemination by interfering with cell proliferation, apoptosis, and angiogenesis via adenosine receptors expressed on cancer cells and endothelial cells [14–16].

Tumor microenvironment (TME) immunosuppression has emerged as a sentinel mechanism in lung cancer progression and, thus, a viable phenotypic target for treatment [17, 18]. In this context, numerous therapeutic approaches are currently under development with the goal of skewing the TME toward an immune effective phenotype [19]. More recently, in preclinical studies, agents that target the adenosine pathway, including anti-CD73 antibodies and adenosine A2A receptor antagonists, were shown to also attenuate immunosuppression [20, 21].

While CD73 expression in LUAD was noted previously [22], the association of this immune enzyme mediator of the adenosine pathway with other relevant clinical biomarkers such as PD-L1, immune infiltrates, and tumor mutation burden remains unknown. We surmised that understanding the contextual expression patterns of CD73 in LUAD can help us better understand the role of the adenosine pathway in

NSCLC and in the immune pathobiology of this malignancy. Here, we sought to characterize the immunohistochemical expression of CD73 in a richly annotated cohort of early stage LUADs in association with various clinicopathological, molecular, immune features, and other markers involved in adenosine generation. We demonstrate that the extent of CD73 expression in malignant cells (MCs) defines groups of LUADs with distinct immune profiles and that thus may guide future personalized immunotherapeutic strategies.

Materials and methods

Patient samples

We first interrogated CD73 RNA expression in a set of 83 FFPE specimens from 50 patients representing different lesions in the sequence of LUAD pathogenesis including normal-appearing lung tissue ($n=38$), adenomatous atypical hyperplasia (AAH; $n=9$), adenocarcinoma in situ (AIS; $n=11$), minimally invasive adenocarcinoma (MIA; $n=21$), as well as invasive adenocarcinoma ($n=4$), and that were profiled using the nCounter, PanCancer Immune Profiling Panel (NanoString Technologies) (Supplementary Fig. 1) in the manner described previously [23]. To determine associations of CD73 and LUAD clinicopathological, molecular, and immune features, we studied a cohort of LUADs ($n=106$) from patients with early stage (stages I–III) disease that underwent surgical treatment without neoadjuvant therapy between Feb 1999 and 2012 at The University of Texas MD Anderson Cancer Center (MD Anderson; Houston, TX, USA). This study was approved by the MD Anderson Institutional Review Board and was conducted according to the principles of the Helsinki Declaration. Formalin-fixed paraffin-embedded (FFPE) LUADs tissue was placed in a tissue microarray (TMA); the tumor samples were selected based on the availability of FFPE tissue blocks; three 1 mm-diameter cores that included tissue from the center, intermediate, and peripheral areas of the tumor were used for the TMA, as previously described [24]. Detailed clinicopathological information, including demographics, smoking history, pathologic tumor-node-metastasis stage (staging system from the 8th American Joint Committee on Cancer) [25], histological patterns, and overall and recurrence-free survival were available for all cases and are summarized in Table 1. Briefly, the median age in this cohort was 65 years (range 41–84), with ever smokers representing 86% of patients included, and with a median follow-up of 86 months. Histological growth patterns were categorized as any-solid and non-solid based on the presence of any observed solid growth pattern found [26]. Mutational status of key driver genes, including KRAS, EGFR, STK11, TP53, and mutation burden derived from whole-exome sequencing [27] or Sanger sequencing data,

Table 1 Clinicopathological and molecular characteristics of LUAD patients studied ($N = 106$)

Characteristic	N (%)
Age	
Median (range)	65 (41–84)
Sex	
Female	52 (49%)
Male	54 (51%)
Smoking history	
Never	15 (14%)
Current/former	91 (86%)
TNM 8th edition	
I	58 (55%)
II	26 (25%)
III	22 (20%)
Pathological T (8th)	
pT1a—pT2a	70 (66%)
pT2b—T4	36 (34%)
Pathological N (8th)	
N0	78 (74%)
N1	20 (19%)
N2	8 (7%)
Histologic pattern	
Any-solid	46 (43%)
Non-solid	60 (57%)
Molecular characteristics	
<i>EGFR</i> mutated	15 (15%)
<i>EGFR</i> wild type	85 (85%)
<i>KRAS</i> mutated	26 (25%)
<i>KRAS</i> wild type	77 (75%)
<i>TP53</i> mutated	27 (43%)
<i>TP53</i> wild type	36 (57%)
<i>STK11</i> mutated	7 (11%)
<i>STK11</i> wild type	56 (89%)
Mutation burden (number of mutations)	
Median (range)	145 (2–993)
Overall survival (median)	108.9 months
Death	59
Alive	47
Recurrence-free survival (median)	117.2 months
Recurrence	49
No recurrence	57

were available in a subset of the cases (Table 1). Also, in a subset of this cohort ($n = 65$), next-generation sequencing RNA-based data using HTG EdgeSeq Precision Immuno-Oncology panel were employed to examine associations between CD73, CD38, and CD39 expression in LUAD and immune gene expression signatures [28–34] (SupplementaryTable 1), CD73 gene expression and its protein product by IHC.

Immunohistochemistry staining

We performed immune histochemistry (IHC) to detect the protein expression of CD73 (D7F9A), and CD39 (EPR20461). Antibody optimization of CD73 and CD39 was performed using tonsil tissue as control and multiple tumor specimens (including non-small cell lung carcinoma among others) to reach an optimal signal to noise ratio that can permit specific evaluation of cellular and subcellular expression patterns. Validation of the IHC assay included evaluation of FFPE lung cancer cell line pellets available with known mRNA expression of *CD73* and *CD39* (Supplementary Fig. 2). PD-L1 (E1L3N) and CD38 (SPC32) antibody immunohistochemistry validation, staining, and pathology evaluation were previously reported by our team [35]. The immunohistochemistry protocol is briefly described: tissue sections (4 μ m) were stained in a Leica Bond Max automated stainer (Leica Biosystems Nussloch GmbH). The tissue sections were deparaffinized and rehydrated following the Leica Bond protocol. Antigen retrieval was performed for 20 min with Bond Solution #2 (Leica Biosystems, equivalent EDTA, pH 9.0) or Bond Solution #1 (Leica Biosystems, equivalent Citrate Buffer, pH6). Primary antibodies were incubated for 15 min at room temperature and detected using the Bond Polymer Refine Detection kit (Leica Biosystems) with DAB as chromogen. The slides were counterstained with hematoxylin, dehydrated, and cover-slipped. Antibody clones and their vendor information as well as dilution and antigen retrieval conditions are summarized in SupplementaryTable 2.

Immunohistochemistry scoring

Immunohistochemistry expression levels of CD73, was evaluated in malignant cells (MCs) by two pathologists (RS and LS), using standard microscopy. The percentage of MCs with any membrane CD73 expression was estimated. Basolateral (BL) (cell membrane not adjacent to luminal spaces) and luminal (L) membrane (cell membrane facing luminal spaces) expression levels of CD73 were separately scored when evaluable (Fig. 1). To determine total CD73 (T) expression in MCs, the average of BL and L scores was computed. Tumors were categorized as CD73 positive (T+, BL+ or L+,) based on the presence of any membrane expression in > 1% of MCs. LUADs were stratified into three groups based on the extent of CD73 expression: ‘T Negative tumors’ (TN), $\leq 1\%$, $n = 27$; ‘T Low group’ (TL), $< 55\% > 1\%$, $n = 53$, and ‘T High group’ (TH), \geq to 55%, $n = 26$. Lower quartile of CD73 percentage in malignant cells was used as cutoff for T Negative group, while the upper quartile was used as cutoff for T High group (Supplementary Fig. 3a).

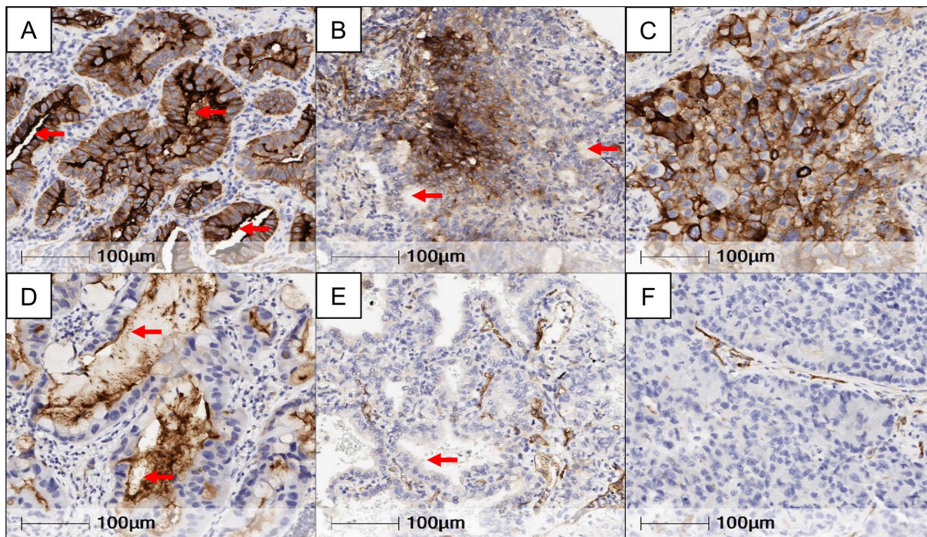


Fig. 1 Immunohistochemical expression and localization of CD73 in resectable lung adenocarcinoma. Representative microphotographs showing different patterns of CD73 expression in the luminal and/or basolateral membrane of LUAD. **a** Luminal and basolateral membrane expression. **b** Basolateral membrane expression and with no immunoreactivity in the luminal compartment. **c** Basolateral mem-

brane expression, with the absence of a lumen for evaluation. **d** Luminal membrane expression and with no immunoreactivity in the basolateral compartment. **e** Absence of expression in both the luminal and basolateral membranes. **f** No expression in the basolateral membrane and absence of a lumen. Red arrows indicate luminal membranes

Membrane or cytoplasmic CD39 expression in malignant cells was evaluated by two pathologists (DL and LS); since expression in malignant cells was not observed in any sample (0/95), expression levels of CD39 were evaluated in tumor stromal cells using digital image analysis supervised by a pathologist (DL). Briefly, the IHC-stained TMA slides were scanned using Aperio AT2 scanner (Leica Biosystem) at 20x. The digital images were visualized and analyzed with the HALO (IndicaLabs) software. A pathologist selected tumor stroma areas in each TMA core and applied algorithms to detect positive cells with cytoplasm or membrane expression of these markers; the results were expressed as cell densities (n/mm²) of the whole tumor stroma area analyzed; necrosis and artifacts were not included in the analysis.

Membrane PD-L1 was evaluated by two pathologists (DL and LS) as percentage of MCs with positive expression based on the International Association for the Study of Lung Cancer (IASLC) guidelines [36]. CD38 IHC expression annotated data included the evaluation in MCs and in tumor stromal cells, and were previously published by our team [35].

Digital image analysis of tumor-associated immune cells

Immunohistochemistry and digital image analysis previously performed for a subset of LUADs ($n=94$), included the analysis of cell densities of tumor-associated immune cells (TAICs): CD3+ (T cells), CD4+ (helper T cell), CD8+ (cytotoxic T cell), CD57+ (NK cells), granzyme B+ (NK/cytotoxic T cells), CD45RO+ (memory T cell), PD-1+, FOXP3+ (regulatory T cell), and CD68+ (tumor-associated macrophages). The IHC methodology and image data analysis were performed as previously reported by our group [37, 38].

Statistical analysis

CD73 mRNA expression across normal, preneoplastic, and malignant issues in the sequence of LUAD development was statistically determined using ANOVA and Benjamini–Hochberg correction. Targeted immune gene expression data were first median-normalized and then log₂-transformed for further analysis. Scores of previously curated

immune gene signatures were calculated by computing average expression of genes within each signature. To determine the association of categorical CD73 expression (T+, BL+, and L+, and T high, T Low, and T negative) with clinicopathological characteristics, we used Fisher's exact test, as appropriate for categorical data. To test association between continuous and categorical variables, Wilcoxon signed-rank test and Kruskal–Wallis were applied for categorical variables with two levels or more than two levels, respectively. To correlate the association between continuous CD73 expression, immune markers, and immune signatures, we used Spearman's rank correlation, and scatterplots. For survival analysis, we used Cox proportional-hazard model with CD73 expression as continuous and categorical variables separately. Heat maps of CD73 expression and tumor-associated immune cells and PD-L1 expression were generated after normalizing values for better visualization of data.

Results

Membrane expression patterns of CD73 and their association with clinicopathological features and immune biomarkers

We first interrogated expression patterns of CD73 in the pathogenesis of LUAD. We evaluated the expression of *CD73* mRNA in a series of premalignant lesions, along with malignant tumors, representing the sequence of pathogenesis of LUAD (83 specimens from 50 patients). We found that *CD73* expression was significantly and progressively increased across normal-appearing lung tissue, AAH, AIS, MIA, and adenocarcinoma ($p < 0.0001$; Supplementary Fig. 1). These findings prompted us to comprehensively examine CD73 protein expression patterns in a larger cohort of early stage LUAD.

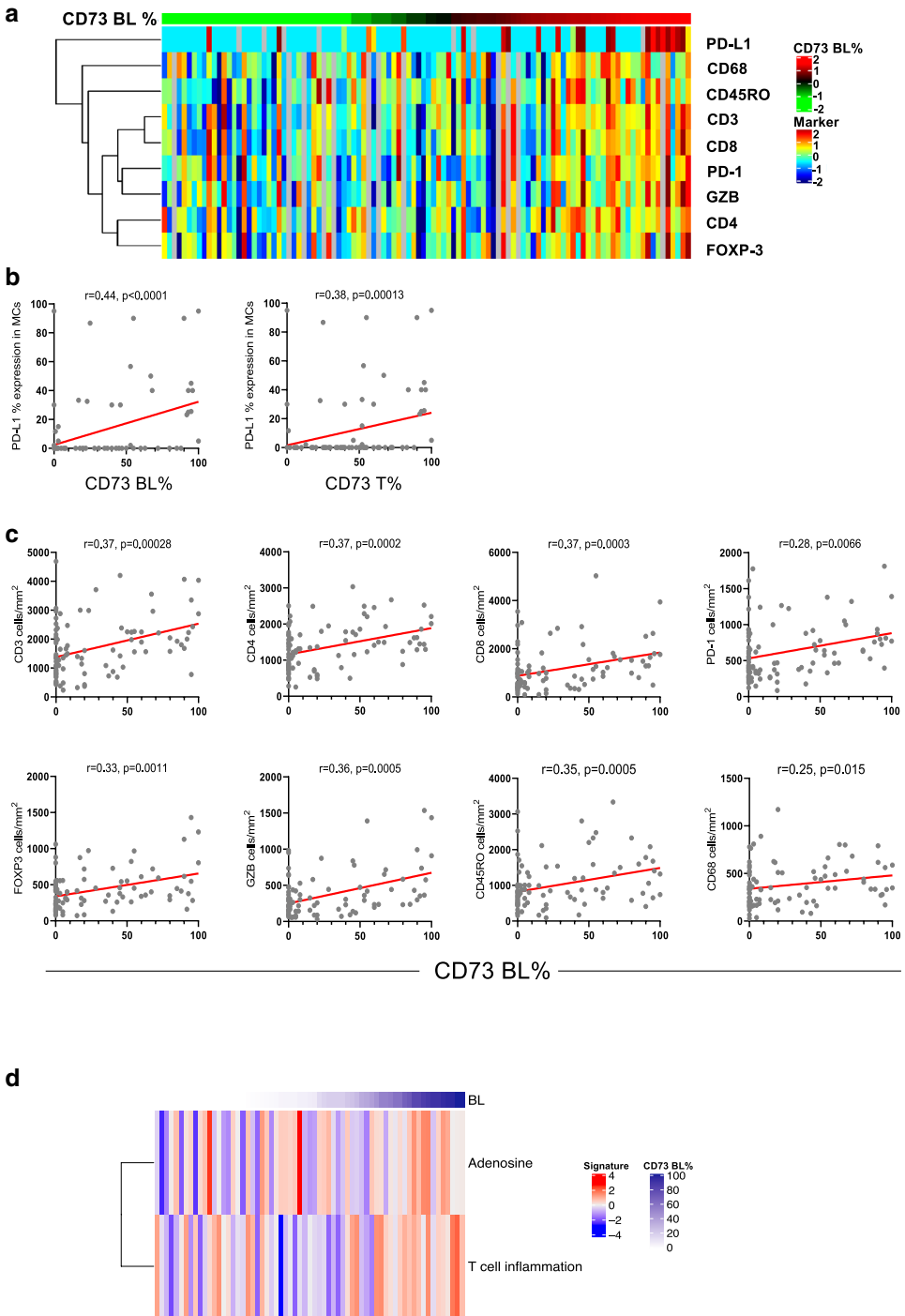
In our cohort of resectable early stage LUAD, immunohistochemistry evaluation revealed a positive total (T+) CD73 expression (> 1%) in 75% (79/106) of LUADs. Positive basolateral (BL+) expression was found in 60% (68/106); positive luminal (L+) was present in 83% (60/72) of LUADs that had luminal structures in the TMA cores. Positive correlation was found between BL and L CD73 expression ($r = 0.49$, $p = 0.0042$). Detailed information on L and BL co-expression is presented in Supplementary Table 3. Associations of CD73 expression with clinicopathological characteristics are shown in Supplementary Table 4. In our cohort, never smokers showed higher rates of T+CD73 expression (15/15, 100%) compared to ever smoker patients (64/91, 70%) ($p = 0.0107$). Tumors with any-solid histological pattern were associated with lower frequencies of T+CD73 ($p = 0.0243$). LUADs from female patients had higher frequency of BL+CD73

($p = 0.0268$). We did not find correlations between CD73 expression and survival outcomes (data not shown). T and BL expression levels showed positive correlation with most immune biomarkers evaluated by IHC (Fig. 2a and Supplementary Fig. 4a). Specifically, CD73 T and BL expression levels correlated with higher PD-L1 expression ($r = 0.38$, $p = 0.0013$ and $r = 0.44$, $p < 0.0001$, respectively) (Fig. 2b) and with higher densities of CD3, CD4, CD8, CD45RO, CD68, PD-1, FOXP3, and Granzyme B positive cells (all $p < 0.05$; Fig. 2c, and Supplementary Fig. 4a). L CD73 levels positively correlated with CD3 and CD4 cell densities (Supplementary Fig. 4b).

In a subset of patients ($N = 65$), we performed RNA-sequencing-based analysis of immune genes and signatures using the HTG EdgeSeq platform. Corroborating our immunohistochemical analyses, BL CD73 gene expression was positively associated with increased expression of T-cell inflammation ($p = 0.013$) and adenosine signatures ($p = 0.035$) (Fig. 2d).

CD73 expression defines subgroups of LUADs with disparate clinicopathological and immune features

We then defined groups of LUADs (designated as high, low, and negative) based on the extent of CD73 membrane expression. CD73 IHC expression across the three groups significantly and positively correlated with its RNA counterpart ($p < 0.0001$, Supplementary Fig. 3b). Based on the extent of CD73 expression, we stratified our cohort into three groups: 'T Negative tumors' (TN), $\leq 1\%$, $n = 27$; 'T Low group' (TL), $> 1\%$ and $< 55\%$, $n = 53$; and 'T High group' (TH), $\geq 55\%$, $n = 26$. L+ and BL+ expressions in these groups are shown in Supplementary Table 4. We found that these CD73-defined groups correlated with tobacco history ($p = 0.0194$); most LUADs from never smoker patients were TL (73%) and none of them were TN. TL LUADs showed more frequent non-solid histological patterns, while TH and TN showed similar proportions of tumors with any-solid histological pattern ($p = 0.0003$) (Table 2). Notably, the CD73-defined groups correlated with most of the immune markers examined (Fig. 3a). TH showed the highest PD-L1 expression in MCs ($p = 0.002$) (Fig. 3b), and significantly higher cell densities of CD3 CD4, CD8, PD-1, FOXP3, Granzyme B, CD45RO, and CD68-positive cells (Fig. 3c). In addition, 22.2% of tumors evaluated co-expressed CD73 and PD-L1. We did not find significant differences in immune marker expression between TN and TL LUADs. No differences in survival outcomes among the three groups were observed (Supplementary Fig. 5).



◀**Fig. 2** Basolateral CD73 expression is associated with higher immune infiltration in lung adenocarcinoma. **a** Heat map of TAIC densities and PD-L1 (% of expression) in MCs from 95 LUADs sorted according to BL CD73 expression (red, relatively higher BL CD73 expression; green, lower BL CD73 expression). Rows represent immune marker and columns denote samples (red, relatively higher TAIC density or PD-L1%; blue, lower TAIC density or PD-L1%). **b** Spearman correlation analysis of PD-L1 expression in MCs with BL and T CD73. **c** Spearman correlation analyses of TAICs (y-axis) with BL CD73 expression (x-axis)

Association of CD73 expression with molecular features

We then examined the association of CD73 expression with genomic features in LUAD. TH and TN groups showed significantly higher proportion of *TP53* mutant tumors ($p=0.0035$) compared to TL group. Somatic mutation burdens were significantly lower in the TL group compared to TH and TN groups ($p=0.0018$) (Table 2). We found that L negative CD73 LUADs comprised more *STK11* mutant LUADs rates compared to L+ ($p=0.0041$), although in our cohort, we only have a small number of *STK11* mutations ($n=7$). We did not find associations between *KRAS* and *EGFR* mutations with CD73 expression.

Association of CD73 with other markers involved in adenosine generation

We next interrogated other critical enzymes in the adenosine pathway, namely CD38 and CD39. CD38 expression in malignant cells was found in 20% (20/98) of LUADs and 18 (89%) of them co-expressed T CD73. Assessment of CD38 in tumor stroma showed that higher number of CD38⁺ cells positively associated with the TN group ($p=0.02$) (Supplementary Fig. 6a). In addition, our immune gene profiling analysis showed that CD38 cell densities in tumor stroma were associated with specific immune cell signatures indicative of T-cell inflammation, cytotoxic T lymphocytes, expanded host immune responses, tumor inflammation (TIS), interferon-gamma signaling, as well as peripheral T-cell infiltration and M1 macrophage polarization (Supplementary Fig. 6b). In contrast, CD39 expression was not observed in malignant cells in our cohort, and CD39⁺ cell densities in the tumor stroma did not exhibit significant association with CD73 expression (Supplementary Fig. 6c) or with immune signatures obtained by gene expression analysis.

Discussion

The immunosuppressive adenosine pathway, in which CD73 plays a critical role, has been proposed as one of the possible mechanisms of resistance to ICI [9, 35, 39].

The current combination of ICI therapies and anti-CD73 antibodies are attractive therapeutic approaches, and are under evaluation [40] with the aim to improve the outcome in patients with NSCLC that did not response to ICI (monotherapy or combination with chemotherapy). Yet, the role of CD73 in the pathobiology and immune contexture of LUAD is poorly understood. To begin to fill this void, we examined the expression patterns of CD73 in a richly annotated cohort of early stage LUADs in association with various features including clinicopathological, molecular, and immune covariates. We found that CD73 was expressed in a significant fraction (75%) of LUADs and categorized subsets of LUAD with distinct histological, molecular, and immune features.

In contrast to previous studies that mostly focused on total CD73 expression assessment, we interrogated CD73 in different membrane compartments (basolateral and luminal; BL and L, respectively) of MCs. Our pathological analyses demonstrated that tumors with different CD73 expression patterns exhibited distinct clinicopathological (e.g., histological patterns) and molecular associations, possibly pointing to causal links between CD73 expression or membrane localization and tumor differentiation [9, 41]. This hypothesis is also supported by our finding on progressively increased expression of *CD73* across premalignant lung lesions representing different stages in the sequence of LUAD pathogenesis. We also found that the localization of CD73 in cells from well-differentiated LUADs was predominantly luminal, which may as well be related to the physiological protective and mitigating properties of CD73 against inflammation (45). Of note, we found distinct associations between not only the presence or absence of CD73 but also the extent of expression of this antigen with smoking status, molecular features, and immune infiltration (Table 1). Consistent with previous reports [22], our cohort showed that all (100%) never smoker LUADs exhibited positive CD73 expression when compared to smoker tumors (70%). However, among positive CD73 tumors, never smoker patients had lower extent of CD73 expression (T Low group), along with more differentiated tumors, less mutation burden, and lower rates of p53 mutation. These results suggest that extensive expression of CD73 in tumors from smoker patients could be in part explained by the higher immune infiltration observed in these tumors. Interestingly, CD73 membrane localization was also predominantly luminal (Supplementary Table 5), while the group with higher extent of CD73 expression, the predominant localization was basolateral. It is reasonable to surmise that CD73, viz., its disparate localization, may have distinct roles in the molecular pathogenesis of smoker and non-smoker LUADs. It is also plausible to suggest that CD73 membrane localization may have important implications on the effectiveness of anti-CD73 therapy.

Table 2 Clinicopathological and molecular features of LUAD patients grouped based on extent of CD73 expression

Characteristic	N	T high (TH) (26/106, 25%) N (%)	T low (TL) (53/106, 50%) N (%)	T negative (TN) (27/106, 25%) N (%)	p values ^a
Age					
≤ 65	53	17 (32%)	21 (40%)	15 (28%)	0.2069
> 65	53	11 (21%)	30 (57%)	12 (23%)	
Sex					
Female	52	15 (29%)	26 (50%)	11 (21%)	0.6116
Male	54	13 (24%)	25 (46%)	16 (30%)	
Smoking history					
Never	15	4 (27%)	11 (73%)	0 (0%)	0.0194
Current/former	91	24 (26%)	40 (44%)	27 (30%)	
TNM 8th edition					
I	58	18 (31%)	28 (48%)	12 (20%)	0.4244
II	26	4 (15%)	12 (46%)	10 (39%)	
III	22	6 (27%)	11 (50%)	5 (23%)	
Pathological T (8th)					
pT1a—pT2a	70	19 (27%)	35 (50%)	16 (23%)	0.6934
pT2b—T4	36	9 (25%)	16 (44%)	11 (31%)	
Pathological N (8th)					
N0	78	22 (28%)	37 (47%)	19 (24%)	0.9041
N1	20	5 (25%)	10 (50%)	5 (25%)	
N2	8	1 (13%)	4 (50%)	3 (37%)	
Histologic pattern					
Any-solid	46	15 (32%)	14 (30%)	17 (37%)	0.0003
Non-solid	60	11 (18%)	39 (65%)	10 (17%)	
Molecular features					
<i>EGFR</i> mutated	15	5 (33%)	9 (60%)	1 (7%)	0.1717
<i>EGFR</i> wild type	85	22 (26%)	38 (45%)	25 (29%)	
<i>KRAS</i> mutated	26	8 (31%)	13 (50%)	5 (19%)	0.7039
<i>KRAS</i> wild type	77	20 (26%)	36 (47%)	21 (27%)	
<i>TP53</i> mutated	27	11 (41%)	7 (26%)	9 (33%)	0.0035
<i>TP53</i> wild type	36	5 (14%)	24 (67%)	7 (19%)	
<i>STK11</i> mutated	7	1 (14%)	2 (29%)	4 (57%)	0.1901
<i>STK11</i> wild type	56	15 (27%)	29 (52%)	12 (21%)	
Mutational burden					
Median	63	353 (2–955)	154 (3–914)	392 (33–993)	0.0018

It is important to mention that we observed that tumor BL CD73 expression positively correlated with features of a “hot” immune environment such as PD-L1 and immune cell infiltration rendering the plausible supposition that CD73 immune function may be disparate between BL and L compartments of LUAD cells. Similarly, when we analyzed immune cell densities within LUADs grouped based on CD73 positivity, the TH group displayed elevated PD-L1 and immune cell infiltration compared with the TL and TN groups. It is noteworthy, that CD73 was shown to suppress anti-tumor immunity and promote immune evasion [9, 42, 43]. Thus, given our findings along with the previous reports on CD73 function, it is not unreasonable to suggest

that expression of CD73 may underlie inferior response to ICI even in tumors with concomitant high tumoral PD-L1 expression and immune cell infiltration [44, 45]. In line with our results, a previous report demonstrated that high levels of adenosine correlated with elevated infiltration of immune cells, but with a decreased response to ICI [32]. It is intriguing to suppose that targeting CD73 may enhance anti-tumor immunity, particularly in tumors with high levels of CD73, as well as augment the effect of ICI. Indeed, targeting CD73 was shown to skew the immune TME to a more anti-tumor phenotype in preclinical models [46, 47]. In separate context, our findings also suggest that targeting CD73 may help augment anti-tumor immunity in LUADs with low yet

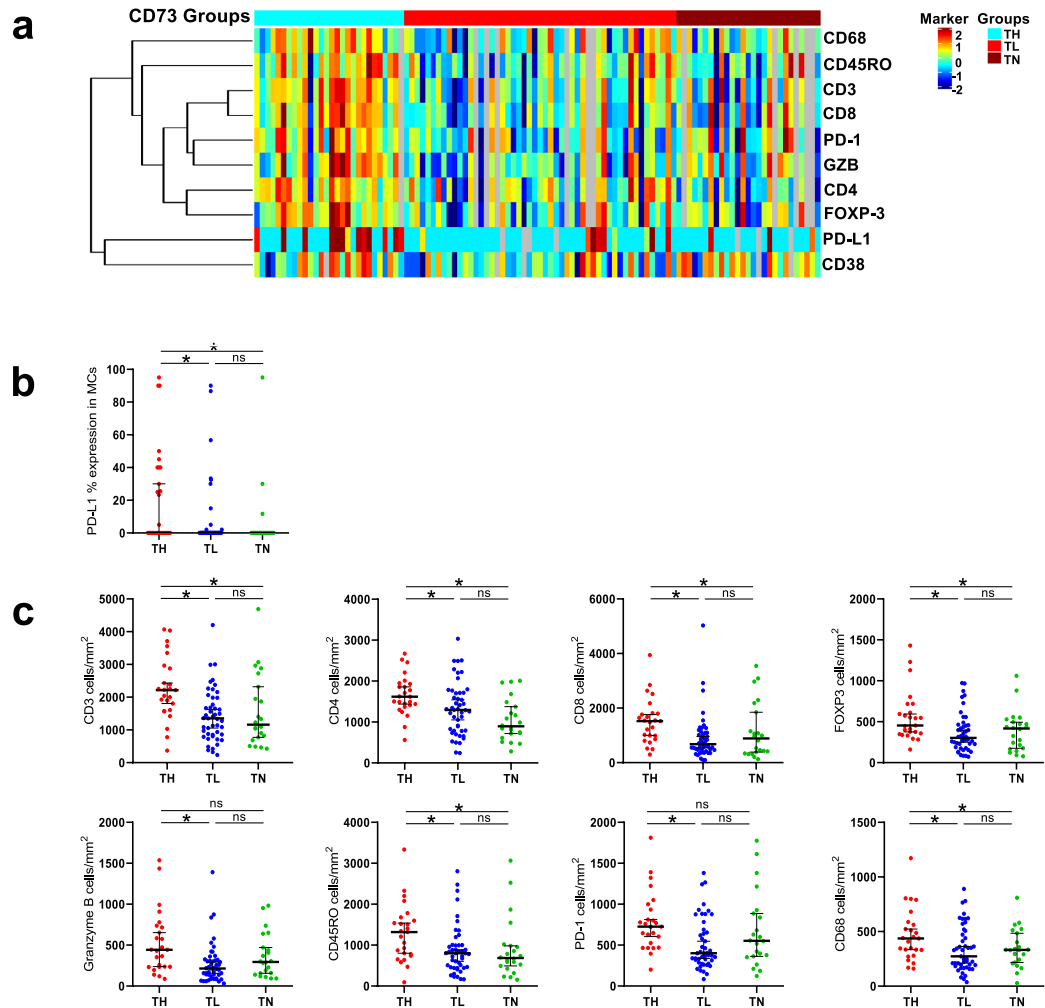


Fig. 3 Extent of CD73 expression defines groups of lung adenocarcinoma with disparate tumor immune infiltration. **a** Heat map of TAIC densities and PD-L1 (% of expression) in MCs of 95 LUADs grouped based on the extent of CD73 expression (TH, TL, and TN). Rows represent immune markers and columns denote samples (red, relatively

higher TAIC density or PD-L1%; blue, relatively lower TAIC density or PD-L1%). **b** Plots showing PD-L1% expression among the TH, TL, and TN groups. **c** Plots showing TAIC densities among the TH, TL, and TN groups (* $p < 0.05$ based on the Kruskal–Wallis test, *n.s.* not significant, bars correspond to median values \pm 95% CI)

positive CD73, and which we find here to exhibit a relatively “cold” immune contexture [48]. Of note, we found that a fraction of LUADs that were CD73 negative displayed abundant expression of CD38 concomitant with a muted host immune response, suggesting redundant activation of the non-canonical adenosine pathway [9, 11] in these tumors and their potential tractability by agents that target this pathway. Our study points to the potential role of CD73, and

other members of the adenosine signaling pathway, as potential mechanisms of tumor immune evasion and resistance to ICI, thus providing additional rationale for propagating anti-CD73 antibodies in new combinatorial immunotherapeutic regimens. As mentioned before, we found that differential (e.g., BL vs. L) CD73 localization was associated with distinct clinicopathological and molecular features in LUAD. It is intriguing to propose that in-depth assessment

of CD73 expression along with its membrane localization will provide comprehensive assessment of patients who may benefit from agents targeting this immune marker.

Our study is not without limitations. It is important to mention that we interrogated tissue microarrays of LUAD, with these arrays typically harboring relatively small tissue cores which may bring about increased tumor and, thus, immune marker heterogeneity and under-representation of luminal structures of adenocarcinomas—thus warranting future studies probing CD73 in whole tissue specimens. It is also noteworthy, given our study design and goals, that our cohort was primarily comprised of resectable early stage tumors with, thus, under-representation of relatively more advanced (e.g., metastatic) LUADs. In this context, our study is unable to ascertain relative patterns of CD73 expression (and localization), along with features of host anti-tumor immunity and immune evasion, between early stage and more advanced LUADs. Since mechanisms of host immune evasion by the tumor, along with genomic and mutational complexity, are expectantly more pronounced in advanced-stage tumors, future studies are warranted to fully probe CD73, and other members of the adenosine pathway, along the continuum of different stages (e.g., early, local/oligometastatic to distant metastatic) in LUAD. Furthermore, the expression patterns of CD73 in patients who have received ICI, preoperatively or in the advanced setting, are not yet discerned. It also cannot be neglected that our study is retrospective in nature and comprises a cohort of limited number of patients and from a single center warranting validation of our findings by external cohorts. Additionally, future studies are warranted that further probe mechanisms involving CD73 expression and its interaction with host immune responses in LUAD. It is important to note that, unlike earlier work [22], we did not find associations between CD73 with clinical outcome and *EGFR* mutation status. This discrepancy may be attributable to the disparate patient molecular and clinicopathological profiles in our cohort compared to those earlier studies that focused on East Asian patients [22]. Due to the lack of tissue availability, the analysis of *CD73* gene expression in AAH, MIA, AIS, LUAD, and normal lung tissue was not validated by IHC. Nonetheless, our study provides new and comprehensive insights into diverse patterns of CD73 expression and localization, in association with genomic, immune, and clinical features, in early stage LUAD, thus offering a roadmap in the future to interrogate the role of CD73 expression in immunotherapy and/or response to ICI.

In conclusion, we comprehensively surveyed the expression, abundance, and membrane tumor localization of CD73 in early stage LUAD, and found that this immune marker with distinct clinicopathological, molecular, and immune characteristics. Our findings on increased expression of the immune evasion mediator CD73 in LUADs with elevated

PD-L1 and immune cell infiltration offer potential insight into why some patients with augmented immune response still respond poorly or modestly to ICI. Our data also provide the plausible rationale for exploring immunotherapeutic regimens consisting of anti-CD73 antibodies in combination with ICI.

Supplementary Information The online version contains supplementary material available at <https://doi.org/10.1007/s00262-020-02820-4>.

Acknowledgements The author would like to thank the laboratory members of the Translational Molecular Pathology Immune-Profiling Laboratory (TMP-IL), especially Lakshmi Kakarala, Mei Jiang, Auriole Tamegnon, Jocelyn Coronel, and Jianling Zhou for their technical assistance.

Author contributions Study concept and design: LS, CB, and IW; Develop of methodology: PR, RS, BM, WL, and LS; Data acquisition: RS, DL, PV, HD, DD, CB, KG, AW, EP, DR, BS, NK, CM, AV, TC, JH, DG, JZ, and LS; Data interpretation: PR, CB, HK, and LS; Statistical analysis: JZ, LD, and JL; Writing of the manuscript: PR, CB, HK, IW, and LS; Edition and approval of the manuscript: all authors.

Funding This work was partially supported by the NCI Specialized Program of Research Excellence (SPORE) in Lung Cancer (P50CA70907), by the Cancer Prevention and Research Institute of Texas Multi-Investigator Research Award (CPRIT MIRA) grant (RP160668) at The University of Texas M.D. Anderson Cancer Center, and by SEOM (Sociedad Española de Oncología Médica).

Data availability Data are available upon reasonable request. The data that support the findings of our study are available upon request from the corresponding author. The data are not publicly available due to privacy or ethical restrictions.

Code availability Not applicable.

Compliance with ethical standards

Conflict of interest None.

Ethical approval This study was approved by the MD Anderson Institutional Review Board and was conducted according to the principles of the Helsinki Declaration.

Open Access This article is licensed under a Creative Commons Attribution 4.0 International License, which permits use, sharing, adaptation, distribution and reproduction in any medium or format, as long as you give appropriate credit to the original author(s) and the source, provide a link to the Creative Commons licence, and indicate if changes were made. The images or other third party material in this article are included in the article's Creative Commons licence, unless indicated otherwise in a credit line to the material. If material is not included in the article's Creative Commons licence and your intended use is not permitted by statutory regulation or exceeds the permitted use, you will need to obtain permission directly from the copyright holder. To view a copy of this licence, visit <http://creativecommons.org/licenses/by/4.0/>.


References

- Siegel RL, Miller KD, Jemal A (2020) Cancer statistics, 2020. *CA Cancer J Clin* 70:7–30. <https://doi.org/10.3322/caac.21590>
- Borghaei H, Paz-Ares L, Horn L et al (2015) Nivolumab versus docetaxel in advanced nonsquamous non-small-cell lung cancer. *N Engl J Med* 373:1627–1639. <https://doi.org/10.1056/NEJMoa1507643>
- Reck M, Rodríguez-Abreu D, Robinson AG et al (2016) Pembrolizumab versus chemotherapy for PD-L1-positive non-small-cell lung cancer. *N Engl J Med* 375:1823–1833. <https://doi.org/10.1056/NEJMoa1606774>
- Gandhi L, Rodríguez-Abreu D, Gadgeel S et al (2018) Pembrolizumab plus chemotherapy in metastatic non-small-cell lung cancer. *N Engl J Med*. <https://doi.org/10.1056/NEJMoa1801005>
- Gettinger S, Horn L, Jackman D et al (2018) Five-year follow-up of Nivolumab in previously treated advanced non-small-cell lung cancer: results from the CA209–003 study. *J Clin Oncol* 003:2017770412. <https://doi.org/10.1200/JCO.2017.77.0412>
- Forde PM, Chaft JE, Smith KN et al (2018) Neoadjuvant PD-1 blockade in resectable lung cancer. *N Engl J Med* 378:1976–1986. <https://doi.org/10.1056/NEJMoa1716078>
- Antonia SJ, Villegas A, Daniel D et al (2017) Durvalumab after chemoradiotherapy in stage III non-small-cell lung cancer. *N Engl J Med* 377:1919–1929. <https://doi.org/10.1056/NEJMoa1709937>
- Gao ZW, Dong K, Zhang HZ (2014) The roles of CD73 in cancer. *Biomed Res Int* 2014:460654. <https://doi.org/10.1155/2014/460654>
- Allard B, Allard D, Buisseret L, Stagg J (2020) The adenosine pathway in immuno-oncology. *Nat Rev Clin Oncol*. <https://doi.org/10.1038/s41571-020-0382-2>
- Fridman WH, Zitvogel L, Sautès-Fridman C, Kroemer G (2017) The immune contexture in cancer prognosis and treatment. *Nat Rev Clin Oncol* 14:717–734. <https://doi.org/10.1038/nrcli.nonc.2017.101>
- Horenstein AL, Chillemi A, Zaccarello G et al (2013) A CD38/CD203a/CD73 ectoenzymatic pathway independent of CD39 drives a novel adenosinergic loop in human T lymphocytes. *Oncimmunology* 2:e26246. <https://doi.org/10.4161/onci.26246>
- de Andrade MP, Coutinho-Silva R, Savio LEB (2017) Multifaceted effects of extracellular adenosine triphosphate and adenosine in the tumor-host interaction and therapeutic perspectives. *Front Immunol* 8:1526. <https://doi.org/10.3389/fimmu.2017.01526>
- Regateiro FS, Cobbold SP, Waldmann H (2013) CD73 and adenosine generation in the creation of regulatory microenvironments. *Clin Exp Immunol* 171:1–7. <https://doi.org/10.1111/ij.1365-2249.2012.04623.x>
- Beavis PA, Divisekera U, Paget C et al (2013) Blockade of A2A receptors potently suppresses the metastasis of CD73⁺ tumors. *Proc Natl Acad Sci* 110:14711–14716. <https://doi.org/10.1073/pnas.1308209110>
- Antonioni L, Blandizzi C, Pacher P, Haskó G (2013) Immunity, inflammation and cancer: a leading role for adenosine. *Nat Rev Cancer* 13:842–857. <https://doi.org/10.1038/nrc3613>
- Chen S, Wainwright DA, Wu JD et al (2019) CD73: an emerging checkpoint for cancer immunotherapy. *Immunotherapy* 11:983–997. <https://doi.org/10.2217/imt-2018-0200>
- Chen DS, Mellman I (2013) Oncology meets immunology: the cancer-immunity cycle. *Immunity* 39:1–10. <https://doi.org/10.1016/j.immuni.2013.07.012>
- Cogdill AP, Andrews MC, Wargo JA (2017) Hallmarks of response to immune checkpoint blockade. *Br J Cancer* 117:1–7. <https://doi.org/10.1038/bjc.2017.136>
- Marshall HT, Djamgoz MBA (2018) Immuno-oncology: emerging targets and combination therapies. *Front Oncol* 8:1–29. <https://doi.org/10.3389/fonc.2018.00315>
- Young A, Ngiew SF, Barkauskas DS et al (2016) Co-inhibition of CD73 and A2AR adenosine signaling improves anti-tumor immune responses. *Cancer Cell* 30:391–403. <https://doi.org/10.1016/j.ccell.2016.06.025>
- Stagg J, Divisekera U, McLaughlin N et al (2010) Anti-CD73 antibody therapy inhibits breast tumor growth and metastasis. *Proc Natl Acad Sci* 107:1547–1552. <https://doi.org/10.1073/pnas.0908801107>
- Inoue Y, Yoshimura K, Kurabe N et al (2017) Prognostic impact of CD73 and A2A adenosine receptor expression in non-small-cell lung cancer. *Oncotarget* 8:8738–8751. <https://doi.org/10.18632/oncotarget.14434>
- Kudo Y, Haymaker C, Zhang J et al (2019) Suppressed immune microenvironment and repertoire in brain metastases from patients with resected non-small-cell lung cancer. *Ann Oncol Off J Eur Soc Med Oncol* 30:1521–1530. <https://doi.org/10.1093/annonc/mdz207>
- Solis LM, Behrens C, Dong W et al (2010) Nrf2 and Keap1 abnormalities in non-small cell lung carcinoma and association with clinicopathologic features. *Clin Cancer Res* 16:3743–3753. <https://doi.org/10.1158/1078-0432.CCR-09-3352>
- Rami-Porta R, Asamura H, Travis WD, Rusch VW (2017) Lung cancer-major changes in the American joint committee on cancer eighth edition cancer staging manual. *CA Cancer J Clin*. 67:138–155. <https://doi.org/10.3322/caac.21390>
- Solis LM, Behrens C, Raso MG et al (2012) Histologic patterns and molecular characteristics of lung adenocarcinoma associated with clinical outcome. *Cancer* 118:2889–2899. <https://doi.org/10.1002/cncr.26584>
- Kadara H, Choi M, Zhang J et al (2017) Whole-exome sequencing and immune profiling of early-stage lung adenocarcinoma with fully annotated clinical follow-up. *Ann Oncol Off J Eur Soc Med Oncol* 28:75–82. <https://doi.org/10.1093/annonc/mdw436>
- Ayers M, Lunceford J, Nebozhyn M et al (2017) IFN- γ -related mRNA profile predicts clinical response to PD-1 blockade. *J Clin Invest* 127:2930–2940. <https://doi.org/10.1172/JCI91190>
- Spranger S, Bao R, Gajewski TF (2015) Melanoma-intrinsic β -catenin signalling prevents anti-tumour immunity. *Nature* 523:231–235. <https://doi.org/10.1038/nature14404>
- Jiang P, Gu S, Pan D et al (2018) Signatures of T cell dysfunction and exclusion predict cancer immunotherapy response. *Nat Med* 24:1550–1558. <https://doi.org/10.1038/s41591-018-0136-1>
- Hwang S, Kwon A-Y, Jeong J-Y et al (2020) Immune gene signatures for predicting durable clinical benefit of anti-PD-1 immunotherapy in patients with non-small cell lung cancer. *Sci Rep* 10:643. <https://doi.org/10.1038/s41598-019-57218-9>
- Sidders B, Zhang P, Goodwin K et al (2020) Adenosine signaling is prognostic for cancer outcome and has predictive utility for immunotherapeutic response. *Clin Cancer Res* 26:2176–2187. <https://doi.org/10.1158/1078-0432.CCR-19-2183>
- Danaher P, Warren S, Lu R et al (2018) Pan-cancer adaptive immune resistance as defined by the tumor inflammation signature (TIS): results from The Cancer Genome Atlas (TCGA). *J Immunother Cancer* 6:63. <https://doi.org/10.1186/s40425-018-0367-1>
- Qi Z, Wang L, Desai K et al (2019) Reliable gene expression profiling from small and hematoxylin and eosin-stained clinical formalin-fixed, paraffin-embedded specimens using the HTG edgeSeq platform. *J Mol Diagn* 21:796–807. <https://doi.org/10.1016/j.jmoldx.2019.04.011>
- Chen L, Diao L, Yang Y et al (2018) CD38-mediated immunosuppression as a mechanism of tumor cell escape from PD-1/PD-L1 blockade. *Cancer Discov* 8:1156–1175. <https://doi.org/10.1158/2159-8290.CD-17-1033>

36. Lantuejoul S, Sound-Tsao M, Cooper WA et al (2020) PD-L1 testing for lung cancer in 2019: perspective from the IASLC Pathology Committee. *J Thorac Oncol* 15:499–519. <https://doi.org/10.1016/j.jtho.2019.12.107>
37. Parra ER, Behrens C, Rodriguez-Canales J et al (2016) Image analysis-based assessment of pd-11 and tumor-associated immune cells density supports distinct intratumoral microenvironment groups in non-small cell lung carcinoma patients. *Clin Cancer Res* 22:6278–6289. <https://doi.org/10.1158/1078-0432.CCR-15-2443>
38. Parra ER, Villalobos P, Zhang J et al (2018) Immunohistochemical and image analysis-based study shows that several immune checkpoints are co-expressed in non-small cell lung carcinoma tumors. *J Thorac Oncol* 13:779–791. <https://doi.org/10.1016/j.jtho.2018.03.002>
39. Hay CM, Sult E, Huang Q et al (2016) Targeting CD73 in the tumor microenvironment with MEDI9447. *Oncoimmunology* 5:e1208875. <https://doi.org/10.1080/2162402X.2016.1208875>
40. NIH-U.S. National Library of Medicine (2019) ClinicalTrials.gov. <https://clinicaltrials.gov/ct2/results?cond=Lung+Cancer&term=CD73&cntry=&state=&city=&dist=&Search=Search>
41. Pervez S, Arshad S, Abro B (2018) HER2 basolateral versus circumferential IHC expression is dependent on polarity and differentiation of epithelial cells in gastric/GE adenocarcinoma. *Patholog Res Int* 2018:6246493. <https://doi.org/10.1155/2018/6246493>
42. Vigano S, Alatzoglou D, Irving M et al (2019) Targeting adenosine in cancer immunotherapy to enhance T-Cell function. *Front Immunol* 10:925. <https://doi.org/10.3389/fimmu.2019.00925>
43. Chen S, Fan J, Zhang M et al (2019) CD73 expression on effector T cells sustained by TGF- β facilitates tumor resistance to anti-4-1BB/CD137 therapy. *Nat Commun* 10:150. <https://doi.org/10.1038/s41467-018-08123-8>
44. Teng F, Meng X, Kong L, Yu J (2018) Progress and challenges of predictive biomarkers of anti PD-1/PD-L1 immunotherapy: a systematic review. *Cancer Lett* 414:166–173. <https://doi.org/10.1016/j.canlet.2017.11.014>
45. Minor M, Alcedo KP, Battaglia RA, Snider NT (2019) Cell type- and tissue-specific functions of ecto-5'-nucleotidase (CD73). *Am J Physiol Cell Physiol*. <https://doi.org/10.1152/ajpcell.00285.2019>
46. Beavis PA, Milenkovski N, Henderson MA et al (2015) Adenosine receptor 2A blockade increases the efficacy of anti-PD-1 through enhanced antitumor T-cell responses. *Cancer Immunol Res* 3:506–517. <https://doi.org/10.1158/2326-6066.CIR-14-0211>
47. Perrot I, Michaud H-A, Giraudon-Paoli M et al (2019) Blocking antibodies targeting the CD39/CD73 immunosuppressive pathway unleash immune responses in combination cancer therapies. *Cell Rep* 27:2411–2425.e9. <https://doi.org/10.1016/j.celrep.2019.04.091>
48. Mazzarella L, Duso BA, Trapani D et al (2019) The evolving landscape of “next-generation” immune checkpoint inhibitors: a review. *Eur J Cancer* 117:14–31. <https://doi.org/10.1016/j.ejca.2019.04.035>

Publisher's Note Springer Nature remains neutral with regard to jurisdictional claims in published maps and institutional affiliations.

Authors and Affiliations

Pedro Rocha^{1,2} · Ruth Salazar¹ · Jiexin Zhang³ · Debora Ledesma¹ · Jose L. Solorzano¹ · Barbara Mino¹ · Pamela Villalobos¹ · Hitoshi Dejima¹ · Dzifa Y. Douse¹ · Lixia Diao³ · Kyle Gregory Mitchell⁴ · Xiuning Le⁴ · Jianjun Zhang⁴ · Annikka Weissferdt⁶ · Edwin Parra-Cuentas¹ · Tina Cascone⁴ · David C. Rice⁵ · Boris Sepesi⁴ · Neda Kalhor⁶ · Cesar Moran⁶ · Ara Vaporciyan⁵ · John Heymach⁴ · Don L. Gibbons⁴ · J. Jack Lee³ · Humam Kadara¹ · Ignacio Wistuba^{1,4} · Carmen Behrens⁴ · Luisa Maren Solis¹ 

¹ Department of Translational Molecular Pathology, The University of Texas MD Anderson Cancer Center, 2130 West Holcombe Boulevard, Houston, TX 77030, USA

² Universidad de Barcelona, Barcelona, Spain

³ Department of Bioinformatics and Comp Biology, The University of Texas MD Anderson Cancer Center, Houston, TX, USA

⁴ Thoracic/Head and Neck Medical Oncology, The University of Texas MD Anderson Cancer Center, Houston, TX, USA

⁵ Thoracic and Cardiovascular Surgery, The University of Texas MD Anderson Cancer Center, Houston, TX, USA

⁶ The University of Texas MD Anderson Cancer Center, Houston, TX, USA

4.2 Distinct immune gene programs associated with host tumor immunity, neoadjuvant chemotherapy and chemoimmunotherapy in resectable NSCLC.

Pedro Rocha, Jiexin Zhang, Raquel Laza-Briviesca, Alberto Cruz-Bermúdez, Katsuhiko Yoshimura, Carmen Behrens, Apar Pataer, Edwin R Parra, Cara Haymaker, Junya Fujimoto, Stephen G Swisher, John V Heymach, Don L Gibbons, J. Jack Lee, Boris Sepesi, Tina Cascone, Luisa M Solis, Mariano Provencio, Ignacio I Wistuba, Humam Kadara. *Clinical Cancer Research*, 2022.

Distinct Immune Gene Programs Associated with Host Tumor Immunity, Neoadjuvant Chemotherapy, and Chemoimmunotherapy in Resectable NSCLC



Pedro Rocha^{1,2}, Jiexin Zhang³, Raquel Laza-Briviesca⁴, Alberto Cruz-Bermúdez⁴, Neus Bota-Rabasedas¹, Beatriz Sanchez-Espiridon¹, Katsuhiko Yoshimura¹, Carmen Behrens⁵, Wei Lu¹, Ximing Tang¹, Apar Pataer⁶, Edwin R. Parra¹, Cara Haymaker¹, Junya Fujimoto¹, Stephen G. Swisher⁶, John V. Heymach⁵, Don L. Gibbons⁵, J. Jack Lee³, Boris Sepesi⁶, Tina Cascone⁵, Luisa M. Solis¹, Mariano Provencio⁴, Ignacio I. Wistuba¹, and Humam Kadara¹

ABSTRACT

Purpose: Our understanding of the immunopathology of resectable non-small cell lung cancer (NSCLC) is still limited. Here, we explore immune programs that inform of tumor immunity and response to neoadjuvant chemotherapy and chemoimmunotherapy in localized NSCLC.

Experimental Design: Targeted immune gene sequencing using the HTG Precision Immuno-Oncology panel was performed in localized NSCLCs from three cohorts based on treatment: naïve ($n = 190$), neoadjuvant chemotherapy ($n = 38$), and neoadjuvant chemoimmunotherapy ($n = 21$). Tumor immune microenvironment (TIME) phenotypes were based on the location of CD8⁺ T cells (inflamed, cold, excluded), tumoral PD-L1 expression (<1% and ≥1%), and tumor-infiltrating lymphocytes (TIL). Immune programs and signatures were statistically analyzed on the basis of tumoral PD-L1 expression, immune phenotypes, and pathologic response and were cross-compared across the three cohorts.

Results: PD-L1-positive tumors exhibited increased signature scores for various lymphoid and myeloid cell subsets ($P < 0.05$). TIME phenotypes exhibited disparate frequencies by stage, PD-L1 expression, and mutational burden. Inflamed and PD-L1⁺/TILs⁺ NSCLCs displayed overall significantly heightened levels of immune signatures, with the excluded group representing an intermediate state. A cytotoxic T-cell signature was associated with favorable survival in neoadjuvant chemotherapy-treated NSCLCs ($P < 0.05$). Pathologic response to chemoimmunotherapy was positively associated with higher expression of genes involved in immune activation, chemotaxis, as well as T and natural killer cells ($P < 0.05$ for all). Among the three cohorts, chemoimmunotherapy-treated NSCLCs exhibited the highest scores for various immune cell subsets including T effector and B cells ($P < 0.05$).

Conclusions: Our findings highlight immune gene programs that may underlie host tumor immunity and response to neoadjuvant chemotherapy and chemoimmunotherapy in resectable NSCLC.

Introduction

While non-small cell lung cancer (NSCLC) remains the leading cause of cancer-related mortality, death rates due to this ominous cancer have declined in the past few years (1). Enhanced early

screening and diagnosis have increased the numbers of early-stage NSCLCs (2, 3). Also, new approaches using stereotactic body radiation for inoperable early-stage lung cancer (4) and immune checkpoint inhibitors (ICI) in the adjuvant setting are increasingly being established for clinical management of stage II to IIIA NSCLC with ≥1% tumoral PD-L1 expression (5). Improved treatment of early-stage NSCLC heavily relies on understanding the molecular and immune biology of the malignancy. Indeed, recent emerging evidence points to reprogramming of the immune contexture in early stages in the pathogenesis of NSCLC, (6–8) thus providing rationale for immunotherapeutic strategies such as ICI in the resectable disease setting (9, 10).

Immunosuppression mediated by the PD-1/PD-L1 checkpoint pathway has been shown to underlie immune evasion by NSCLC (11, 12). Clinical studies have shown that ICIs targeting the PD-(L)1 axis mount an antitumor immune response that leads to favorable and, in some cases, durable responses in patients with cancer, including those with advanced/unresectable NSCLC (8, 9). Of note, patients with NSCLC exhibit variable responses to ICIs targeting PD-1 or PD-L1 (13, 14). Expression of PD-L1 protein by IHC is used to guide immunotherapeutic strategies in NSCLC (15). Previous clinical trials (14) showed that high tumoral and immune PD-L1 expression predict overall favorable response to ICI. Yet, a significant fraction of patients with PD-L1-positive (≥1%) tumors do not respond to ICIs (14) and, conversely, other studies have

¹Department of Translational Molecular Pathology, The University of Texas MD Anderson Cancer Center, Houston, Texas. ²Universidad de Barcelona, Barcelona, Spain. ³Department of Bioinformatics and Computational Biology, The University of Texas MD Anderson Cancer Center, Houston, Texas. ⁴Hospital Universitario Puerta de Hierro-Majadahonda, Madrid, Spain. ⁵Department of Thoracic Head and Neck Medical Oncology, The University of Texas MD Anderson Cancer Center, Houston, Texas. ⁶Department of Thoracic and Cardiovascular Surgery, The University of Texas MD Anderson Cancer Center, Houston, Texas.

Note: Supplementary data for this article are available at Clinical Cancer Research Online (<http://clincancerres.aacrjournals.org/>).

P. Rocha and J. Zhang contributed equally to this article.

Corresponding Authors: Humam Kadara, Department of Translational Molecular Pathology, The University of Texas MD Anderson Cancer Center, Houston, TX 77030. E-mail: hkadara@mdanderson.org; and Ignacio I. Wistuba, Department of Translational Molecular Pathology, The University of Texas MD Anderson Cancer Center, Houston, TX 77030. E-mail: iiwistuba@mdanderson.org

Clin Cancer Res 2022;28:2461–73

doi: 10.1158/1078-0432.CCR-21-3207

©2022 American Association for Cancer Research

Translational Relevance

Neoadjuvant treatment with immune checkpoint inhibitors alone or in combination with chemotherapy have recently shown promising results in non–small cell lung cancer (NSCLC). Yet, mechanisms that promote response to these strategies remain inadequately understood. Here we report immune programs that inform of host antitumor immunity and response in resectable NSCLC. In treatment-naïve tumors, we found that tumor immune microenvironment phenotypes (inflamed, cold, and excluded) based on the cell densities and spatial distribution of CD8⁺ T cells exhibited disparate frequencies by stage, PD-L1 expression, and mutational burden. Cytotoxic T-cell signature was associated with favorable survival in neoadjuvant chemotherapy–treated NSCLCs. Patients achieving major pathologic response after chemoimmunotherapy exhibited higher CD8⁺ T cells, while Th1 cells were significantly reduced post chemoimmunotherapy. Among the three cohorts, chemoimmunotherapy–treated NSCLCs significantly exhibited the highest scores for various immune cell subsets including T effector and B cells. Our findings highlight immune gene programs that may underlie host tumor immunity and response to immunotherapy in resectable NSCLC.

demonstrated responses in patients whose NSCLCs are PD-L1 negative (<1%; ref. 16), thus highlighting the need for more reliable biomarkers to predict response to ICI.

Recent reports (17–23) demonstrated promising results using neoadjuvant ICI for treatment of resectable NSCLC. For instance, the phase II clinical trial by Provencio and colleagues [neoadjuvant chemotherapy and nivolumab in resectable non–small cell lung cancer (NADIM)] showed that chemoimmunotherapy (combination of nivolumab and platinum-based chemotherapy) elicited major pathologic response (MPR) in the majority of resected patients (17). More recently, a phase III clinical trial by Forde and colleagues showed that neoadjuvant chemoimmunotherapy resulted in higher MPR rate (36.8%) compared with chemotherapy alone (8.6%; ref. 24). While these results are encouraging, the mechanisms by which neoadjuvant ICI in combination with chemotherapy elicit MPR in early-stage NSCLC are still largely unknown (25).

To fill this void, we interrogated three cohorts with localized NSCLC that underwent upfront surgery or neoadjuvant chemotherapy, as currently established standard of care in this setting, and compared with patients who received neoadjuvant chemoimmunotherapy (platinum-based therapy plus anti-PD-1). Our results show that an augmented immune response is often observed in treatment-naïve patients with high tumor PD-L1 expression, while PD-L1–negative tumors exhibit heterogeneous host immune expression programs. We also find that chemoimmunotherapy elicits immune gene expression programs and phenotypes that are distinct from or absent in treatment-naïve or chemotherapy only–treated patients, thus highlighting potential markers and targets for immunotherapeutic response in early-stage NSCLC.

Materials and Methods

Patient cohorts

Patients with resectable NSCLC were classified based on preoperative treatment. A cohort of 190 treatment-naïve patients that underwent upfront surgery and a set of 38 patients that received neoadjuvant

platinum-based chemotherapy followed by surgery were evaluated and treated at The University of Texas MD Anderson Cancer Center (Houston, TX). The third cohort included patients who were enrolled in a multi-institutional clinical trial (NADIM clinical trial, NCT03081689, primary institution: Hospital Puerta de Hierro, Madrid, Spain) and treated with neoadjuvant chemotherapy plus anti-PD-1 (nivolumab; chemoimmunotherapy cohort; ref. 17). Our study and analyses were approved by the relevant Institutional Review Boards and were conducted according to the principles of the Helsinki Declaration. Informed written consent was obtained from each subject or subject's guardian. Detailed clinicopathologic information including demographics, smoking history, pathologic tumor–node–metastasis stage, as well as overall and recurrence-free survival for all cases are summarized in **Table 1**. Mutational status of key driver genes, including *KRAS*, *EGFR*, *STK11*, and *TP53*, as well as tumor mutation burden (TMB) were previously characterized (26) by whole-exome sequencing and were available for a subset of the cases (**Table 1**). Pathologic response to therapy was assessed by estimating the percentage of viable tumor cells (VTC), necrosis, and fibrosis. Pathologic response to neoadjuvant therapies was performed following a standardized approach to assess the percentage of VTCs, necrosis and stroma (including inflammation and fibrosis)—all amounting to 100% of analyzed cells. Pathologic response was categorized as incomplete pathologic response (i.e., no MPR; >10% VTCs), MPR (≤10% VTCs), and pathologic complete response (pCR; no remaining VTCs; refs. 27, 28). For cases with MPR or pCR after neoadjuvant chemotherapy or chemoimmunotherapy, the tumor bed was histopathologically identified and subsequently interrogated by targeted immune gene profiling.

IHC analysis

IHC and digital image analysis were performed previously (29) for a subset of NSCLCs ($n = 177$). This included analysis of densities of tumor-associated immune cells: CD4⁺ (Th), CD8⁺ (cytotoxic T), CD45RO⁺ (memory T), and FOXP3⁺ (regulatory T; Supplementary Table S1). Briefly, tissue sections (4 μm) were stained using a Leica Bond Max automated stainer (Leica Biosystems Nussloch GmbH). Sections were then deparaffinized and rehydrated according to the manufacturer's protocol. Antigen retrieval was performed for 20 minutes with Bond Solution #2 (Leica Biosystems, equivalent EDTA, pH 9.0) or Bond Solution #1 (Leica Biosystems, equivalent Citrate Buffer, pH6). Primary antibodies were incubated for 15 minutes at room temperature and detected using the Bond Polymer Refine Detection kit (Leica Biosystems) with DAB as chromogen. Tissue slides were counterstained with hematoxylin, dehydrated, and coverslipped.

Membrane PD-L1 was evaluated by a pathologist (L.M. Solis) as percentage of tumor cells with positive expression based on the International Association for the Study of Lung Cancer guidelines (30). Pathologic evaluation was done for each sample to confirm the presence of tumor and adjacent normal uninvolved tissue. For those cases in which the presence of both compartments was confirmed, the invasive margin was delineated (red line in **Fig. 2A**). Subsequently, and using IHC analysis, CD8⁺ T-cell densities were separately evaluated within (tumoral) and surrounding (peritumoral or adjacent normal tissue) tumors in whole sections using digital image analysis as previously described by our group (29). Based on this compartment classification (tumoral vs. peritumoral), we categorized tumors into three tumor immune microenvironment (TIME) patterns similar to what was performed by previous studies in NSCLC (31): (i) inflamed, ≥1,000 CD8⁺ T cells/mm² within the tumor compartment and a

Table 1. Clinicopathologic characteristics of the three cohorts: Treatment-naïve ($n = 190$), neoadjuvant chemotherapy cohort ($n = 38$) from MD Anderson, and the neoadjuvant chemoimmunotherapy cohort from the NADIM trial ($n = 21$; NCT03081689).

Clinicopathologic variables	Treatment-naïve (MD Anderson) ($n = 190$)		Neoadjuvant chemotherapy (MD Anderson) ($n = 38$)		Neoadjuvant chemoimmunotherapy (NADIM trial) ($n = 21$)	
		%		%		%
Age median (range)	67 (41–86)		62 (43–81)		64 (41–76)	
Sex						
Female	80	42.1	17	44.7	5	23.8
Male	110	57.9	21	55.3	16	76.2
Smoking status						
Current	83	43.7	23	60.5	8	38.1
Former	92	48.4	15	39.5	13	61.9
Never	15	7.9	0	0.0	0	0.0
Histology						
LUAD	107	56.3	20	52.6	11	52.4
LUSC	83	43.7	18	47.4	10	47.6
TNM stage						
I	73	38.4	1	2.6	0	0.0
II	49	25.8	7	18.4	0	0.0
III	68	35.8	30	79.0	21	100.0
PD-L1 (IHC)						
<1%	80	42.1	4	10.5	8	38.1
≥1%	38	20	7	18.4	9	42.9
NA	72	37.9	27	71.1	4	19.0
Recurrence						
Yes	91	47.9	21	55.3	5	23.8
No	99	52.1	17	44.7	16	76.2
Survival						
Alive	56	29.5	8	21.1	19	90.5
Dead	134	70.5	30	78.9	2	9.5

Abbreviations: IHC, immunohistochemistry; LUAD, lung adenocarcinoma; LUSC, lung squamous cell carcinoma; NA, not available.

peritumoral CD8⁺/tumoral CD8⁺ ratio < 2.75, denoting homogeneous infiltration across both compartments; (ii) cold, < 1,000 CD8⁺ T cells/mm² within the tumor compartment and ratio < 2.75, denoting lack of infiltration across both compartments; and (iii) excluded, with a peritumoral CD8⁺/tumoral CD8⁺ ratio > 2.75, lacking CD8⁺ T cells in the tumor area and exhibiting CD8⁺ T-cell infiltrates that reside at the periphery of the tumor. Tumors were also categorized into four groups based on PD-L1 IHC expression (<1% and ≥1%) and tumor-infiltrating lymphocyte (TIL) infiltration using CD3⁺ T-cell densities (<median = TILs⁻ and ≥median = TILs⁺): (i) PD-L1⁻/TILs⁻; (ii) PD-L1⁻/TILs⁺; (iii) PD-L1⁺/TILs⁻; and (iv) PD-L1⁺/TILs⁺.

Multiplex immunofluorescence analysis

Multiplex immunofluorescence (mIF) was available for a subset of patients in the neoadjuvant chemoimmunotherapy cohort ($n = 27$) and were reported previously (17). Briefly, mIF staining was performed on 4 μm histologic tumor sections using the Opal 7-Color IHC Kit (PerkinElmer). Slides were scanned by a Vectra multispectral microscope (PerkinElmer). The immune markers CD3, CD8, and FOXP3, and pancyokeratin AE1/AE3 were then analyzed and reported as number of cells per mm square (cells/mm²).

Targeted RNA sequencing of immune genes

The HTG EdgeSeq Precision Immuno-Oncology panel (HTG Molecular) was employed to examine immune-centric expression programs in samples from all three cohorts. This panel comprised 1,392 genes with a focus on tumor-immune interaction. We then used the available HTG EdgeSeq Reveal software (HTG Molecular) to

in silico deconvolute the immune gene expression data into gene signatures that characterize distinct cell populations and phenotypes (Supplementary Table S2; ref. 32). Furthermore, gene programs that predict immune cell infiltration and functional states were compiled (Supplementary Table S3) and interrogated in the three cohorts. For validation, we studied publicly available bulk and transcriptome sequencing data of 481 stage I to III lung adenocarcinomas (LUAD) from The Cancer Genome Atlas (TCGA) cohort. LUAD samples were ranked by their expression of *CD274*, with upper quartile of tumors constituting those with relatively high expression (PD-L1 positive).

Statistical analysis

Targeted immune gene expression data were first median-normalized and then log₂ transformed for further analysis. Scores of previously curated immune gene signatures were calculated by computing average expression of genes within each signature. To test association between continuous and categorical variables, Mann-Whitney *U* and Kruskal-Wallis tests were applied for categorical variables with two levels or more than two levels, respectively. To test association between two continuous variables, the Spearman rank correlation test was applied. For survival analysis, we used Cox proportional hazards models. Benjamini and Hochberg method was used for multiple testing correction of *P* values.

Data availability statement

Raw data were generated in the HTG Molecular Diagnostics core facility. Processed data are available from the authors and derived data

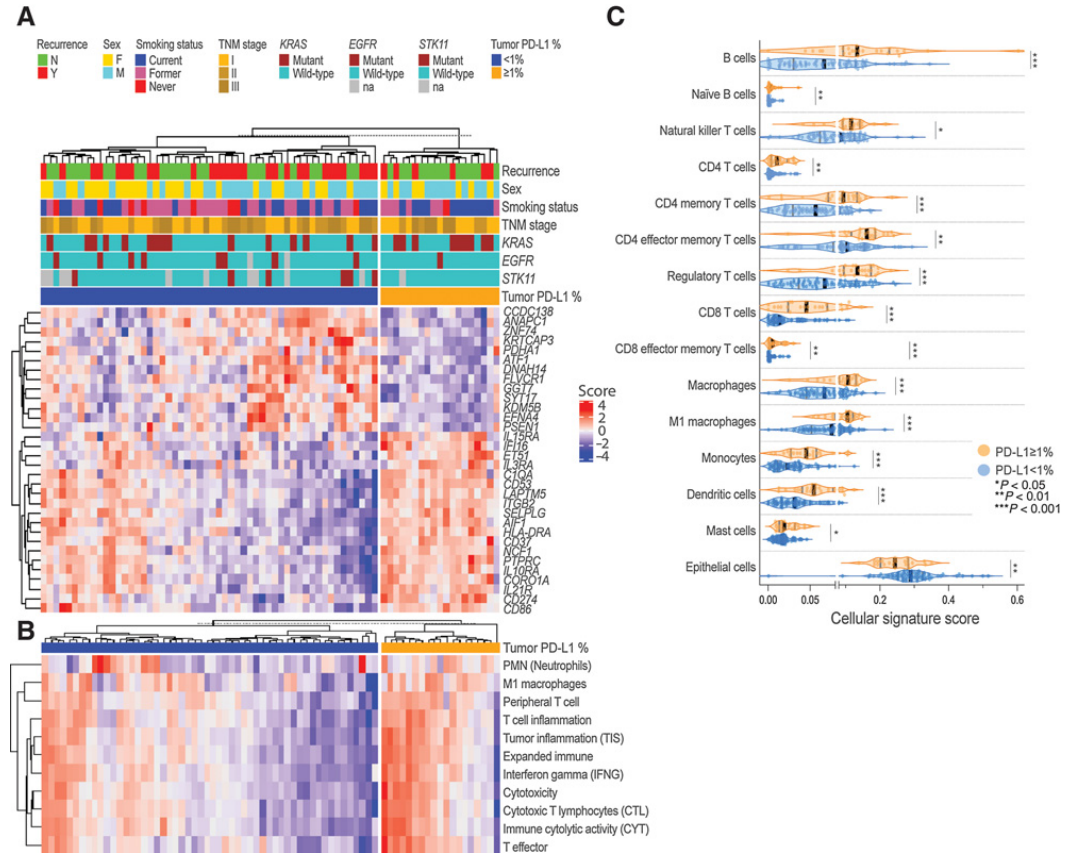


Figure 1. Immune expression programs differentially expressed in PD-L1-positive and PD-L1-negative treatment-naïve LUADs. **A**, Heatmap showing DEGs between PD-L1-positive ($\geq 1\%$) and PD-L1-negative ($< 1\%$) treatment-naïve LUADs. DEGs were selected on the basis of a statistical threshold of adjusted $P < 0.05$. Columns denote samples which were annotated with clinicopathologic and molecular features, and rows represent DEGs (red, relatively higher expression; blue, relatively lower expression). **B**, Differential expression of functional gene signatures (red, higher expression; blue, relatively lower expression; adjusted $P < 0.05$) between PD-L1-positive and PD-L1-negative LUADs. **C**, Violin plots for cellular signatures scores in PD-L1-positive ($\geq 1\%$, orange) and PD-L1-negative ($< 1\%$, blue) tumors. P values were calculated on the basis of the Mann-Whitney test, black lines represent the median, and gray lines correspond to 95% confidence interval (CI). DEGs, differentially expressed genes; LUADs, lung adenocarcinomas.

supporting the findings of this study are available from the corresponding author upon request.

Results

Immune expression programs are associated with PD-L1 positivity in treatment-naïve NSCLC

We performed targeted immune gene sequencing using the HTG EdgeSeq Precision Immuno-Oncology platform (32) of 190 treatment-naïve early-stage NSCLCs (Table 1) and compared immune expression programs and phenotypes between PD-L1-positive and PD-L1-negative tumors. We first compared protein IHC expression levels of CD4⁺, CD8⁺, FOXP3⁺, CD45RO⁺, and CD68⁺ cell densities with corresponding immune cell scores derived by targeted gene sequencing ($n = 177$ patients). We found significant correlation between all

four immune cell densities with the corresponding gene scores ($r = 0.58$, $r = 0.67$, $r = 0.35$, $r = 0.32$, $r = 0.22$, respectively, $P < 0.0001$ for all; Supplementary Fig. S1A). PD-L1 protein expression in tumor cells by IHC significantly and highly correlated with CD274 expression ($r = 0.55$, $P < 0.0001$; Supplementary Fig. S1B). In addition, CD8 T and CD8 memory effector T-cell immune gene programs were significantly and highly positively correlated with previous published gene signatures denoting cytotoxic T lymphocytes (CTL; ref. 33; $P < 0.0001$; $r = 0.7761$) and cytotoxicity (ref. 34; $P < 0.0001$; $r = 0.8037$; Supplementary Fig. S2). These data point to the robustness of the targeted immune sequencing approach to quantify immune subsets in the TIME of early-stage NSCLC.

Relative to PD-L1-negative ($< 1\%$ tumoral PD-L1) LUADs, PD-L1-positive ($\geq 1\%$) LUADs displayed elevated expression of genes associated with antigen presentation (e.g., *HLA-DRA* and *CD86*;

Fig. 1A), various immune programs such as IFN γ signaling (35), and immune cytolytic activity (36) as well as immune subsets such as CTLs (33) and T effector cells (37, 38). In addition, PD-L1–positive tumors showed increased signature scores for immunoregulatory mediators such as neutrophils (Fig. 1B; ref. 39). These findings were validated when we studied localized LUADs from the TCGA cohort. PD-L1–high LUADs from TCGA cohort similarly exhibited relatively higher expression of genes implicated in antigen presentation and several immune programs implicated in host antitumor responses (e.g., IFN γ , immune cytolytic activity, M1 macrophages, T effector cells; Supplementary Fig. S3A and S3B). PD-L1–positive LUADs also showed elevated immune cell scores for B ($P = 0.0005$), CD4 T ($P = 0.0029$), regulatory T, and effector memory CD8 T cells (all $P < 0.05$; Fig. 1C). Of note, we observed heterogeneous expression of these immune gene programs in PD-L1–negative LUADs, with a subset of tumors exhibiting elevated inflammation-associated signatures. In close alignment with previous studies (26, 40), LUADs harboring *EGFR* or *STK11* mutations more frequently exhibited negative tumoral PD-L1 expression concomitant with reduced expression of various immune cell scores (Supplementary Fig. S4A). Among lung squamous cell carcinomas (LUSC), PD-L1–positive tumors only showed increased abundance of macrophages and M1 macrophages signatures and decreased scores for plasma cells relative to those that were negative for PD-L1, perhaps suggesting distinct immune biology programs associated with PD-L1 between both subtypes of NSCLC (Supplementary Fig. S4B–S4D). Of note, tumoral PD-L1 in both LUADs and LUSCs was not significantly associated with recurrence (Supplementary Fig. S5A). Notably, nonrecurrent LUADs, compared with their recurrent counterparts, exhibited increased abundance of specific immune subsets such as B and plasma cells as well as M1 macrophages (all $P < 0.05$; Supplementary Fig. S5B). Our findings suggest immune genes and programs that further inform of the immunopathology of early-stage NSCLC.

Gene expression programs associated with immunologically inflamed, cold, and excluded TIME phenotypes

We next categorized treatment-naïve NSCLCs into distinct TIME phenotypes (inflamed, cold, and excluded) based on cell density and spatial distribution of CD8⁺ T cells by IHC (Fig. 2A). The fraction of LUADs harboring an excluded phenotype increased with pathologic stage ($P = 0.0273$; Fig. 2B). In accordance with our previous findings above, PD-L1–positive LUADs displayed increased frequency of the inflamed TIME phenotype (66.7%) compared with PD-L1–negative tumors (38.1%; $P = 0.0207$; Fig. 2B). In addition, LUADs with relatively higher TMB more frequently displayed an inflamed phenotype (58.6%; $P < 0.0001$; Fig. 2B). Notably, 9 of 13 *EGFR*-mutant LUADs were classified as cold tumors (Supplementary Fig. S6A) in close agreement with previous studies (26, 40). We found a trend for reduced survival in the excluded group albeit not reaching statistical significance (Supplementary Fig. S6B).

We next performed *in silico* deconvolution to identify differences in the abundance of immune cell types across the three TIME phenotypes. Inflamed LUADs exhibited significantly higher signature scores for CD8 T cells ($P < 0.0001$) including effector memory T cells ($P < 0.0001$; Fig. 2C), consistent with the CD8⁺ IHC analysis. Inflamed LUADs also showed increased abundance of B-cell populations (naïve B cells and B cells, both $P < 0.0001$). In addition, macrophage and M1 macrophage subsets were significantly lower in cold LUADs ($P = 0.0008$ and $P = 0.0003$, respectively). Similarly, we found by IHC analysis significantly decreased CD68⁺ cell densities in the cold group

($P < 0.0001$; Supplementary Fig. S7). Of note, signature scores for M2 macrophages were significantly increased in LUADs with an excluded phenotype ($P = 0.0219$; Fig. 2C). We identified 94 differentially expressed genes (DEG) among treatment-naïve LUADs across the three phenotypes. Inflamed LUADs showed increased expression of genes that were consistent with elevated immune cell infiltration (e.g., *CD3E*, *CD3G*, *CD8A*, *CD8B*), cytolytic activity (*GZMA*, *GZMB*, *GZMK*, *NKG7*), immune cell chemotaxis (*CXCL9*, *CXCL10*, *CXCL13*), and antigen presentation (*TAP1*, *TAP2*). In sharp contrast, LUADs with a cold phenotype exhibited the lowest levels for these immune profiles, concomitant with increased expression of tumor promoting factors (*MTOR*, *FGFR3*, *IL6R*). Excluded LUADs displayed immune profiles that were in an intermediate state between inflamed and cold phenotypes (Fig. 2D).

We also performed similar analysis of tumors that we categorized into four groups based on PD-L1 expression and TILs (CD3⁺ T cell) infiltration (Supplementary Fig. S8A). We found increased frequencies of PD-L1⁺/TILs⁺ tumors in cases with an inflamed or excluded TIME phenotype and in those with higher TMB (Supplementary Fig. S8B). Conversely, fractions of PD-L1⁺/TILs⁺ tumors were markedly reduced and of PD-L1⁻/TILs⁻ greatly increased in the cold TIME group (Supplementary Fig. S8B). We found that PD-L1⁺/TILs⁺ tumors when compared with their PD-L1⁻/TILs⁻ counterparts overall exhibited increased signature scores for various immune populations, programs, and genes—echoing our findings when comparing inflamed and cold tumors (Supplementary Fig. S8C and S8D). Also, among PD-L1–negative tumors, those that were TILs⁺ displayed higher CD4 T-cell signatures including memory, effector memory and regulatory cell subsets compared with their TILs⁻ counterparts (Supplementary Fig. S8C). We also interrogated expression levels of various immune checkpoints (*PDCD1*, *CD274*, *CTLA4*, *HAVCR2*, *ICOSLG*, *TIGIT*, and *LAG3*) across the TIME phenotypes and PD-L1/TILs groups. We found increased expression of *CTLA4*, *TIGIT*, and *LAG3* in the inflamed group, and elevated levels of *HAVCR2* and *ICOSLG* in the excluded phenotype (Supplementary Fig. S9A). We did not find significant differences in the expression of these immune checkpoints among the four subgroups based on PD-L1 expression and TILs, while significant differences were observed on the basis of PD-L1 status (<1% vs. $\geq 1\%$) with positive tumors exhibiting increase expression of *CD274*, *CTLA4*, *HAVCR2*, and *TIGIT* ($P < 0.05$ for all; Supplementary Fig. S9B and S9C).

Immune expression changes linked with pathologic response after neoadjuvant chemotherapy in early-stage NSCLC

We next sought to interrogate immune programs in early-stage NSCLCs treated with neoadjuvant chemotherapy. We studied immune genes that were associated with pathologic response. Among LUADs, we found that immune genes implicated in innate immune responses (*CD14*, *TLR4*, *MAF*) and those pertinent to B-cell biology (*CD79A*, *JCHAIN*, *CXCL12*, *BLNK*) were significantly and positively associated with pathologic response (lower % VTCs; $P < 0.01$). In contrast, LUADs with relatively lower or no response to neoadjuvant chemotherapy displayed upregulation of genes implicated in DNA replication, cell cycle, and inhibition of apoptosis (e.g., *MCM6*, *FOXM1*, *FOXA1*) consistent with increased % VTCs (Fig. 3A). In accordance, percentage of VTCs was significantly correlated with the identified DEGs ($r = 0.84$, $P < 0.001$) and with an epithelial cell gene signature ($r = 0.62$, $P = 0.0065$; Fig. 3B). Also, LUADs with a relatively higher signature score for CTLs (33) displayed significantly improved overall survival (OS; $P = 0.0055$; Fig. 3C). Of note, recurrent LUADs showed significantly upregulated expression of the adenosine pathway

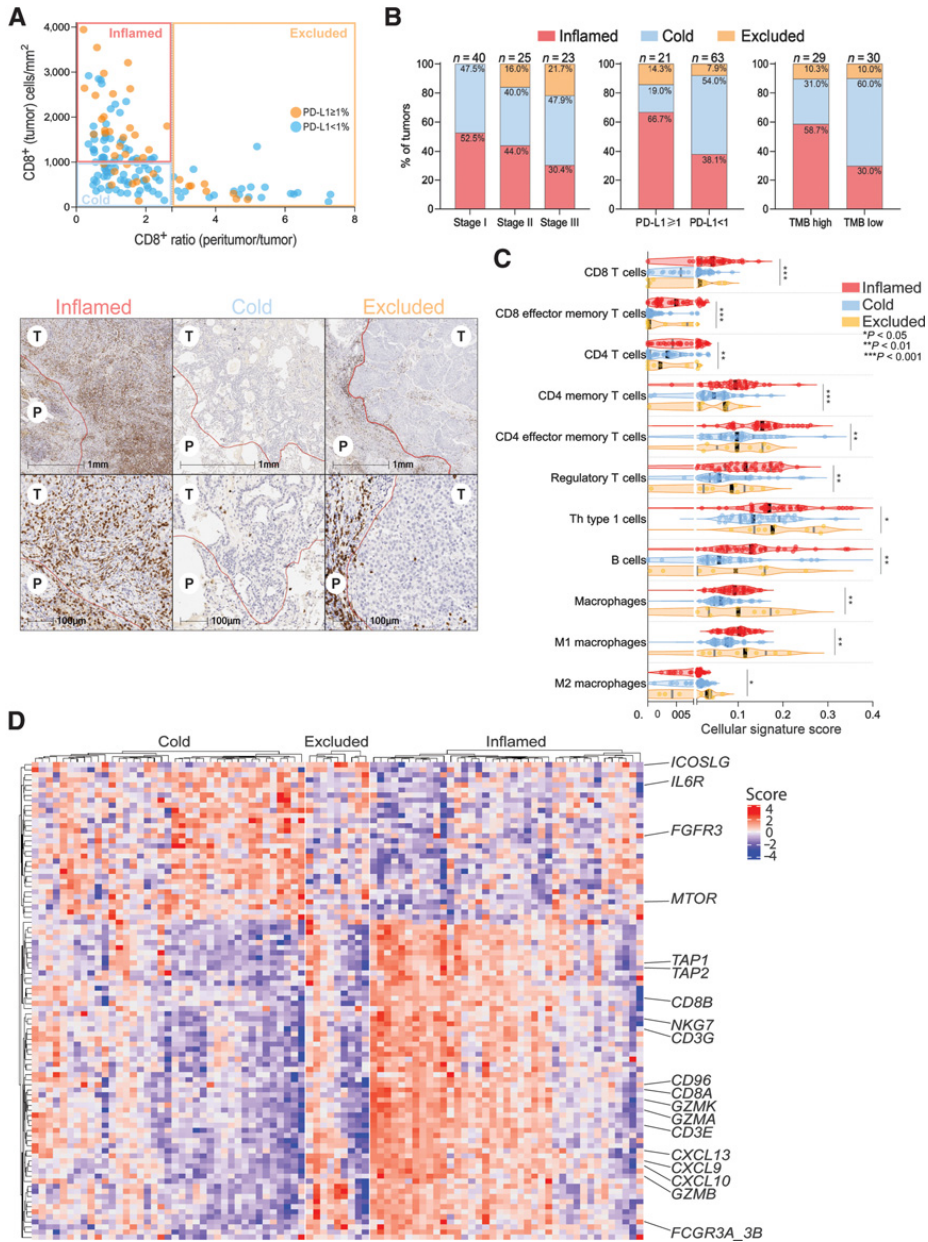


Figure 2.

Gene expression programs associated with immunologically inflamed, cold, and excluded TIME phenotypes in treatment-naïve LUADs. **A**, Scatter plot showing distribution of LUADs based on tumoral cell densities of CD8⁺ T cells (y-axis) and peritumoral/tumoral ratios for CD8⁺ T cells (x-axis). LUADs were classified into inflamed (red rectangle), cold (blue rectangle), and excluded (yellow rectangle) phenotypes (top); representative images for the three different phenotype patterns are shown at the bottom (P, peritumoral; T, tumor area). LUADs were also color coded by PD-L1 expression (orange, ≥1%; blue, <1%). **B**, Frequencies of TIME phenotypes in LUAD by pathologic stage, tumoral PD-L1 expression, as well as TMB [TMB high, ≥ median (171); TMB low, < median]. *P* values were calculated on the basis of the Fisher exact test. **C**, Violin plots depicting cellular signature scores across the three TIME phenotypes. *P* values were calculated on the basis of the Kruskal-Wallis test, black lines represent median levels, and gray lines correspond to 95% CI. **D**, Heatmap showing 94 DEGs (*P*_{adjusted} < 0.05) between the three TIME phenotypes. Rows represent genes and columns denote samples (red, relatively higher expression; blue, relatively lower expression).

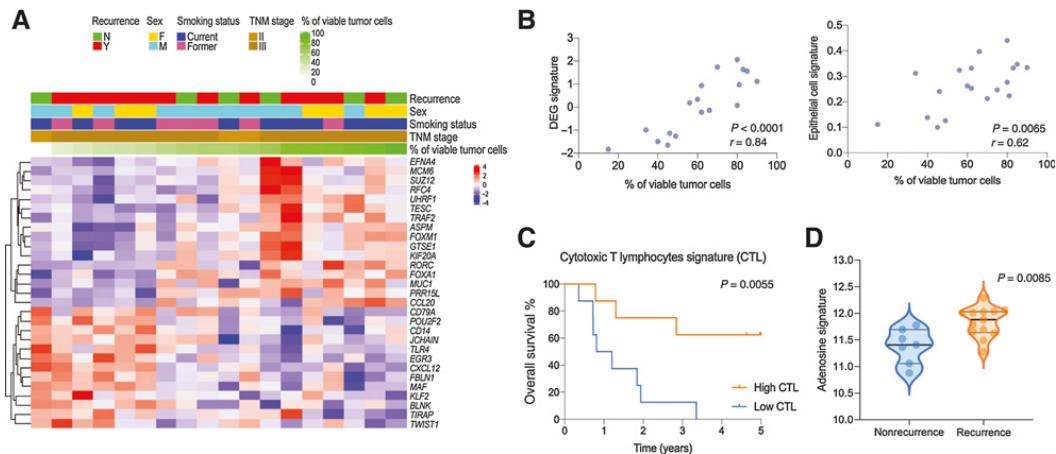


Figure 3.

Immune expression changes linked with pathologic response after neoadjuvant chemotherapy in early-stage NSCLC. **A**, Heatmap showing 29 DEGs (unadjusted $P < 0.01$) that are associated with the percent of viable tumor cells in early-stage NSCLCs treated with neoadjuvant chemotherapy. Columns denote patients who are annotated with clinicopathologic and molecular features and rows represent DEGs (red, relatively higher expression; blue, relatively lower expression). **B**, Scatter plot showing statistically positive correlation of the identified DEGs (left) and an epithelial cell signature (right) with percent viable tumor cells. Correlation was statistically assessed using Spearman correlation. **C**, Analysis of the association of a signature score for CTLs with OS using Kaplan–Meier method for estimation of survival probability and of an adenosine signature (**D**) with recurrence (P value was calculated on the basis of the Mann–Whitney test, black lines represent the median, and gray lines correspond to 95% CI).

($P = 0.0085$; **Fig. 3D**), an immune program previously shown by our group and others to be associated with tumor immune evasion and lack of response to ICI (34, 41). Recurrent LUADs in this cohort also showed a tendency for increased abundance of macrophages ($P = 0.0811$), M2 macrophages ($P = 0.0557$), and CD4 memory T cells ($P = 0.0557$; Supplementary Fig. S10). In LUSCs, % VTCs was positively correlated with a natural killer (NK) cell exhaustion signature (ref. 34; $r = 0.61$, $P = 0.022$), and inversely correlated with abundance of M2 macrophages ($r = -0.61$, $P = 0.0187$; Supplementary Fig. S11A and S11B).

Chemoimmunotherapy elicits pronounced immune-wide expression changes in resectable NSCLC

Comparison of patients with NSCLC who showed pCR/MPR relative to those with incomplete response to neoadjuvant chemoimmunotherapy revealed that the former group overall displayed higher immune scores (i.e., abundance) for various cell subsets such as B cells ($P = 0.0110$) and CD8 T cells ($P = 0.0293$; **Fig. 4A**) indicative of elevated immune infiltration associated with response. On the other hand, NSCLCs that did not respond to neoadjuvant chemoimmunotherapy exhibited elevated fractions of Th type 1 cells as well as of epithelial cells ($P < 0.05$; **Fig. 4A**) consistent with increased percentage of VTCs. Of note, we also performed orthogonal confirmation of CD8 T and regulatory T cell signatures using mIF. CD3⁺CD8⁺ and CD3⁺FOXP3⁺CD8⁻ cell densities by mIF closely and positively correlated with RNA sequencing (RNA-seq)-derived CD8 T and regulatory T cell signatures, respectively (Supplementary Fig. S12A and S12B). CD3⁺CD8⁺ cell densities by mIF and the CD8 T-cell signature were both concordantly and significantly increased between chemoimmunotherapy-treated patients with MPR/pCR and those with no MPR (Supplementary Fig. S12A, right) whereas there were no statistically significant changes in both CD3⁺FOXP3⁺CD8⁻ cell

densities and the regulatory T cell signature between both patient groups (Supplementary Fig. S12B, right).

Next, we interrogated immune genes that were associated with pathologic response. We identified 223 genes significantly associated with % VTCs ($P_{\text{adjusted}} < 0.05$). Patients with less % VTCs after neoadjuvant chemoimmunotherapy exhibited higher expression of genes involved in immune activation and chemotaxis (*IL1R1*, *CCL14*, *IL33*, *IL7R*, *IRF8*, *CXCR4*), T and NK (*TARP*, *CD226*, *CD69*, *KLRD1*), and myeloid cells (*CLEC9A*, *MARCO*). Conversely, tumors with relatively higher % VTCs following neoadjuvant chemoimmunotherapy displayed upregulation of genes implicated in DNA replication and cell cycle (e.g., *BRCA1*, *CDK4*, *TOP2A*, *AURKA*) as well as of the major immunosuppressive transcriptional factor *FOXP3* (**Fig. 4B**).

We next interrogated evolution of immune responses in a subset of these patients ($n = 13$) with available paired pretherapy and posttherapy samples. Differential expression analysis revealed 128 DEGs that were significantly modulated between paired posttreatment and pretreatment samples. Chemoimmunotherapy increased expression of genes that are implicated in inflammation and chemotaxis of immune cells (*IL1R1*, *CXCR4*, *CCL14*, *CXCL12*), regulatory T cells ($P = 0.0479$), and M2 macrophages ($P = 0.0398$; **Fig. 4C** and **D**; Supplementary Fig. S13). Chemoimmunotherapy also reduced overall abundance of Th type 1 ($P < 0.0001$) and epithelial ($P < 0.0001$) cells (**Fig. 4D**).

We next compared immune gene programs across NSCLCs that are treatment-naïve, treated with neoadjuvant chemotherapy, and those treated with neoadjuvant chemoimmunotherapy. Because of the design of our study, and the currently approved treatment approaches (42), stage I NSCLCs were more frequently found in the treatment-naïve cohort (38%) compared with neoadjuvant chemotherapy (2.6%) and the chemoimmunotherapy (0%) cohorts. We thus excluded stage I NSCLCs from this comparative analysis. We observed

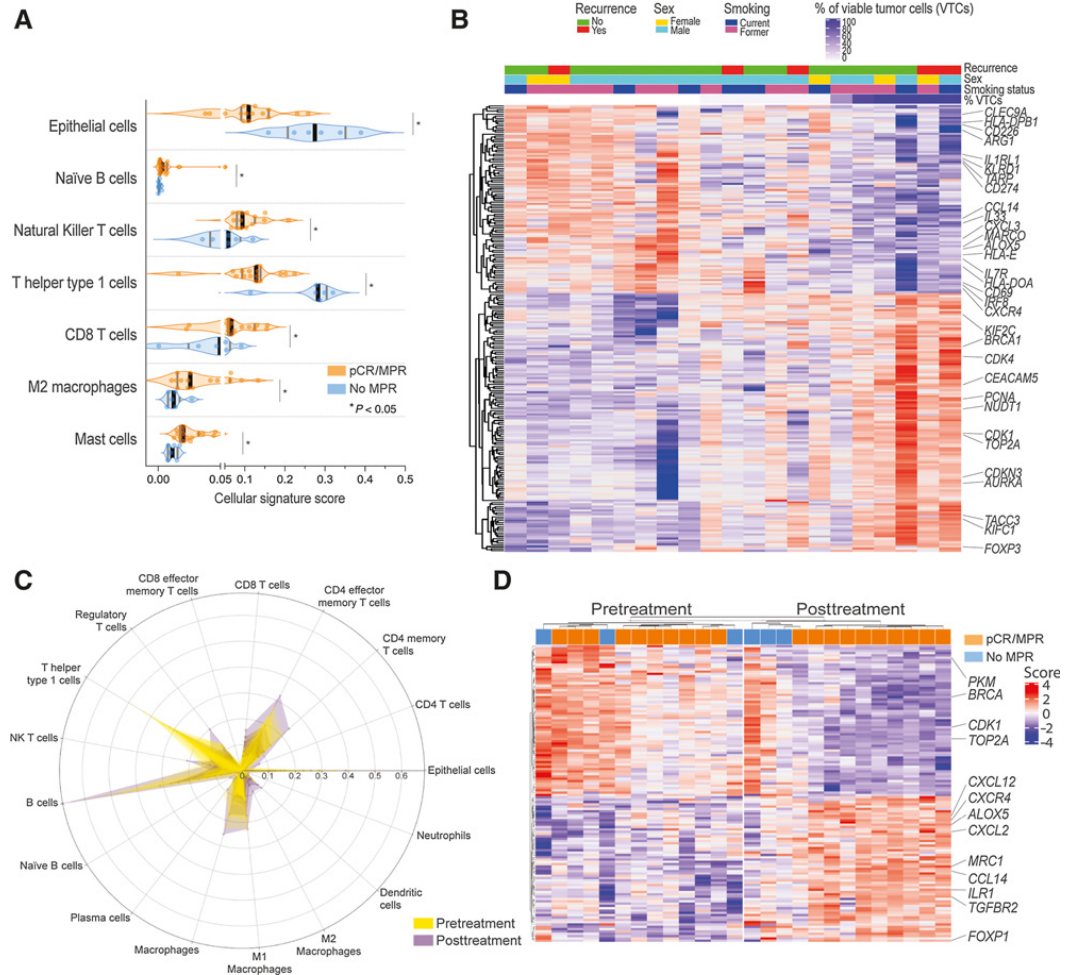


Figure 4. Chemoimmunotherapy elicits pronounced immune-wide expression changes in resectable NSCLC. **A**, Violin plots for cellular signature scores in patients with pCR/MPR (% of viable tumor cells $\leq 10\%$, orange) and without pCR/MPR ($>10\%$ of viable tumor cells, blue). *P* values were calculated on the basis of the Mann-Whitney test; black lines represent median values, and gray lines correspond to 95% CI. **B**, Heatmap showing 223 DEGs ($P_{\text{adjusted}} < 0.05$) that are associated with percent viable tumor cells in early-stage NSCLCs treated with neoadjuvant chemoimmunotherapy. **C**, Radar plot highlighting differences between pretreatment (red) and posttreatment samples (blue) for the cellular signature scores. **D**, Heatmap showing 128 DEGs between pretreatment and posttreatment samples ($P_{\text{adjusted}} < 0.05$). Columns denote samples and rows represent genes (red, relatively higher expression; blue, relatively lower expression). MPR: major pathologic response; pCR: pathologic complete response.

that 532 genes were differentially expressed between the three groups (Fig. 5A). Patients with NSCLC treated with chemoimmunotherapy exhibited upregulated expression of profiles indicative of elevated T and B cell (e.g., *CD3G*, *CD8A*, *MS4A1*, *CD19*, *CD22*) and myeloid (*CD68*, *CD163*, *CXCR2*, *ALOX15B*) cell infiltration (Fig. 5A) and, conversely, attenuated levels of genes involved in cell cycle (*PKM*, *CDK4*) and DNA repair (*BRCA1*, *PCNA*; Fig. 5A). In addition, most immune cell gene signatures were found to be elevated in the chemoimmunotherapy cohort (Fig. 5B). Chemoimmunotherapy-treated

patients with NSCLC displayed markedly and significantly upregulated abundance of B and plasma cells (both $P < 0.05$) as well as CD4 ($P = 0.0031$) and cytotoxic CD8 ($P < 0.0001$) T cells. Notably, and for many of these cell subsets, we found gradual changes across the three patient groups, that is, chemoimmunotherapy-treated NSCLCs exhibiting the highest fractions of these immune populations and the treatment-naïve group showing the lowest levels (Fig. 5B). Our findings underscore immune gene programs that may underlie effects of and response to neoadjuvant chemoimmunotherapy.

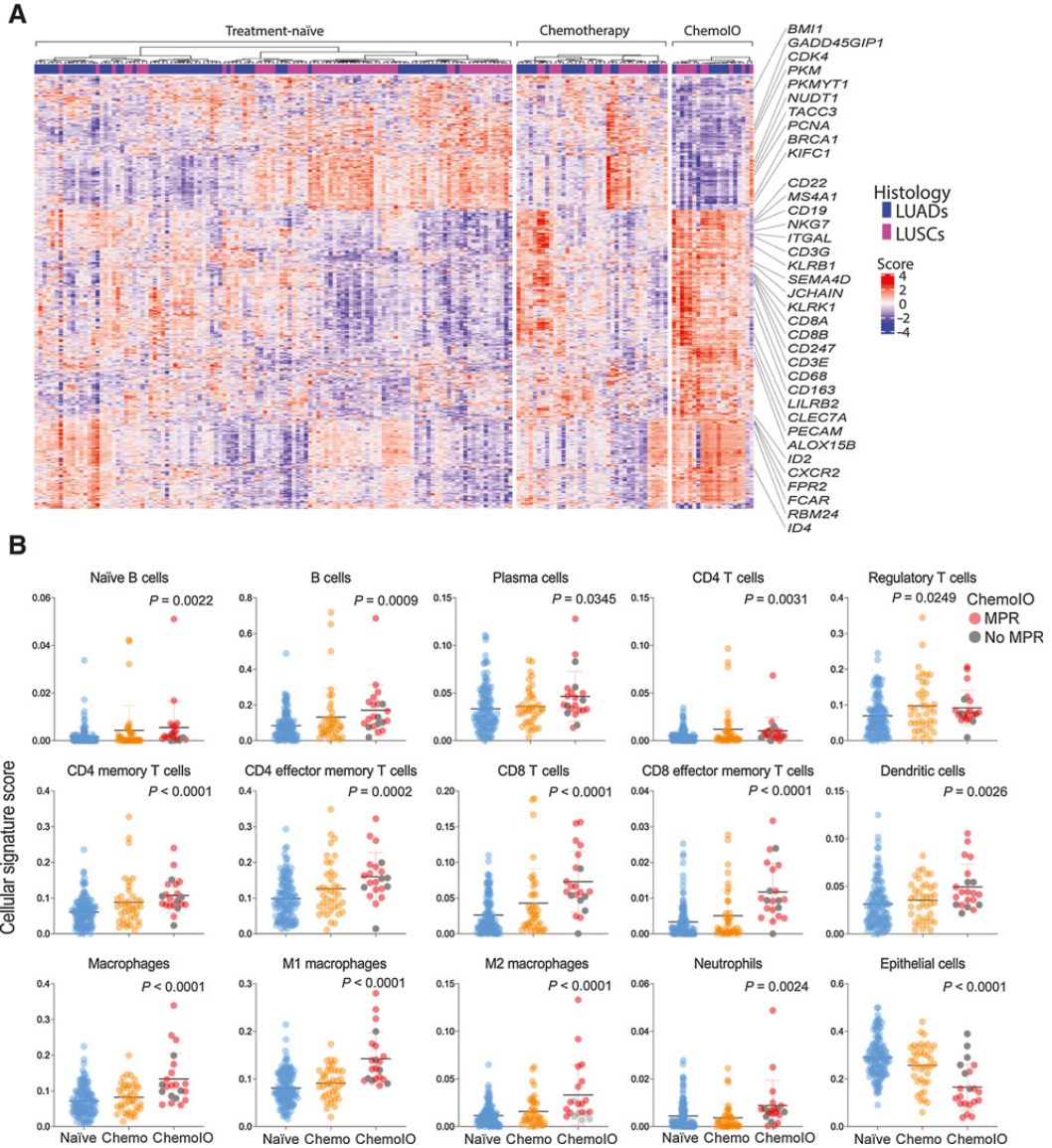


Figure 5. Immune gene programs that are differentially modulated between treatment-naïve NSCLCs and those treated with neoadjuvant chemotherapy and chemoimmunotherapy. **A**, Heatmap showing 532 DEGs between treatment-naïve, neoadjuvant chemotherapy-treated (Chemotherapy), and NSCLCs treated with chemoimmunotherapy (ChemoIO; $P_{\text{adjusted}} < 0.05$). Columns denote samples, and rows represent genes (red, relatively higher expression; blue, relatively lower expression). **B**, Dot plots for cellular signature scores across the three cohorts (blue, treatment-naïve; orange, neoadjuvant chemotherapy; red, neoadjuvant chemoimmunotherapy). P values were calculated on the basis of Kruskal-Wallis tests. Bars correspond to median values \pm 95% CI.

Discussion

Immune phenotypes underlying the pathobiology of NSCLC including its response to neoadjuvant therapy remain poorly under-

stood. Here, we performed targeted RNA-seq of an immune gene panel to interrogate immune programs in three cohorts of resectable NSCLC that underwent upfront surgery (treatment-naïve), neoadjuvant chemotherapy, or chemoimmunotherapy. We found that the majority of

treatment-naïve NSCLCs that expressed PD-L1 displayed elevated immune cell scores. We further defined three TIME phenotypes (inflamed, cold, and excluded) in NSCLCs based on the presence and spatial distribution of CD8⁺ T cells and that showed distinct immune and inflammatory features. We then described immune gene sets that were associated with response to neoadjuvant chemotherapy or chemoimmunotherapy. Finally, comparative analysis of immune programs across the three cohorts showed progressive increases in various immune cell scores along the spectrum of treatment-naïve, to neoadjuvant chemotherapy-treated tumors, up to those treated with neoadjuvant chemoimmunotherapy. Our study points to immune programs and phenotypes that may underlie tumor immunity and responses to neoadjuvant therapies, including chemotherapy and immune-based treatment, in resectable NSCLC.

Several clinical trials have demonstrated that tumoral and immune cell PD-L1 expression is associated with increased likelihood of response to antibodies against PD-1 or PD-L1 in metastatic NSCLC (14, 43–45). In our analysis of early-stage NSCLCs, and consistent with previous reports (46–48), we found that PD-L1-positive LUADs displayed overall augmented immune gene scores and programs compared with PD-L1-negative LUADs. Interestingly, we found that a subset of PD-L1-negative LUADs displayed relatively high levels of immune cell scores. It is noteworthy that previous studies demonstrated favorable responses to anti-PD-1/PD-L1 therapy in localized NSCLCs that were negative for tumoral PD-L1 (17–20, 23). Our findings set the stage for a reasonable supposition that patients with early-stage NSCLC with negative tumoral PD-L1 may comprise additional immune-centric signatures that play a role in shaping tumor responsiveness to ICI. These immune programs can be further explored to improve our understanding of how the TIME may impact responses to anti-PD-1/PD-L1-based therapies in the early-stage disease setting. It is worthwhile to mention that when we stratified each of LUADs and LUSCs based on PD-L1 expression status, we found overall higher immune cell scores and signatures in the former lung tumor type and less so in LUSCs. In addition, we found distinctively modulated immune signatures (e.g., plasma cells and macrophage subsets) between PD-L1-positive LUSCs relative to their negative counterparts and which were not prevalent in the LUAD analysis. Our findings point to immune programs that denote disparate immunopathology between LUADs and LUSCs. Interestingly, recent studies have shown that PD-L1-negative LUSCs exhibited more favorable responses to combined anti-PD-1 and -CTLA-4 treatment relative to PD-L1-negative LUADs (49, 50), emphasizing different immune biology between both major subtypes of NSCLC.

Earlier work has shown that the extent and spatial pattern (intratumoral or peritumoral) of lymphocyte infiltration impinge on host immunity and response to ICIs (51, 52). Here, we defined three different TIME phenotypes based on CD8⁺ T cells: inflamed, excluded, and cold. We found that inflamed tumors, in contrast to tumors exhibiting a cold TIME phenotype, showed upregulation for CD8 memory/effector and CD4 memory T cells as well as B cells and reduced scores for M2 macrophages, all features known to promote antitumor immune responses (53). We also found that early-stage LUADs with an inflamed phenotype exhibited elevated levels of *CXCL9* and *CXCL13* along with increased expression of genes involved in antigen presentation (e.g., *TAP1* and *TAP2*). Our findings are in close agreement with a recently reported meta-analysis which described elevated expression of *CXCL9* and *CXCL13* as predictors of response of advanced/metastatic cancers to ICI (54). Interestingly, LUADs with an excluded TIME phenotype displayed an overall intermediate “immune-state,” in line with the study by Abduljabbar

and colleagues (55), and with notably higher signature scores for M2 macrophages relative to both inflamed and cold LUADs. These data are in agreement with earlier work demonstrating immune cell exclusion by protumor macrophage subsets including tumor-associated and tissue-resident macrophages (56, 57). On that theme, a recent report that employed transcriptomic analysis for multicancer TIME classification found that tumors with lowest ratios of M1/M2 macrophage signatures exhibited poor prognosis (58). Also, another study by Herbst and colleagues similarly stratified tumors treated with anti-PD-L1 therapy into distinct TIME phenotypes and found that metastatic tumors exhibiting a cold or an excluded TIME phenotype did not respond, suggesting that preexisting immunity may be important for response (31). Conversely, other studies exploring the combination of CTLA-4 plus PD-1 blockade have shown responses independent of baseline CD8 T cells (59). Nonetheless, our study highlights heterogeneity of immune phenotypes and antitumor immunity in early-stage NSCLC.

Recent studies have shown encouraging results when interrogating the use of ICI, alone or in combination with chemotherapy, as a neoadjuvant therapeutic approach for resectable NSCLC, with MPR rates ranging from 20% to 86% (17–23, 60). Yet, as in the metastatic setting, there are very limited, if any, available biomarkers to predict response to neoadjuvant ICI (18, 43). Analysis of surgically resected NSCLCs treated with neoadjuvant ICI or chemoimmunotherapy underscored immune markers or targets that were associated with MPR (17–19). Despite these insights, a comprehensive view of immune programs that are associated with response to neoadjuvant ICI or chemoimmunotherapy is still lacking. Our gene profiling analysis demonstrated immune cell scores and programs that were associated with MPR to neoadjuvant chemoimmunotherapy. Our findings are in line with recent studies showing positive association between CD8 T cells, including memory T and antigen-experienced subsets, with ICI response (18, 19, 22, 60, 61). Also, our longitudinal profiling analysis of paired pretreatment and posttreatment samples showed increased scores for M2 macrophages postchemoimmunotherapy. While these findings may first appear counterintuitive, they are in accordance with recent independent studies by Forde and colleagues and Cascone and colleagues showing increased fractions of macrophages expressing PD-L1 (CD68⁺PD-L1⁺) following ICI (18, 19). It is intriguing to speculate whether cotargeting protumor myeloid programs may enhance response to neoadjuvant immunotherapy. Of note, a recent phase III clinical trial (CheckMate 816) showed strikingly increased MPR following neoadjuvant chemoimmunotherapy (36.8%) versus chemotherapy alone (8.6%; ref. 24). Here, our gene profiling analysis showed that NSCLCs that were treated with neoadjuvant chemoimmunotherapy displayed relatively highest signature scores for various immune cells such as CD8 and CD4 T cells as well as B-cell subsets. Our work offers a comprehensive overview of immune gene programs that may underlie response to and effects of chemoimmunotherapy in resectable NSCLC.

Our work is not without limitations. Our analysis centered on interrogating immune programs in retrospective cohorts of patients with resectable NSCLC. It is not clear how our data will compare with immune profiles in NSCLCs in the metastatic setting. Also, our findings when comparing the three cohorts should be interpreted with caution due to the small number of patients in the treated groups, differences in pathologic stage, PD-L1 expression, and disease course among the three cohorts, along with the multicenter nature of the chemoimmunotherapy cohort. Thus, our findings warrant validation in future studies that include larger cohorts. Nonetheless, given the ongoing efforts exploring ICI in early-stage NSCLC our work

provides new insights on immune programs that are disparate among early-stage NSCLCs and in the context of neoadjuvant therapy. It is noteworthy that we described TIME phenotypes based on CD8⁺ T-cell densities and it cannot be neglected that markers for other immune cells could impact these phenotypes. Nevertheless, we found that TIME phenotypes based on extent and infiltration of CD8⁺ T cells still showed robust differences in their frequencies by pathologic stage, PD-L1 expression, and TMB. Also, our study focused on immune gene profiling of different cohorts of resectable NSCLC. A paucity of adequate tissues from patients treated with chemotherapy and chemoimmunotherapy impeded a more comprehensive examination of TIME phenotypes, for instance by high-plex spatial analysis of immune cells. Future studies are warranted to perform spatial immune profiling of neoadjuvant-treated NSCLCs. Still, our targeted sequencing analysis identified immune programs that were tightly correlated with their corresponding immune cell densities (measured by protein analysis) and distinctively modulated on the basis of various immune phenotypes (e.g., PD-L1 expression).

In conclusion, using targeted gene sequencing analysis, we characterized immune programs across patients that underwent upfront surgery, neoadjuvant chemotherapy, or neoadjuvant chemoimmunotherapy. We identified immune gene programs that are unique to PD-L1-positive and PD-L1-negative NSCLCs as well as those that are shared between both groups. Spatial distribution of CD8⁺ T cells unveiled distinctive TIME phenotypes whose frequencies differed on the basis of major clinicopathologic and genomic features. Longitudinal analysis of patients following neoadjuvant chemoimmunotherapy showed strong upregulation of immune cells signatures within the TIME. Comparative analysis underscored immune programs and signatures that overall were progressively modulated along the spectrum of treatment-naïve, neoadjuvant chemotherapy-treated, up to those treated with chemoimmunotherapy—pointing to an association between perturbation of an expanded repertoire of immune gene sets with neoadjuvant chemoimmunotherapy. All in all, our study showcases immune gene signatures, programs, and phenotypes that inform of the immunopathology of localized NSCLC as well as its response to early immunotherapy.

Authors' Disclosures

A. Cruz-Bermúdez reports grants from BMS and “Instituto de Salud Carlos III” (ISCIII) during the conduct of the study. C.L. Haymaker reports grants from Lovance, Sanofi, and Dragonfly; personal fees from Nanobiotix; and other support from Briacell outside the submitted work. J.V. Heymach reports other support from AstraZeneca, Boehringer-Ingelheim, Bristol-Myers Squibb, EMD Serono, Catalyst, Genentech, GlaxoSmithKline, Hengrui Therapeutics, Eli Lilly, Spectrum, Sanofi, Takeda, Mirati Therapeutics, BrightPath Biotherapeutics, Janssen Global Services, Pneuma Respiratory, Kairos Venture investments, Leads Biolabs, RefleXion, and Chugai Pharmaceuticals outside the submitted work; in addition, J.V. Heymach has a patent for Spectrum licensed and with royalties paid. D.L. Gibbons reports grants from CPRIT and NCI during the conduct of the study; grants and personal fees from AstraZeneca, Janssen, Astellas, and Ribon Therapeutics; personal fees from Eli Lilly; and grants from Sanofi, Takeda, and NGM Therapeutics outside the submitted work. B. Sepesi reports speakers fees from AstraZeneca and Peer View consultation fees

from Bristol Myers Squibb and Medscape. T. Cascone reports personal fees and other support from MedImmune/AstraZeneca and EMD Serono; grants, personal fees, and other support from Bristol Myers Squibb; and personal fees from Merck & Co., Genentech, Arrowhead Pharmaceuticals, Society for Immunotherapy of Cancer, Roche, Medscape, and PeerView outside the submitted work. M. Provencio reports grants and personal fees from Roche and BMS, and personal fees from AstraZeneca, Takeda, and MSD outside the submitted work. I.I. Wistuba reports grants and personal fees from Genentech/Roche, Bayer, Bristol-Myers Squibb, AstraZeneca, Pfizer, HTG Molecular, Merck, Novartis, Sanofi, and Amgen; personal fees from GlaxoSmithKline, Guardant Health, Flame, Daiichi Sankyo, Oncocyte, Janssen, and MSD; and grants from Adaptive, Adaptimmune, EMD Serono, Takeda, Karus, Johnson & Johnson, Bayer, Iovance, 4D, and Akoya outside the submitted work. H. Kadara reports grants from Johnson and Johnson during the conduct of the study. No disclosures were reported by the other authors.

Authors' Contributions

P. Rocha: Conceptualization, data curation, formal analysis, validation, investigation, visualization, methodology, writing—original draft, writing—review and editing. **J. Zhang:** Conceptualization, data curation, software, formal analysis, investigation, visualization, methodology, writing—original draft, writing—review and editing. **R. Laza-Briviesca:** Data curation, investigation, writing—review and editing. **A. Cruz-Bermúdez:** Formal analysis, investigation, writing—review and editing. **N. Bota-Rabasedas:** Resources, project administration, writing—review and editing. **B. Sanchez-Espiridon:** Resources, project administration, writing—review and editing. **K. Yoshimura:** Formal analysis, investigation, writing—review and editing. **C. Behrens:** Conceptualization, investigation, writing—review and editing. **W. Lu:** Resources, validation, writing—review and editing. **X. Tang:** Resources, investigation, writing—review and editing. **A. Pataer:** Conceptualization, resources, investigation, writing—review and editing. **E.R. Parra:** Investigation, writing—review and editing. **C. Haymaker:** Conceptualization, investigation, writing—review and editing. **J. Fujimoto:** Formal analysis, writing—review and editing. **S.G. Swisher:** Resources, investigation, writing—review and editing. **J.V. Heymach:** Investigation, writing—review and editing. **D.L. Gibbons:** Conceptualization, investigation, writing—review and editing. **J. Lee:** Resources, writing—review and editing. **B. Sepesi:** Resources, writing—review and editing. **T. Cascone:** Conceptualization, investigation, writing—review and editing. **L.M. Solis:** Conceptualization, supervision, investigation, visualization, writing—review and editing. **M. Provencio:** Resources, investigation, writing—review and editing. **I.I. Wistuba:** Conceptualization, resources, supervision, funding acquisition, investigation, writing—original draft, writing—review and editing. **H. Kadara:** Conceptualization, resources, data curation, supervision, funding acquisition, validation, investigation, methodology, writing—original draft, writing—review and editing.

Acknowledgments

This work was partially supported by The University of Texas Lung Specialized Programs of Research Excellence (SPORE) grant from the NCI P50CA70907, the NCI Cancer Center Support Grant P30CA016672 (supporting the Institutional Tissue Bank), NCI Cooperative Agreement U24CA224285 (to the MDACC CIMAC), and the Cancer Prevention and Research Institute of Texas grant RP160668. P. Rocha was supported by SEOM (Sociedad Española de Oncología Médica).

The costs of publication of this article were defrayed in part by the payment of page charges. This article must therefore be hereby marked *advertisement* in accordance with 18 U.S.C. Section 1734 solely to indicate this fact.

Received September 4, 2021; revised February 12, 2022; accepted March 30, 2022; published first April 8, 2022.

References

1. Siegel RL, Miller KD, Fuchs HE, Jemal A. Cancer statistics, 2022. *CA Cancer J Clin* 2022;72:7–33.
2. Siegel RL, Miller KD, Fuchs HE, Jemal A. Cancer statistics, 2021. *CA Cancer J Clin* 2021;71:7–33.
3. National Lung Screening Trial Research Team; Church TR, Black WC, Aberle DR, Berg CD, Clingan KL, et al. Results of initial low-dose computed tomographic screening for lung cancer. *N Engl J Med* 2013; 368:1980–91.
4. Timmerman R. Stereotactic body radiation therapy for inoperable early stage lung cancer. *JAMA* 2010;303:1070–6.
5. Felip E, Altorki N, Zhou C, Csőszi T, Vynnychenko I, Goloborodko O, et al. Adjuvant atezolizumab after adjuvant chemotherapy in resected stage IB–IIIA

- non-small-cell lung cancer (IMpower010): a randomised, multicentre, open-label, phase 3 trial. *Lancet* 2021;398:1344–57.
6. Sinjab A, Han G, Treekitkammongkol W, Hara K, Brennan PM, Dang M, et al. Resolving the spatial and cellular architecture of lung adenocarcinoma by multi-region single-cell sequencing. *Cancer Discov* 2021;11:2506–23.
 7. Dejima H, Hu X, Chen R, Zhang J, Fujimoto J, Parra ER, et al. Immune evolution from preneoplasia to invasive lung adenocarcinomas and underlying molecular features. *Nat Commun* 2021;12:2722.
 8. Remark R, Lupo A, Alifano M, Biton J, Ouakrim H, Stefani A, et al. Immune contexture and histological response after neoadjuvant chemotherapy predict clinical outcome of lung cancer patients. *Oncoimmunology* 2016;5:e1255394.
 9. Munari E, Marconi M, Querzoli G, Lunardi G, Bertoglio P, Ciompi F, et al. Impact of PD-L1 and PD-1 expression on the prognostic significance of CD8+ tumor-infiltrating lymphocytes in non-small cell lung cancer. *Front Immunol* 2021;12:680973.
 10. Mascaux C, Angelova M, Vasaturo A, Beane J, Hijazi K, Anthoine G, et al. Immune evasion before tumour invasion in early lung squamous carcinogenesis. *Nature* 2019;571:570–5.
 11. Mahoney KM, Rennett PD, Freeman GJ. Combination cancer immunotherapy and new immunomodulatory targets. *Nat Rev Drug Discov* 2015;14:561–84.
 12. Gill J, Prasad V. A reality check of the accelerated approval of immune-checkpoint inhibitors. *Nat Rev Clin Oncol* 2019;16:656–8.
 13. Gettinger S, Horn L, Jackman D, Spigel D, Antonia S, Hellmann M, et al. Five-year follow-up of nivolumab in previously treated advanced non-small-cell lung cancer: results from the CA209–003 study. *J Clin Oncol* 2018;36:1675–84.
 14. Reck M, Rodriguez-Abreu D, Robinson AG, Hui R, Csösz T, Fülöp A, et al. Five-year outcomes with pembrolizumab versus chemotherapy for metastatic non-small-cell lung cancer with PD-L1 tumor proportion score \geq 50. *J Clin Oncol* 2021;39:2339–49.
 15. Doroshow DB, Bhalla S, Beasley MB, Sholl LM, Kerr KM, Gnjatich S, et al. PD-L1 as a biomarker of response to immune-checkpoint inhibitors. *Nat Rev Clin Oncol* 2021;18:345–62.
 16. Lucibello G, Mograbi B, Milano G, Hofman P, Brest P. PD-L1 regulation revisited: impact on immunotherapeutic strategies. *Trends Mol Med* 2021;27:868–81.
 17. Provencio M, Nadal E, Insa A, Garcia-Campelo MR, Casal-Rubio J, Dómine M, et al. Neoadjuvant chemotherapy and nivolumab in resectable non-small-cell lung cancer (NADIM): an open-label, multicentre, single-arm, phase 2 trial. *Lancet Oncol* 2020;21:1413–22.
 18. Cascone T, William WN, Weissferdt A, Leung CH, Lin HY, Pataer A, et al. Neoadjuvant nivolumab or nivolumab plus ipilimumab in operable non-small cell lung cancer: the phase 2 randomized NEOSTAR trial. *Nat Med* 2021;27:504–14.
 19. Forde PM, Chaft JE, Smith KN, Anagnostou V, Cottrell TR, Hellmann MD, et al. Neoadjuvant PD-1 blockade in resectable lung cancer. *N Engl J Med* 2018;378:1976–86.
 20. Shu CA, Gainer JF, Awad MM, Chiuhan C, Grigg CM, Pabani A, et al. Neoadjuvant atezolizumab and chemotherapy in patients with resectable non-small-cell lung cancer: an open-label, multicentre, single-arm, phase 2 trial. *Lancet Oncol* 2020;21:786–95.
 21. Gao S, Li N, Gao S, Xue Q, Ying J, Wang S, et al. Neoadjuvant PD-1 inhibitor (Sintilimab) in NSCLC. *J Thorac Oncol* 2020;15:816–26.
 22. Altorki NK, McGraw TE, Borczuk AC, Saxena A, Port JL, Stiles BM, et al. Neoadjuvant durvalumab with or without stereotactic body radiotherapy in patients with early-stage non-small-cell lung cancer: a single-centre, randomised phase 2 trial. *Lancet Oncol* 2021;22:824–35.
 23. Rothschild SL, Zippelius A, Eboulet EI, Savic Prince S, Betticher D, Bettini A, et al. SAKK 16/14: Durvalumab in addition to neoadjuvant chemotherapy in patients with stage IIIA(N2) non-small-cell lung cancer—a multicenter single-arm phase II trial. *J Clin Oncol* 2021;39:2872–80.
 24. Spicer J, Wang C, Tanaka F, Saylor GB, Chen K-N, Liberman M, et al. Surgical outcomes from the phase 3 CheckMate 816 trial: Nivolumab (NIVO) + platinum-doublet chemotherapy (chemo) vs chemo alone as neoadjuvant treatment for patients with resectable non-small cell lung cancer (NSCLC). *J Clin Oncol* 2021;39:8503.
 25. Versluis JM, Long GV, Blank CU. Learning from clinical trials of neoadjuvant checkpoint blockade. *Nat Med* 2020;26:475–84.
 26. Kadara H, Choi M, Zhang J, Parra ER, Rodriguez-Canales J, Gaffney SG, et al. Whole-exome sequencing and immune profiling of early-stage lung adenocarcinoma with fully annotated clinical follow-up. *Ann Oncol* 2017;28:75–82.
 27. Travis WD, Dacic S, Wistuba I, Sholl L, Adusumilli P, Bubendorf L, et al. IASLC multidisciplinary recommendations for pathologic assessment of lung cancer resection specimens after neoadjuvant therapy. *J Thorac Oncol* 2020;15:709–40.
 28. Pataer A, Kalhor N, Correa AM, Raso MG, Erasmus JJ, Kim ES, et al. Histopathologic response criteria predict survival of patients with resected lung cancer after neoadjuvant chemotherapy. *J Thorac Oncol* 2012;7:825–32.
 29. Parra ER, Behrens C, Rodriguez-Canales J, Lin H, Mino B, Blando J, et al. Image analysis-based assessment of PD-L1 and tumor-associated immune cells density supports distinct intratumoral microenvironment groups in non-small cell lung carcinoma patients. *Clin Cancer Res* 2016;22:6278–89.
 30. Tsoo MS, Kerr KM, Dacic S, Yatabe Y, Hirsch FR. IASLC Atlas of PD-L1 immunohistochemistry testing in lung cancer. *Rx Press*; 2017.
 31. Herbst RS, Soria J-C, Kowanetz M, Fine GD, Hamid O, Gordon MS, et al. Predictive correlates of response to the anti-PD-L1 antibody MPDL3280A in cancer patients. *Nature* 2014;515:563–7.
 32. Jaramillo MC, Laroche D, Ran D, Navratil M. Gene expression profiling signatures for immunophenotyping of tumor microenvironment using HTG EdgeSeq Precision Immuno-Oncology Panel. *J Clin Oncol* 2021;39:e14528.
 33. Jiang P, Gu S, Pan D, Fu J, Sahu A, Hu X, et al. Signatures of T cell dysfunction and exclusion predict cancer immunotherapy response. *Nat Med* 2018;24:1550–8.
 34. Sidders B, Zhang P, Goodwin K, O'connor G, Russell DL, Borodovsky A, et al. Adenosine signaling is prognostic for cancer outcome and has predictive utility for immunotherapeutic response. *Clin Cancer Res* 2020;26:2176–87.
 35. Ayers M, Luceford J, Nebozhyn M, Murphy E, Loboda A, Kaufman DR, et al. IFN- γ -related mRNA profile predicts clinical response to PD-1 blockade. *J Clin Invest* 2017;127:2930–40.
 36. Rooney MS, Shukla SA, Wu CJ, Getz G, Hacohen N. Molecular and genetic properties of tumors associated with local immune cytolytic activity. *Cell* 2015;160:48–61.
 37. McDermott DF, Huseni MA, Atkins MB, Motzer RJ, Rini BI, Escudier B, et al. Clinical activity and molecular correlates of response to atezolizumab alone or in combination with bevacizumab versus sunitinib in renal cell carcinoma. *Nat Med* 2018;24:749–57.
 38. Hwang S, Kwon A-Y, Jeong J-Y, Kim S, Kang H, Park J, et al. Immune gene signatures for predicting durable clinical benefit of anti-PD-1 immunotherapy in patients with non-small cell lung cancer. *Sci Rep* 2020;10:643.
 39. Kargl J, Zhu X, Zhang H, Yang GHY, Friesen TJ, Shipley M, et al. Neutrophil content predicts lymphocyte depletion and anti-PD1 treatment failure in NSCLC. *JCI Insight* 2019;4:e130850.
 40. Le X, Negrao MV, Reuben A, Federico L, Diao L, McGrail D, et al. Characterization of the immune landscape of EGFR-tumor negative NSCLC identifies CD73/Adenosine pathway as a potential therapeutic target. *J Thorac Oncol* 2021;16:583–600.
 41. Rocha P, Salazar R, Zhang J, Ledesma D, Solorzano JL, Mino B, et al. CD73 expression defines immune, molecular, and clinicopathological subgroups of lung adenocarcinoma. *Cancer Immunol Immunother* 2021;70:1965–76.
 42. Chaft JE, Rimmer A, Weder W, Azzoli CG, Kris MG, Cascone T. Evolution of systemic therapy for stages I–III non-metastatic non-small-cell lung cancer. *Nat Rev Clin Oncol* 2021;18:547–57.
 43. Grant MJ, Herbst RS, Goldberg SB. Selecting the optimal immunotherapy regimen in driver-negative metastatic NSCLC. *Nat Rev Clin Oncol* 2021;18:625–44.
 44. Tang H, Liang Y, Anders RA, Taube JM, Qiu X, Mulgaonkar A, et al. PD-L1 on host cells is essential for PD-L1 blockade-mediated tumor regression. *J Clin Invest* 2018;128:580–8.
 45. Lin H, Wei S, Hurt EM, Green MD, Zhao L, Vatan L, et al. Host expression of PD-L1 determines efficacy of PD-L1 pathway blockade-mediated tumor regression. *J Clin Invest* 2018;128:805–15.
 46. Teng MWL, Ngiew SF, Ribas A, Smyth MJ. Classifying cancers based on T-cell infiltration and PD-L1. *Cancer Res* 2015;75:2139–45.
 47. Roepman P, Jassem J, Smit EF, Muley T, Niklinski J, Van De Velde T, et al. An immune response enriched 72-gene prognostic profile for early-stage non-small-cell lung cancer. *Clin Cancer Res* 2009;15:284–90.
 48. Prat A, Navarro A, Paré L, Reguart N, Galván P, Pascual T, et al. Immune-related gene expression profiling after PD-1 blockade in non-small cell lung carcinoma, head and neck squamous cell carcinoma, and melanoma. *Cancer Res* 2017;77:3540–50.
 49. Paz-Ares LG, Ciuleanu T-E, Lee J-S, Urban L, Bernabe Caro R, Park K, et al. Nivolumab (NIVO) plus ipilimumab (IPI) versus chemotherapy (chemo) as first-line (1L) treatment for advanced non-small cell lung cancer (NSCLC): 4-year update from CheckMate 227. *J Clin Oncol* 2021;39:9016.

50. Reck M, Ciuleanu T-E, Cobo M, Schenker M, Zurawski B, Janoski De Menezes J, et al. First-line nivolumab (NIVO) plus ipilimumab (IPI) plus two cycles of chemotherapy (chemo) versus chemo alone (4 cycles) in patients with advanced non-small cell lung cancer (NSCLC): Two-year update from CheckMate 9LA. *J Clin Oncol* 2021;39:9000-.
51. Patel SS, Weirather JL, Lipschitz M, Lako A, Chen PH, Griffin GK, et al. The microenvironmental niche in classic Hodgkin lymphoma is enriched for CTLA-4-positive T cells that are PD-1-negative. *Blood* 2019;134:2059-69.
52. Lavin Y, Kobayashi S, Leader A, Amir E-AD, Elefant N, Bigenwald C, et al. Innate immune landscape in early lung adenocarcinoma by paired single-cell analyses. *Cell* 2017;169:750-65.
53. Bruni D, Angell HK, Galon J. The immune contexture and Immunoscore in cancer prognosis and therapeutic efficacy. *Nat Rev Cancer* 2020;20:662-80.
54. Litchfield K, Reading JL, Puttick C, Thakkar K, Abbosh C, Bentham R, et al. Meta-analysis of tumor- and T cell-intrinsic mechanisms of sensitization to checkpoint inhibition. *Cell* 2021;184:596-614.
55. Abduljabbar K, Raza SEA, Rosenthal R, Jamal-Hanjani M, Veeriah S, Akarca A, et al. Geospatial immune variability illuminates differential evolution of lung adenocarcinoma. *Nat Med* 2020;26:1054-62.
56. Denardo DG, Ruffell B. Macrophages as regulators of tumour immunity and immunotherapy. *Nat Rev Immunol* 2019;19:369-82.
57. Casanova-Acebes M, Dalla E, Leader AM, Leberichel J, Nikolic J, Morales BM, et al. Tissue-resident macrophages provide a pro-tumorigenic niche to early NSCLC cells. *Nature* 2021;595:578-84.
58. Bagaev A, Kotlov N, Nomie K, Svekolkin V, Gafurov A, Isaeva O, et al. Conserved pan-cancer microenvironment subtypes predict response to immunotherapy. *Cancer Cell* 2021;39:845-65.
59. van Dijk N, Gil-Jimenez A, Silina K, van Montfoort ML, Einerhand S, Jonkman L, et al. Preoperative ipilimumab plus nivolumab in locoregionally advanced urothelial cancer: the NABUCCO trial. *Nat Med* 2020;26:1839-44.
60. Lee J, Chaff J, Nicholas A, Patterson A, Waqar S, Toloza E, et al. PS01.05 surgical and clinical outcomes with neoadjuvant atezolizumab in resectable stage IB-IIIb NSCLC: LCMC3 trial primary analysis. *J Thorac Oncol* 2021; 16:S59-61.
61. Juneja VR, McGuire KA, Manguso RT, Lafleur MW, Collins N, Haining WN, et al. PD-L1 on tumor cells is sufficient for immune evasion in immunogenic tumors and inhibits CD8 T cell cytotoxicity. *J Exp Med* 2017;214: 895-904.

4.3 Pre-existing tumor host immunity characterization in resected Non-Small Cell Lung Cancer.

Pedro Rocha, Maite Rodrigo, Laura Moliner, Silvia Menendez, Nil Navarro, Laura Masfarré, Raúl Del Rey-Vergara, Miguel Galindo, Álvaro Taus, Mario Giner, Ignacio Sanchez, Lara Pijuan, Alberto Rodríguez, Rafael Aguiló, Roberto Chalela, Albert Font, Josep Belda, Victor Curull, David Casadevall, Sergi Clavé, Beatriz Bellosillo, Júlia Perera, Laura Comerma, Edurne Arriola. In preparation.

Pre-existing tumor host immunity characterization in resected Non-Small Cell Lung Cancer.

Authors: Pedro Rocha^{1,2*}, Maite Rodrigo^{3*}, Laura Moliner¹, Silvia Menendez², Nil Navarro¹, Laura Masfarré¹, Raúl Del Rey-Vergara², Miguel Galindo², Álvaro Taus¹, Mario Giner³, Ignacio Sanchez³, Lara Pijuan³, Alberto Rodríguez^{4,5,6}, Rafael Aguiló⁴, Roberto Chalela⁷, Albert Font⁷, Josep Belda⁴, Víctor Curull⁷, David Casadevall^{1,2}, Sergi Clavé³, Beatriz Bellosillo³, Júlia Perera⁸, Laura Comerma³, Edurne Arriola^{1,2#}

Affiliations:

¹Medical Oncology Department, Hospital del Mar, Barcelona, Spain

²Cancer Research Program – CIBERONC, IMIM, Hospital del Mar, Barcelona, Spain

³Pathology Department, Hospital del Mar, Barcelona, Spain

⁴Thoracic and Cardiovascular Surgery Department, Hospital del Mar, Barcelona, Spain

⁵IMIM (Instituto Hospital del Mar de Investigaciones Médicas), Barcelona, Spain

⁶Centro de Investigación en Red de Enfermedades Respiratorias (CIBERES), Instituto de Salud Carlos III (ISCIII), Barcelona, Spain

⁷Neumology Department, Hospital del Mar, Barcelona, Spain.

* These authors contributed equally: Pedro Rocha, Maite Rodrigo

Corresponding author: Edurne Arriola, Medical Oncology Department, Hospital del Mar, Cancer Research Program, IMIM, Passeig Maritim 2-9, 08003-Barcelona, Spain. Email: earriola@psmar.cat

Abstract.

Introduction: Neoadjuvant and adjuvant immune checkpoint blockade (ICB) have recently become standard of care in resectable NSCLC. Yet, biomarkers that inform patient benefit with this approach remain largely unknown. Here, we interrogated the tumor immune microenvironment (TIME) in early-stage NSCLC patients that underwent up-front surgery.

Methods: A total of 185 treatment-naïve early-stage NSCLC patients, that underwent up-front surgical treatment between 2006 and 2018 at Hospital del Mar were included. Core biopsies from the surgical specimens (124 lung adenocarcinomas (LUADs), and 61 squamous cell carcinoma (LUSCs)) were included in a tissue microarray. Immunohistochemistry for CD3, CD4, CD8, CD68, CD80, CD103, FOXP3, PD-1, PD-L1, PD-L2 and HLA class II were evaluated by digital image analysis (QuPath software). TIME was categorized into four groups using PD-L1 expression in tumor cells (<1% or ≥1%) and tumor infiltrating resident memory (CD103⁺) immune cells (using the median as cut-off): 1) PD-L1⁻/CD103⁻; 2) PD-L1⁻/CD103⁺; 3) PD-L1⁺/CD103⁻; 4) PD-L1⁺/CD103⁺. TIME characteristics and immune markers were statistically compared based on clinicopathological and molecular features and survival outcomes.

Results: We found elevated levels of T cell markers (CD3⁺, CD4⁺, CD8⁺ cells), functional immune markers (FOXP3⁺ cells) as well as, higher HLA-II tumor membrane expression in LUADs ($p < 0.05$ for all). In contrast, LUSCs displayed higher percentage of intratumor macrophages (CD68⁺ cells) as well as, higher PD-L1 and PD-L2 tumor membrane expression ($p < 0.05$ for all). PD-L1 positive (≥1%) LUADs exhibited an augmented infiltration of T cells (CD3⁺, CD4⁺, CD8⁺ cells) along with increase of FOXP3⁺ cells, resident memory cells (CD103⁺) and macrophages (CD68⁺) ($p < 0.05$ for all). Unsupervised analysis revealed three different subsets characterized by membrane tumor expression of PD-L1, PD-L2 and HLA-class II. Enrichment of T cells (CD3⁺, CD8⁺ cells), regulatory T cells (FOXP3⁺ cells) and macrophages (CD68⁺ cells) was observed in the CD103⁺/PD-L1⁺ group ($p < 0.05$ for all), while T helper cells (CD4⁺), antigen experienced immune cells (PD-1⁺) and CD80⁺ immune cells were higher in the CD103⁺/PD-L1⁻ ($p < 0.05$ for all).

Conclusions: TIME analysis in resected NSCLC highlighted differences by histology, PD-L1 expression and molecular subgroups. Biomarker studies using IHC might aid to individually tailor adjuvant treatment in early-stage NSCLC.

Introduction.

After endorsing a paradigm shift in the metastatic setting¹⁻⁴, immune checkpoint blockade (ICB) is now established as a treatment option in early-stage non-small cell lung cancer (NSCLC).

Early trials in 2018, had provided the first evidence that neoadjuvant anti-PD-1 therapy could promote major and complete pathological responses in early-stage NSCLC⁵. These results prompted the initiation of phase 2 and 3 clinical trials exploring the use of ICB in the neoadjuvant and adjuvant settings, as well as their combination with platinum-based chemotherapy⁶⁻⁹. Recently, Forde et al, reported an increase of the pathological completed responses (pCR) when combining ICB plus chemotherapy compared with chemotherapy alone as a neoadjuvant fashion. In this trial, pCR was associated with an increase on event-free survival, suggesting pCR as a surrogate marker for overall survival⁹.

In the adjuvant setting, a phase III trial (IMpower010) evaluating atezolizumab in patients with resected NSCLC (tumors ≥ 4 cm) that received cisplatin-based adjuvant chemotherapy showed a benefit on DFS for the subgroup of patients with stage II-IIIa with increased benefit in tumors expressing PD-L1. Updated analysis suggests that the benefit of adjuvant ICB could be limited to tumors with high PD-L1 expression ($\geq 50\%$), leading to prescription restrictions to this subgroup in some regions¹⁰. The benefit of adjuvant immunotherapy was later confirmed by the PEARLS/KEYNOTE-091 trial. However, in this last trial the benefit in tumors with PD-L1 higher than 50% was not significantly different compared with the control arm¹¹. In both trials, atezolizumab and pembrolizumab, respectively, improved disease-free survival but with contradictory results regarding most benefited populations, emphasizing the need to develop better biomarkers for accurate patient selection.

Likewise in the metastatic setting, no biomarkers for patient selection are available in early-stages, with a potential risk to overtreat patients and life-threatening adverse events, in a population that is potentially cured with surgery alone¹². In the next years, with a wide implementation of screening programs¹³⁻¹⁵, an increase of early-stage NSCLC diagnosis is expected^{16,17}, generating a clear need to better select patients who will benefit for perioperative treatment strategies comprising ICB. Following this line, previous work profiling tumor infiltrating lymphocytes has identify that tissue resident memory T cells, identified as lymphocytes expressing CD103, displayed features of enhanced cytotoxicity suggesting their role in promoting response to ICB¹⁸.

Here, we interrogated the tumor immune microenvironment (TIME) in early-stage NSCLC patients that underwent up-front surgery to understand the host anti-tumor immune response. We observed significant differences in the tumor immune contexture by histology, tumor PD-L1 expression and oncogenic driver mutations in lung adenocarcinomas. Unsupervised

analysis revealed three different subsets characterized by tumor expression of PD-L1, PD-L2 and HLA-class II. Finally, subgroup analysis based on the expression of tumor PD-L1, and resident memory immune cells (CD103⁺ cells) showed an enrichment of immune cell infiltrates (CD3⁺, CD4⁺, CD8⁺, CD68⁺ cells) in tumors harboring higher levels of CD103⁺ immune cells along with an increase of CD80⁺ cells, essential for T cell activation.

Material and Methods.

Patients. A cohort of 185 treatment-naïve early-stage NSCLC patients, that underwent upfront curative surgical treatment between 2006 and 2018 at Hospital del Mar, Barcelona, Spain, were included. Patients that received neoadjuvant therapy were excluded. Adjuvant chemotherapy was administered at physician discretion and following national and international guidelines. None of the patients received adjuvant immunotherapy. Mutational status of key driver genes (*EGFR*, *KRAS* and *ALK*) and *CD274* amplifications were characterized by Sanger sequencing and FISH for a subset of cases. Detailed clinicopathological information including demographics, smoking history, pathological tumor-node-metastasis stage, as well as overall and recurrence-free survival for all cases are summarized in **Table 1**. Two core biopsies (1mm diameter) for every patient sample, obtained from the surgical specimens, were included in a tissue microarray (TMA), for further analysis.

Immunohistochemistry (IHC) and Digital image analysis. IHC for CD3, CD4, CD8, CD68, CD80, CD103, PD-1, FOXP3, PD-L1, PD-L2 and HLA class II were performed following conditions previously optimized and validated at our institution **Supplementary Table 1**. Briefly, tissue sections (4µm) were stained using...

Digital image analysis, QuPath software, was used to evaluate CD3, CD4, CD8, CD68, CD80, CD103, PD-1 and FOXP3, and subsequently manual reviewed by two pathologists (MR and LC). PD-L2 and HLA class II were microscopically evaluated and reported as percentage of membrane expression. Membrane PD-L1 was evaluated by two pathologists (MR, LC) as percentage of tumor cells with positive expression based on the International Association for the Study of Lung Cancer (IASLC) guidelines¹⁹.

Tumor immune microenvironment (TIME) was categorized into four groups using PD-L1 expression in tumor cells (<1% or ≥1%) and tumor resident memory infiltrating lymphocytes based on intratumoral CD103 percentage¹⁸ (median was used as cut-off): 1) PD-L1⁻/CD103⁻, 2) PD-L1⁻/CD103⁺, 3) PD-L1⁺/CD103⁻, 4) PD-L1⁺/CD103⁺. TIME patterns and immune markers were statistically compared based on clinicopathological and molecular features and survival outcomes.

Fluorescence *In Situ* Hybridization (FISH). *CD274* gene copy number and PDL1/CEP9 ratio were evaluated by FISH using ZytoLight SPEC CD274, PDCD1LG2/CEN 9 Dual Color Probe (Zytovision, Bremerhaven, Germany). PDL1 gene amplification was defined as mean PDL1 to mean CEN9 enumeration (ratio) ≥ 2 .

Statistical analysis. To test association between continuous and categorical variables, Mann Whitney U test and Kruskal-Wallis were applied for categorical variables with two levels or more than two levels, respectively. To test association between two continuous variables, the Spearman's rank correlation test was applied. For survival analysis, we used Cox proportional-hazards model. Benjamini & Hochberg's method was used for multiple testing correction of p-values.

Results.

Tumor immune cell contexture characterization by histology, PD-L1 status and oncogenic driver mutations in early-stage NSCLC.

We evaluated immunohistochemical protein expression comprising 12 markers of 185 treatment-naïve early-stage NSCLCs **Table 1**. We first compared the tumor immune microenvironment (TIME) between lung adenocarcinomas (LUADs)(n=124) and lung squamous carcinoma (LUSCs) (n=61) **Supplementary Table 1 and 2**. We found increased levels of T cell markers (CD3⁺, CD4⁺, CD8⁺ cells), functional immune markers (FOXP3⁺ cells) as well as, higher HLA-II tumor membrane expression in LUADs (p<0.05 for all). In contrast, LUSCs displayed higher percentage of intratumor macrophages (CD68⁺ cells) as well as, higher PD-L1 and PD-L2 tumor membrane expression (p<0.05 for all) **Figure 1A**. Altogether, these results suggest a distinctive immune pathobiology between LUADs and indicate that tumor immune contexture analysis should be performed separately by histology.

Relative to PD-L1 negative (<1%), PD-L1 positive ($\geq 1\%$) LUADs exhibited an augmented infiltration of T cells (CD3⁺, CD4⁺, CD8⁺ cells) along with increase of FOXP3⁺ cells, resident memory cells (CD103⁺) and macrophages (CD68⁺) (p<0.05 for all) **Figure 1B**. In stark contrast with LUADs, we did not observe any differences by tumor PD-L1 status for all the markers analyzed in LUSCs **Supplementary Figure 2A**. Of note, PD-L1 positive LUSCs, tended to exhibit higher infiltration by resident memory cells (CD103⁺) (p=0.082)

Supplementary Figure 2A. We next sought to interrogate the TIME composition within the major molecular groups in LUADs (*KRAS* mutant, *EGFR* mutant and wild-type tumors for *KRAS* and *EGFR*). *EGFR* LUADs displayed higher percentage of tumor cells expressing membrane HLA-class II (p<0.0001), while *KRAS* tumors tended to have higher infiltration of

resident memory immune cells (CD103⁺) (p=0.0529) **Figure 1C and Supplementary Figure 3.**

Tumor membrane PD-L1, PD-L2 and HLA-class II defined tumor immune subtypes in LUADs and LUSCs.

We next performed unsupervised cluster analysis in order to identify tumor immune subsets within wild-type LUADs and LUSCs **Figure 2.** We observed that in LUADs three tumor subsets could be defined based on the membrane expression of PD-L1 and HLA class II, and the absence of these markers. PD-L1 and HLA-class II positive LUADs subgroups frequently displayed augmented infiltration levels of immune cell markers while PD-L1 and HLA class II negative tumors showed a lack of tumor immune infiltration **Figure 2A.**

On the other hand, LUSCs subgroups could be defined by the membrane expression of PD-L1 and PD-L2, with a third group characterized by the lack of these two markers **Figure 2B.** Among LUSCs subgroups, PD-L1 and PD-L2 positive tumors tended to have higher infiltration levels of immune cells.

CD103⁺ immune cells and tumor membrane PD-L1 expression define tumor immune microenvironment phenotypes.

Previous work has reported differences on antitumor immune response to anti-PD-L1 in metastatic NSCLC based on the expression of PD-L1 in tumor cells and presence of CD8 T cells by IHC²⁰. In this line, Ganesan et al, reported that CD103 expression in T lymphocytes identifies a intratumor tissue resident T cell population with an augmented expression of cytotoxicity markers¹⁸.

Therefore, we used the percentage of intratumor CD103⁺ immune cells and PD-L1 tumor expression to define tumor subgroups (CD103⁻/PD-L1⁻, CD103⁻/PD-L1⁺, CD103⁺/PD-L1⁻ and CD103⁺/PD-L1⁺) and then interrogated these for all the immune markers analyzed **Figure 3A.** We first observed that the prevalence of the four subgroups were substantially different among NSCLC histology, with CD103⁻/PD-L1⁻ representing the larger group in LUADs (42.9% of all LUADs, compared with 24.6% in LUSCs), while CD103⁺/PD-L1⁺ was the most frequent group observed in LUSCs (39.3%, compared with 24.1% in LUADs). Interestingly, CD103⁺/PD-L1⁻ and CD103⁻/PD-L1⁺ groups exhibited disparate rates among histology (27.8% Vs 6.6% and 5.2% Vs 29.5%) respectively in LUADs and LUSC **Figure 3B.**

In LUADs, analyses focused on oncogenic driver mutations showed that *EGFR* mutant tumors frequently exhibited CD103⁺/PD-L1⁻ phenotype (62.5%). *KRAS* mutant tumors displayed comparable rates for the 4 subgroups as the wild type tumors **Figure 3C.**

Analysis of the immune markers among the 4 groups revealed an enrichment of T cells (CD3⁺, CD8⁺ cells), regulatory T cells (FOXP3⁺ cells) and macrophages (CD68⁺ cells) in the CD103⁺/PD-L1⁺ group ($p < 0.05$ for all). T helper cells (CD4⁺) and antigen experienced immune cells (PD-1⁺) were higher in the CD103⁺/PD-L1⁻ ($p < 0.05$ for all). In contrast, both CD103⁻/PD-L1⁻ CD103⁺/PD-L1⁺ displayed the lower infiltration for all the immune markers, suggesting lack of activation of a proper antitumor immune response. Of note, we observed that CD103⁺ tumors exhibited higher infiltration by immune cells expressing CD80, independently of tumor PD-L1 expression **Figure 4**.

Survival outcomes in early-stage NSCLC: analysis by histology, PD-L1 status, tumor infiltrate immune cells.

Disease-free survival (DFS) and overall survival (OS) was assessed by histology, tumor membrane PD-L1 expression, tumor subgroups derived from unsupervised clustering, and based on the percentage of tumor infiltrating immune cells. Survival analysis by histology showed reduced OS for LUSCs ($p = 0.022$) compared with LUADs, while no differences were observed in DFS **Supplementary Figure 1A**. Regarding PD-L1 status, higher risk of relapse was observed in PD-L1 positive LUADs ($p = 0.041$), while no differences were observed in LUSCs or overall survival **Supplementary Figure 2B**.

We next interrogated survival differences among the unsupervised clusters within LUADs and LUSCs, with no differences observed between these groups (data not shown). Lastly, we evaluated survival differences among the four groups defined by tumor membrane PD-L1 expression and tumor infiltration by CD103⁺ immune cells. Overall, we did not find differences for DFS neither OS (data not shown). Of note, CD103⁺ tumors (using median % as cut-off) showed an improvement in OS with a HR 0.44 (0.2-0.95), $p = 0.031$.

Discussion.

While new treatment approaches in the early-stage NSCLC setting had showed survival advantages, the underlying pathobiology linked to its response to neoadjuvant and adjuvant treatments remains to be elucidated. Here we reported the use of immune markers evaluated by IHC to interrogate the tumor immune microenvironment in a richly annotated early-stage NSCLC cohort. We found marked differences between the two major histological subtypes, adenocarcinoma and squamous lung carcinoma, with LUADs exhibiting an overall augmented immune infiltrate at T cells (CD3⁺, CD4⁺, CD8⁺) and immune functional markers (FOXP3⁺ and CD103⁺) and HLA-II tumor membrane expression, while LUSCs exhibit higher rates of macrophage (CD68⁺) and tumor membrane expression of PD-L1 and PD-L2. We

further explored the use of CD103 and PD-L1 as markers that define tumor microenvironment phenotypes, revealing that CD103, a tissue resident immune marker, identified tumors with higher infiltration and characteristics that could serve as a marker of response to anti-PD-1/PD-L1 treatments to be explored in prospectively clinical trials.

LUADs and LUSCs comprise the two major histologic subtypes in NSCLC²¹. Our results point to differences in the tumor immune contexture between LUADs and LUSCs. In IMpower010, exploratory subgroup analysis by histology showed a hazard ratio (HR) of 0.8(0.54-1.18) in LUSCs histology compared with an HR of (0.78 0.61-0.99) in the LUADs, suggesting a reduced benefit in squamous tumors¹⁰. These results are in concordance with our results emphasizing a different immunopathobiology by these two histologic types, with LUSCs exhibiting lower levels of immune infiltration and suggesting a decreased benefit from anti-PD-1/PD-L1 adjuvant strategies. Interestingly, our LUSCs displayed a higher PD-L1 expression which is the marker that is currently applied for adjuvant treatment decisions. Our work shows that PD-L1 expression might have a different predictive role depending on histology. Unsupervised cluster analysis including all immune markers analyzed by IHC, unveiled that PD-L1 tumor expression characterized a subgroup of tumors in both LUADs and LUSCs, while HLA-class II and PD-L2 defined additional groups in both LUADs and LUSCs respectively. It is then plausible to hypothesize that different markers and perhaps cut-offs should be used for treatment choice in LUADs and LUSCs.

In IMpower010, atezolizumab demonstrated a benefit on DFS for the subgroup of patients with stage II-III A that was driven by PD-L1 positive tumors¹⁰. The benefit of adjuvant immunotherapy was later confirmed by the PEARLS/KEYNOTE-091 trial¹¹. However, in this last trial the benefit in tumors with PD-L1 higher than 50% was not significantly different compared with the control arm, suggesting that PD-L1 alone might not be robust enough as a biomarker to select adjuvant immunotherapy. In our analysis, intratumor immune markers analysis by tumor membrane expression of PD-L1 showed elevated immune infiltrates in PD-L1 positive tumors. These results, once again, align with previous data from randomized clinical trials reporting a higher benefit in tumors harboring high PD-L1 tumor expression, perhaps suggesting the underlying increase of intratumor immune cells that promote response to ICB. It is worthwhile to mention that our study also found, although in a smaller proportion, PD-L1 negative tumors that present similar immune infiltration rates to the PD-L1 positive tumors perhaps partially explaining why some PD-L1 negative tumors present exceptional response to ICB²³⁻²⁵.

Previous work has shown the utility of IHC markers to define the tumor microenvironment in lung cancer, and their association with ICB response. In this work, the authors classified tumor as **1)** ‘immunological ignorance’ – absence of T cells, **2)** ‘non-functional immune response’ – in cases where a lack of increase of T cells were observed after treatment with anti-PD-L1, **3)** ‘immune excluded’ – in cases that CD8 cells were observed in the tumor invasive margin but couldn’t migrate to the intratumor area after administration of ICB ²⁰. Other authors^{20,26,27}, suggested a classification based on the presence of intratumor immune cells and at the tumor invasive margin. This classification proposes three immune phenotypes: **1)** Inflamed, tumors highly infiltrated by immune cells, suggesting a presence of a preexisting immunity, **2)** Cold, tumors lacking immune infiltration and **3)** Excluded, in which immune cells are unable to migrate to the intratumor area and accumulate at the invasive margin. Deconvolution analysis of immune gene programs showed augmented levels of CD8+ memory/effector and CD4+ memory T cells as well as B cells and reduced levels scores for M2 macrophages, all features linked to better outcomes in patients treated with ICB ²⁸. In contrast, cold tumors exhibited lower levels for all immune gene programs, while the excluded phenotype displayed the highest levels of M2 macrophages, and intermediate levels for all the other immune cells ²⁷. Following similar approach, we used tumor PD-L1 expression and intratumor CD103 as markers to define TIME phenotypes. To retain T cells within the tumor, integrins are upregulated in T cell surface ^{29,30}. CD103 (*ITGAE*) is an integrin expressed in dendritic and T cells and defined these cells as tissue resident memory T cells (TRM)²⁹. Transcriptome analysis of purified intratumor T cells showed that tumors displaying enrichment for TRM cells also exhibited features linked to cytotoxicity and T cell proliferation, indicating a more pronounced anti-tumor immune response. In this same study, the authors found that higher densities of CD103⁺ cells were associated with better overall survival independently of CD8⁺ cell densities ¹⁸. Similarly, we observe that tumors with higher infiltration by CD103+ immune cells present better overall survival, compared with those with lower levels (p=0.0031, HR: 0.44 (0.2-0.95)). We next define 4 subgroups based on the tumor PD-L1 expression (<1% Vs ≥1%) and intratumor CD103⁺ cells. We found that CD103⁺/PD-L1⁺ tumors overall present higher T cells (CD3⁺, CD8⁺ cells), regulatory T cells (FOXP3⁺ cells) and macrophages (CD68⁺ cells), in concordance with previous studies reporting a robust anti-tumor immune response in CD103 high tumors. Together our results suggests that CD103⁺/PD-L1⁺ tumors present features linked to ICB benefit, by presenting higher levels of PD-L1 membrane expression and a pre-existing anti-tumor immunity. Of note, the majority of *EGFR* mutant tumors were classified as CD103⁻/PD-L1⁻, suggesting that these tumors lack the capacity to mount a robust anti-tumor immune response, in line with previous data reporting little benefit from ICB in *EGFR* tumors. It is also worthy to mention that CD103+

tumors exhibit higher levels of immune cells expressing CD80⁺ feature linked to a signaling activation of T cells in context of developing an effective immune response. It is then plausible to hypothesize that CD103 and PD-L1 could be used in combination as a predictive biomarker of response to ICB in future clinical trials.

Our study is not without limitations. We focused on the analysis by IHC of a retrospective cohort of patients with resected NSCLC. Of note, we interrogate tissue microarrays (TMAs), and that this arrays classically include relatively small tissue cores which could increase tumor and/or immune marker heterogeneity and under-representation of the tumor invasive margins – thus warranting further studies evaluating these markers in whole tissue specimens. In this context, it is also important to mention that single-plex assess of immune markers does not allow to study immune marker co-localization. Nevertheless, the use of IHC allows a world-wide and timely applicability to the clinical setting, without the need of additional equipment in most of the pathology departments. Also, our study only includes a small cohort of patients that received adjuvant chemotherapy (28%), and it is not clear if our survival analysis could be impacted by this fact.

Overall, our study provides a descriptive characterization of the tumor immune microenvironment by immunohistochemistry that highlights differences by histology, PD-L1 status and oncogenic driver mutations. Based on the tumor infiltration by CD103⁺ immune cells and PD-L1 membrane expression in tumor cells we define a subgroup of patients that exhibited immunological features linked to ICB response, warranting further interrogation of these markers in future clinical trials.

References.

1. Reck, M. *et al.* Five-Year Outcomes With Pembrolizumab Versus Chemotherapy for Metastatic Non-Small-Cell Lung Cancer With PD-L1 Tumor Proportion Score \geq 50. *J. Clin. Oncol.* **39**, 2339–2349 (2021).
2. Reck, M. *et al.* Pembrolizumab versus Chemotherapy for PD-L1-Positive Non-Small-Cell Lung Cancer. *N. Engl. J. Med.* **375**, 1823–1833 (2016).
3. Gandhi, L. *et al.* Pembrolizumab plus Chemotherapy in Metastatic Non-Small-Cell Lung Cancer. *N. Engl. J. Med.* (2018). doi:10.1056/NEJMoa1801005
4. Reck, M. *et al.* First-line nivolumab (NIVO) plus ipilimumab (IPI) plus two cycles of chemotherapy (chemo) versus chemo alone (4 cycles) in patients with advanced non-small cell lung cancer (NSCLC): Two-year update from CheckMate 9LA. *J. Clin. Oncol.* **39**, 9000–9000 (2021).
5. Forde, P. M. *et al.* Neoadjuvant PD-1 Blockade in Resectable Lung Cancer. *N. Engl. J. Med.* **378**, 1976–1986 (2018).
6. Carbone, D. *et al.* OA06.06 Clinical/Biomarker Data for Neoadjuvant Atezolizumab in Resectable Stage IB-IIIB NSCLC: Primary Analysis in the LCMC3 Study. *J. Thorac. Oncol.* **16**, S115–S116 (2021).
7. Provencio, M. *et al.* Neoadjuvant chemotherapy and nivolumab in resectable non-small-cell lung cancer (NADIM): an open-label, multicentre, single-arm, phase 2 trial. *Lancet. Oncol.* **21**, 1413–1422 (2020).
8. Cascone, T. *et al.* Neoadjuvant nivolumab or nivolumab plus ipilimumab in operable non-small cell lung cancer: the phase 2 randomized NEOSTAR trial. *Nat. Med.* **27**, 504–514 (2021).
9. Forde, P. M. *et al.* Neoadjuvant Nivolumab plus Chemotherapy in Resectable Lung Cancer. *N. Engl. J. Med.* **386**, 1973–1985 (2022).
10. Felip, E. *et al.* Adjuvant atezolizumab after adjuvant chemotherapy in resected stage IB-IIIA non-small-cell lung cancer (IMpower010): a randomised, multicentre, open-label, phase 3 trial. *Lancet (London, England)* **398**, 1344–1357 (2021).
11. Paz-Ares, L. *et al.* VP3-2022: Pembrolizumab (pembro) versus placebo for early-stage non-small cell lung cancer (NSCLC) following complete resection and adjuvant chemotherapy (chemo) when indicated: Randomized, triple-blind, phase III EORTC-1416-LCG/ETOP 8-15 – PEARLS/KEYNOTE. *Ann. Oncol.* **33**, 451–453 (2022).
12. Chansky, K. *et al.* The IASLC Lung Cancer Staging Project: External Validation of the Revision of the TNM Stage Groupings in the Eighth Edition of the TNM Classification of Lung Cancer. *J. Thorac. Oncol.* **12**, 1109–1121 (2017).
13. National Lung Screening Trial Research Team *et al.* Results of initial low-dose

- computed tomographic screening for lung cancer. *N. Engl. J. Med.* **368**, 1980–91 (2013).
14. de Koning, H. J. *et al.* Reduced Lung-Cancer Mortality with Volume CT Screening in a Randomized Trial. *N. Engl. J. Med.* **382**, 503–513 (2020).
 15. Mahadevia, P. J. *et al.* Lung cancer screening with helical computed tomography in older adult smokers: a decision and cost-effectiveness analysis. *JAMA* **289**, 313–22 (2003).
 16. Siegel, R. L., Miller, K. D., Fuchs, H. E. & Jemal, A. Cancer statistics, 2022. *CA. Cancer J. Clin.* **72**, 7–33 (2022).
 17. Sung, H. *et al.* Global Cancer Statistics 2020: GLOBOCAN Estimates of Incidence and Mortality Worldwide for 36 Cancers in 185 Countries. *CA. Cancer J. Clin.* **71**, 209–249 (2021).
 18. Ganesan, A.-P. *et al.* Tissue-resident memory features are linked to the magnitude of cytotoxic T cell responses in human lung cancer. *Nat. Immunol.* **18**, 940–950 (2017).
 19. Lantuejoul, S. *et al.* PD-L1 Testing for Lung Cancer in 2019: Perspective From the IASLC Pathology Committee. *J. Thorac. Oncol.* **15**, 499–519 (2020).
 20. Herbst, R. S. *et al.* Predictive correlates of response to the anti-PD-L1 antibody MPDL3280A in cancer patients. *Nature* **515**, 563–7 (2014).
 21. NCCN. NCCN Guidelines - Non-Small Cell Lung Cancer, . Version 3.2022. (2022).
 22. Paz-Ares, L. G. *et al.* Nivolumab (NIVO) plus ipilimumab (IPI) versus chemotherapy (chemo) as first-line (1L) treatment for advanced non-small cell lung cancer (NSCLC): 4-year update from CheckMate 227. *J. Clin. Oncol.* **39**, 9016–9016 (2021).
 23. Borghaei, H. *et al.* Nivolumab versus Docetaxel in Advanced Nonsquamous Non-Small-Cell Lung Cancer. *N. Engl. J. Med.* **373**, 1627–39 (2015).
 24. Rittmeyer, A. *et al.* Atezolizumab versus docetaxel in patients with previously treated non-small-cell lung cancer (OAK): a phase 3, open-label, multicentre randomised controlled trial. *Lancet (London, England)* **389**, 255–265 (2017).
 25. Brahmer, J. *et al.* Nivolumab versus Docetaxel in Advanced Squamous-Cell Non-Small-Cell Lung Cancer. *N. Engl. J. Med.* **373**, 123–35 (2015).
 26. Hegde, P. S. & Chen, D. S. Top 10 Challenges in Cancer Immunotherapy. *Immunity* **52**, 17–35 (2020).
 27. Rocha, P. *et al.* Distinct immune gene programs associated with host tumor immunity, neoadjuvant chemotherapy and chemoimmunotherapy in resectable NSCLC. *Clin. Cancer Res.* (2022). doi:10.1158/1078-0432.CCR-21-3207
 28. Bruni, D., Angell, H. K. & Galon, J. The immune contexture and Immunoscore in cancer prognosis and therapeutic efficacy. *Nat. Rev. Cancer* **20**, 662–680 (2020).

29. Duhén, T. *et al.* Co-expression of CD39 and CD103 identifies tumor-reactive CD8 T cells in human solid tumors. *Nat. Commun.* **9**, 2724 (2018).
30. Mueller, S. N. & Mackay, L. K. Tissue-resident memory T cells: local specialists in immune defence. *Nat. Rev. Immunol.* **16**, 79–89 (2016).

Figure 1.

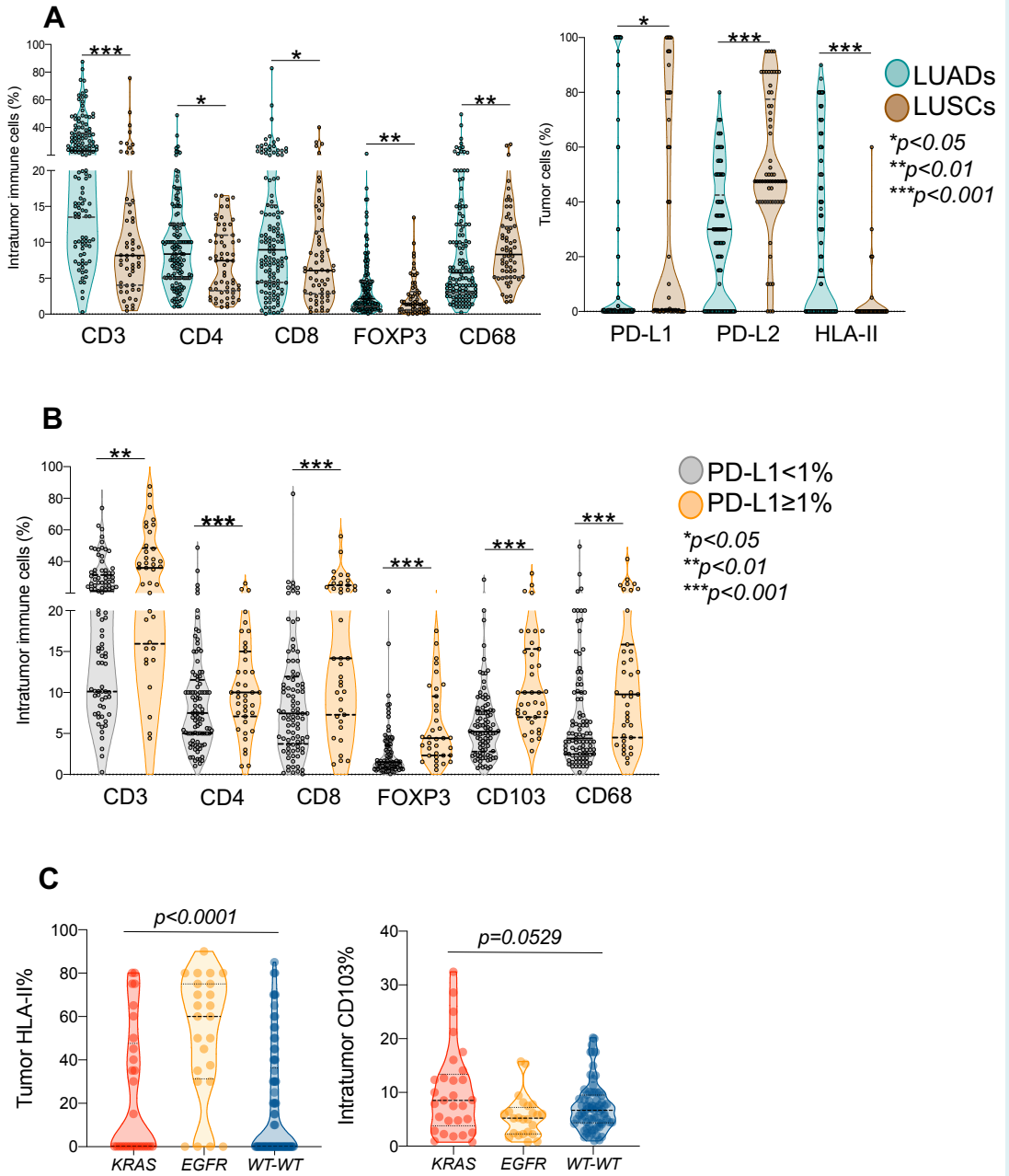


Figure 2.

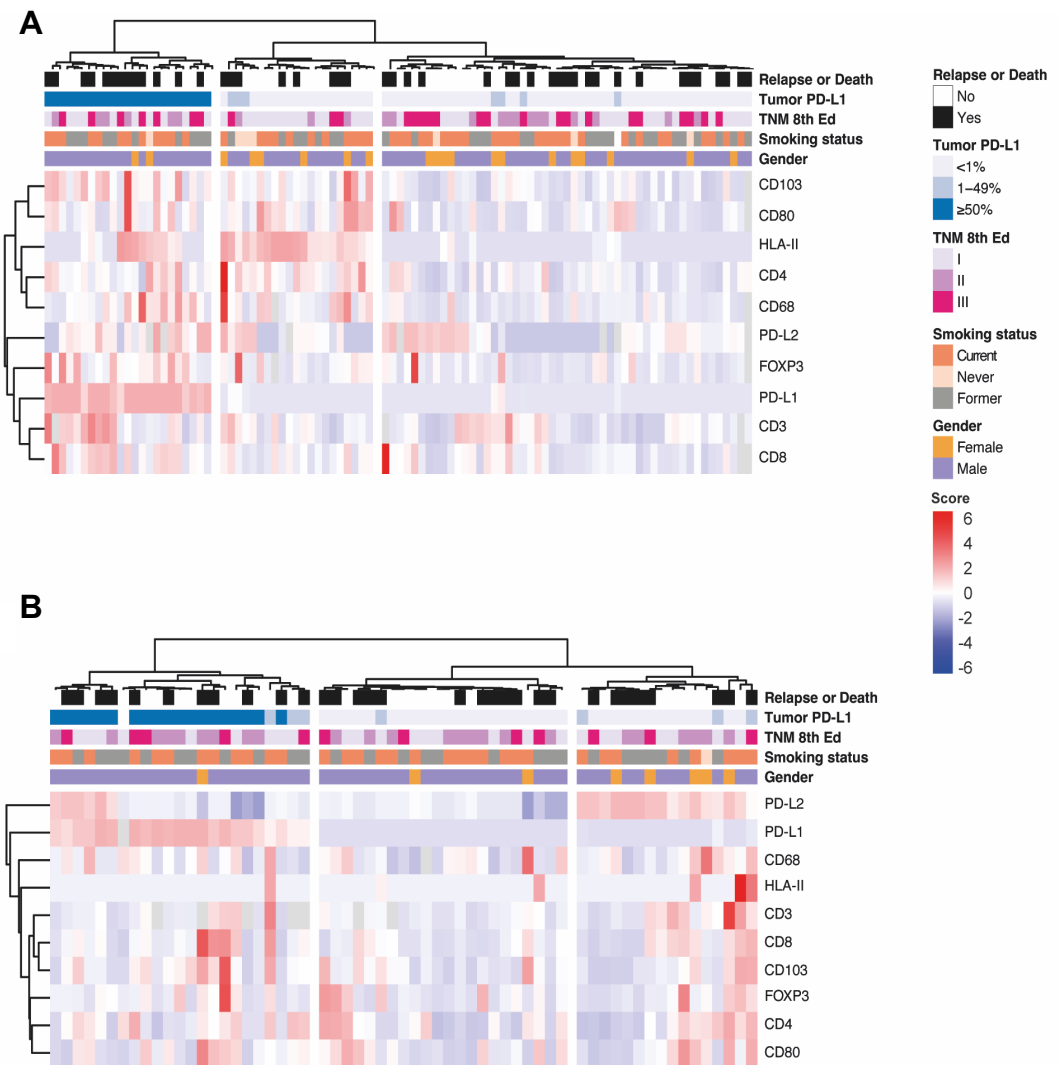
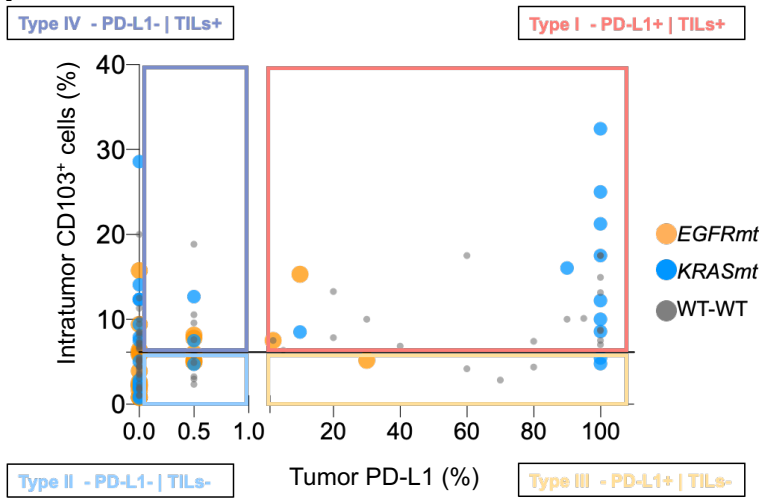
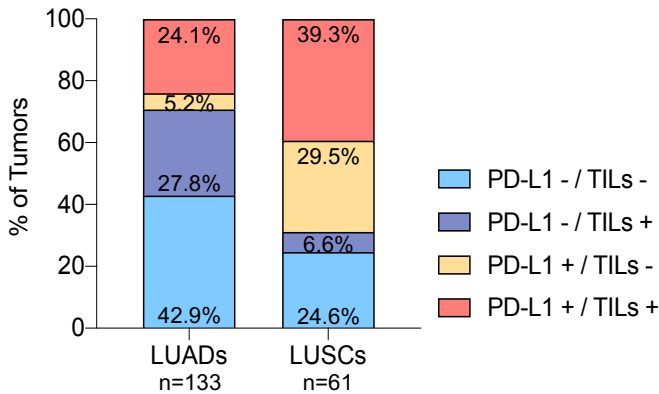


Figure 3.

A



B



C

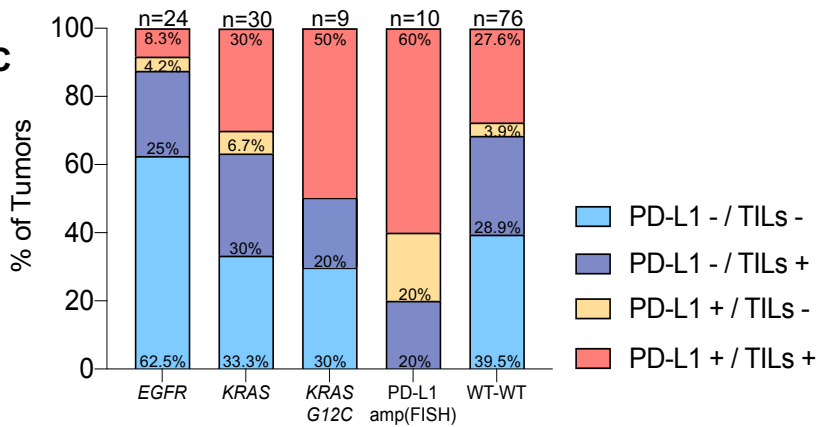
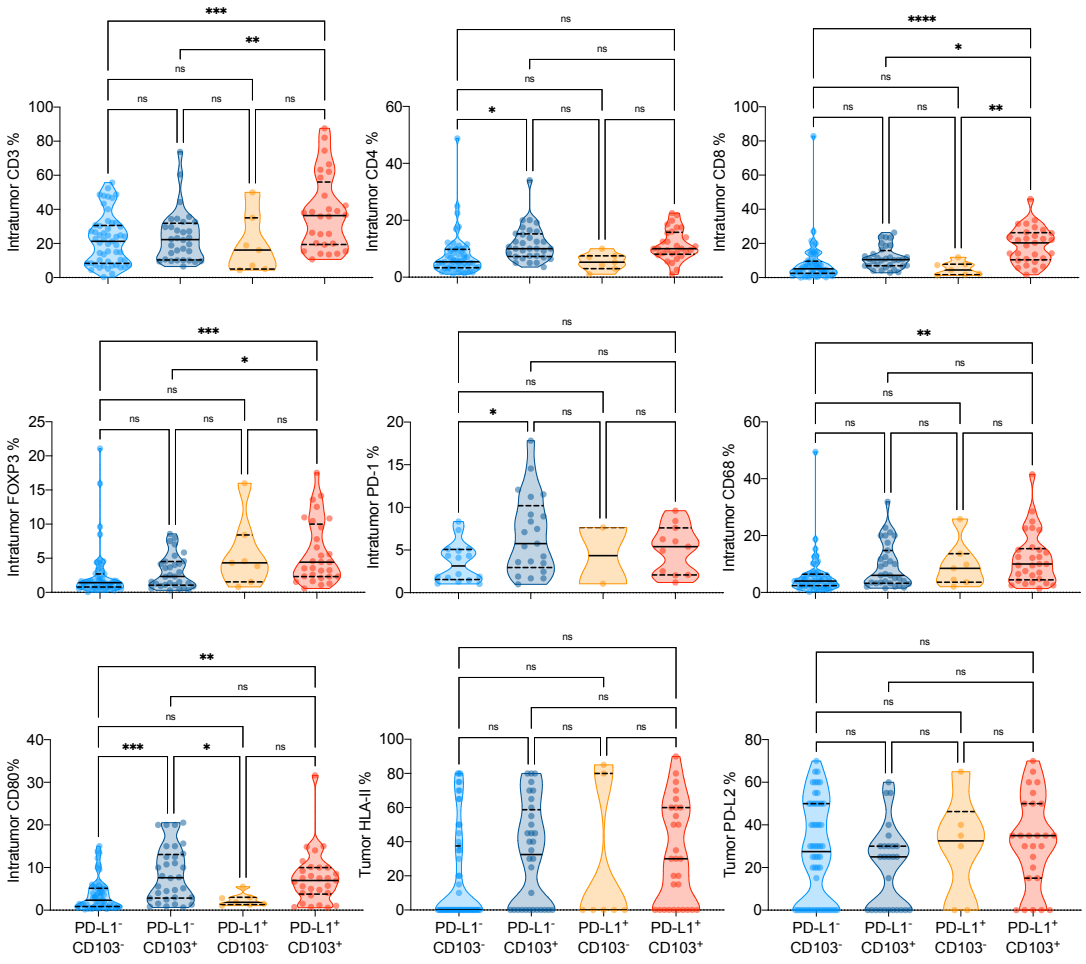


Figure 4.



- PD-L1⁻ / CD103⁻
- PD-L1⁻ / CD103⁺
- PD-L1⁺ / CD103⁻
- PD-L1⁺ / CD103⁺

* $p < 0.05$
 ** $p < 0.01$
 *** $p < 0.001$

Table 1. Demographic, clinical, pathological, and molecular characteristics of all patients included (n=185).

Characteristic (n=185)	N	%
Age - median (range)	67 (42-86)	
Sex		
Female	44	23,8%
Male	141	76,2%
Smoking status		
Never	22	11,9%
Former	76	41,1%
Current	86	46,5%
NA	1	0,5%
Histology		
Adenocarcinoma	124	67,0%
Squamous carcinoma	61	33,0%
TNM 8th Ed.		
I	87	47,0%
II	48	25,9%
III	50	27,0%
Adjuvant Chemotherapy		
Yes	53	28,7%
No	132	72,3%
Molecular features		
KRAS		
Mut	28	15,1%
WT	93	50,3%
NA	64	34,6%
EGFR		
Mut	23	12,4%
WT	94	50,8%
NA	68	36,8%
Tumor PD-L1		
<1%	123	66,5%
≥1%	61	33,0%
NA	1	0,5%
Recurrence		
Yes	57	30,8%
No	128	69,2%
Survival		
Death	74	40,0%
Alive	111	60,0%

Chapter 5

GLOBAL DISCUSSION

90

The work presented here attempts to describe and elucidate the host anti-tumor immune response as well as potential tumor mechanisms that promote tumor growth through immune system evasion with the aim to uncover immune biomarkers in early-stage lung cancer. We first interrogated the expression patterns of CD73 in tumor cells considering the pathobiology and the immune contexture of lung adenocarcinomas. We observed that CD73 was expressed in a significant fraction (75%) of LUADs and categorized subsets of LUAD with distinct histological, molecular, and immune features. We found that higher CD73 expression is associated with an overall augmented host immune response, suggesting potential implications in the immune pathobiology of early-stage lung adenocarcinoma.

In the second part of our work, we performed immunohistochemistry analysis and RNA-sequencing using an immune gene panel to interrogate immune programs in three early-stage NSCLC cohorts that underwent upfront surgery (treatment-naïve) or received neoadjuvant treatment with chemotherapy or chemoimmunotherapy. We found that the majority of treatment-naïve NSCLCs that expressed PD-L1 ($\geq 1\%$) displayed elevated immune cell scores, while PD-L1 negative ($< 1\%$) tumors tended to exhibit a more heterogeneous

immune contexture. We defined three tumor immune microenvironment (TIME) phenotypes – inflamed, cold, and excluded – in NSCLCs based on the presence and spatial distribution of CD8⁺ T cells and that showed distinct immune and inflammatory features. We then described immune gene sets that were associated with response to neoadjuvant chemotherapy or chemoimmunotherapy. Finally, comparative analysis of immune gene programs across the three cohorts showed progressive increases in various immune cell scores along the spectrum of treatment-naïve, to neoadjuvant chemotherapy–treated tumors, up to those treated with neoadjuvant chemoimmunotherapy. Overall, our results point to immune programs and phenotypes that may underlie tumor immunity and responses to neoadjuvant therapies, including chemotherapy and immune-based treatment, in resected NSCLC.

CD73 expression in lung cancer.

The adenosinergic pathway has been proposed as one of the possible mechanisms of resistance to ICI promoting immunosuppression and, hence, tumor immune evasion. Within the canonical adenosine pathway, CD73 plays a critical role as a rate-limiting enzyme in the adenosine production^{82,91,92}. These findings led to the launch of clinical trials exploring ICI combined with anti-CD73 antibodies^{84,85}. Preliminary results in locally advanced NSCLC showed an increase of response rates in the exploratory arm combining durvalumab plus oleclumab (anti-CD73 antibody) after chemo-radiotherapy and also in the neoadjuvant treatment setting. Biomarker analysis from these trials also unveiled that tumors with higher levels of CD73 (by IHC) tended to present greater responses, and a higher likelihood of achieving MPR⁸⁵. Nevertheless, it is worthy to mention that these were phase II studies with a relatively small number of patients and, although promising results were observed, conclusions regarding this combination as well as the magnitude of benefit in lung cancer patients need to be confirmed in phase III clinical trials.

The role of CD73 in the pathobiology and immune contexture of lung adenocarcinoma (LUADs) is poorly understood. To fill this void, we examined the expression patterns of CD73 in a cohort of early stage LUADs and explored their association with various features including clinicopathological, molecular, and immune covariates. In contrast to previous studies that mostly focused on total CD73 expression assessment, we interrogated CD73 in different membrane compartments (basolateral membrane and luminal membrane; BL and L, respectively) of tumor cells. Our comprehensive pathological analyses demonstrated that tumors with different CD73 expression patterns exhibited distinct clinicopathological (e.g., histological patterns) and molecular associations, possibly pointing to causal links between CD73 expression or membrane localization and tumor differentiation – as seen with other membrane proteins^{71,93}. This hypothesis is also supported by our finding on progressively increased expression of CD73 across premalignant lung lesions representing different stages in the sequence of LUAD pathogenesis (normal-appearing lung tissue → adenomatous atypical hyperplasia (AAH) → adenocarcinoma in situ (AIS) → minimally invasive adenocarcinoma (MIA) → lung adenocarcinoma). We observed that the membrane localization of CD73 in cells from well-differentiated LUADs was predominantly luminal, which may as well be related to the physiological protective and mitigating properties of CD73 against inflammation⁹⁴. Of note, we found distinct associations between not only the presence or absence of CD73 but also the extent of expression of this antigen with smoking status, molecular features, and immune infiltration, once again suggesting that patterns of expression may correlate with the underlying biology of these tumors. It is reasonable to surmise that CD73 expression and its disparate localization, may have distinct roles in the molecular pathogenesis of smoker and non-smoker LUADs. It is also plausible to suggest that CD73 membrane localization may have important implications on the effectiveness of anti-CD73 antibodies. It is important to mention that we observed that tumor BL CD73 expression positively

correlated with features of an ‘inflamed’ immune environment such as PD-L1 and immune cell infiltration, rendering the plausible supposition that CD73 immune function may be disparate between the BL and L compartments of LUAD cells. Similarly, when we analyzed immune cell densities within LUADs grouped based on CD73 positivity, the Total CD73 High (TH) group exhibited elevated PD-L1, and immune cell infiltration compared with the Total Low (TL) and Total Negative (TN) groups. Importantly, CD73 was shown to suppress anti-tumor immunity and to promote immune evasion^{71,95,96}. Thus, given our findings along with the previous reports on CD73 function, it is not unreasonable to suggest that expression of CD73 may be associated with inferior response to ICI even in tumors with concomitant high tumoral PD-L1 expression and immune cell infiltration^{94,97}. In line with our results, a previous report demonstrated that high levels of adenosine correlated with elevated infiltration of immune cells, but with a decreased response to anti-PD1 across various tumor types⁸³. It is intriguing to infer that targeting CD73 may enhance anti-tumor immunity, particularly in tumors with high levels of CD73, as well as augment the effect of ICI. Indeed, targeting CD73 was shown to skew the immune TME to a more anti-tumor phenotype in preclinical models^{76,98}. In a separate context, our findings also suggest that targeting CD73 may promote anti-tumor immunity in LUADs with low yet positive CD73, and which we found to exhibit a relatively ‘cold’ immune contexture. Of note, we found that a fraction of LUADs that were CD73 negative displayed abundant expression of CD38 concomitant with a muted host immune response, suggesting redundant activation of the non-canonical adenosine pathway⁸⁸ in these tumors and their potential tractability by agents that target this pathway such as anti-CD38 antibodies.

Tumor microenvironment immune phenotypes.

Immune phenotypes underlying the pathobiology of NSCLC, including its response to neoadjuvant therapy, remain poorly understood. Our study points to

immune programs and phenotypes that may underlie anti-tumor immunity and responses to neoadjuvant therapies, including chemotherapy and immune-based treatment, in resected NSCLC.

Several clinical trials have demonstrated that tumoral and immune cell PD-L1 expression are associated with increased likelihood of response to antibodies against PD-1 or PD-L1 in metastatic NSCLC^{99–102}. Our analysis focused on early-stage NSCLCs, and consistent with previous reports^{103,104}, found that PD-L1 positive LUADs displayed overall augmented immune gene scores and programs compared with PD-L1 negative LUADs, findings then confirmed by IHC in a second cohort. Interestingly, we found in two separated cohorts (MDAnderson Cancer Center cohort, and Hospital del Mar cohort) that a subset of PD-L1 negative LUADs displayed relatively high levels of immune cell scores comparable to PD-L1 positive tumors, that could perhaps partially explain why some PD-L1 negative tumors present exceptional responses to immune checkpoint inhibitors (ICI), and why PD-L1 expression is considered an imperfect biomarker to predict treatment response with ICI. Our findings set the stage for a reasonable supposition that patients with early-stage NSCLC with negative tumoral PD-L1 may comprise additional immune-centric signatures that play a role in shaping tumor responsiveness to ICI. These immune programs can be further explored to improve our understanding of how the TIME may impact responses to anti-PD-1/PD-L1–based therapies in the early-stage disease setting. When we stratified each of LUADs and LUSCs based on PD-L1 expression status, we found overall higher immune cell scores and signatures in the former lung tumor type and less so in LUSCs. In addition, we found distinct modulated immune signatures (e.g., plasma cells and macrophage subsets) between PD-L1–positive LUSCs relative to their negative counterparts and which were not prevalent in the LUAD analysis. Our findings point to immune programs that denote disparate immunopathology between LUADs and LUSCs. Interestingly,

exploratory analysis from CheckMate 227 and CheckMate 9LA have shown that PD-L1 negative LUSCs tend to present higher response rates to anti-PD-1 plus CTLA-4 treatment relative to PD-L1 negative LUADs, supporting different immune biology between both major histologic subtypes in NSCLC^{17,18}.

Previous work has shown that the extent and spatial localization (intra-tumoral or peritumoral) of lymphocyte infiltration impact on host immunity and response to ICIs^{67,105,106}. Here, we defined three different TIME phenotypes based on CD8⁺ T cells spatial distribution: inflamed, excluded, and cold. We found that inflamed tumors, in contrast to tumors exhibiting a cold TIME phenotype, showed upregulation for CD8 memory/effector and CD4 memory T cells as well as B cells and reduced scores for M2 macrophages, all features known to promote antitumor immune responses¹⁰⁷. We also found that early-stage LUADs with an inflamed phenotype exhibited elevated levels of *CXCL9* and *CXCL13* along with increased expression of genes involved in antigen presentation (e.g., *TAP1* and *TAP2*). Our findings are in close agreement with a recently reported meta-analysis which described elevated expression of *CXCL9* and *CXCL13* as predictors of response of advanced/metastatic cancers to ICI¹⁰⁸. Interestingly, LUADs with an excluded TIME phenotype displayed an overall intermediate “immune-state,” in line with the study by AbdulJabbar and colleagues¹⁰⁹, and with notably higher signature scores for M2 macrophages relative to both inflamed and cold LUADs. These findings are in agreement with earlier work demonstrating immune cell exclusion promoted by protumor macrophage subsets, including tumor-associated and tissue-resident macrophages¹¹⁰. On that theme, a recent report that employed transcriptomic analysis for multicancer TIME classification found that tumors with lower ratios of M1/M2 macrophage signatures exhibited poor prognosis when treated with ICI¹¹¹. Another study by Herbst and colleagues similarly stratified tumors treated with anti-PD-L1 therapy into distinct TIME phenotypes and found that metastatic tumors exhibiting a cold or an excluded TIME phenotype did

not respond to atezolizumab monotherapy, overall suggesting that preexisting immunity may be critical to respond to ICI⁷⁰. Conversely, other studies exploring the combination of anti-PD-1 plus CTLA-4 blockade have shown responses independent of baseline CD8 T cells¹¹².

Previous studies showed the potential role of intratumor CD103 expression in immune cells as a marker to identify tumors with an augmented anti-tumor response⁴⁹. In line with previous studies defining TIME based on PD-L1 expression and CD8 T cell infiltration⁷⁰, here we define four TIME phenotypes based on the tumor PD-L1 expression (<1% Vs ≥1%) and intratumor CD103⁺ cells, due to its role previously described as a tissue resident marker associated features of enhanced cytotoxicity and proliferation of immune cells⁴⁹. We found that CD103⁺/PD-L1⁺ tumors overall present higher T cells (CD3⁺, CD8⁺ cells), regulatory T cells (FOXP3⁺ cells) and macrophages (CD68⁺ cells), in concordance with previous studies reporting a robust anti-tumor immune response in CD103 high tumors. Together our results suggest that CD103⁺/PD-L1⁺ tumors present features linked to ICI benefit, by presenting higher levels of PD-L1 membrane expression and a pre-existing anti-tumor immunity. Of note, the majority of EGFR mutant tumors were classified as CD103⁻/PD-L1⁻, suggesting that these tumors lack the capacity to mount a robust anti-tumor immune response, in line with previous data reporting no benefit from ICI in EGFR tumors. It is also worthy to mention that CD103⁺ tumors exhibit higher levels of immune cells expressing CD80⁺, a feature linked to activation of T cells in context of developing an effective immune response. It is then plausible to hypothesize that CD103 and PD-L1 could be used in combination as a predictive biomarker of response to ICI in future clinical trials.

Recent studies have shown encouraging results when interrogating the use of ICI, alone or in combination with chemotherapy, as a neoadjuvant therapeutic

approach for resectable NSCLC, with MPR rates ranging from 20% to 86%^{12,22-24,45,85,113-115}. Yet, as in the metastatic setting, there are very limited, if any, available biomarkers to predict response to neoadjuvant ICI¹⁰⁰. Analysis of surgically resected specimens treated with neoadjuvant ICI or chemoimmunotherapy identified different immune markers or targets that were associated with MPR^{23,24,45}. Despite these insights, a comprehensive view of immune programs that are associated with response to neoadjuvant ICI or chemoimmunotherapy is still lacking. Our gene profiling analysis demonstrated immune cell scores and programs that were associated with MPR to neoadjuvant chemoimmunotherapy. Our findings are in line with recent studies showing positive association between CD8⁺ T cells, including memory T and antigen-experienced subsets, with ICI response^{23,45,113}. Also, our longitudinal profiling analysis of paired pre- and post-treatment samples showed increased scores for M2 macrophages post-chemoimmunotherapy. While these findings may first appear counterintuitive, they are in accordance with recent independent studies by Forde and colleagues and Cascone and colleagues showing increased fractions of macrophages expressing PD-L1 (CD68⁺PD-L1⁺) following ICI^{23,45}. It is intriguing to speculate whether co-targeting protumor myeloid programs may enhance response to neoadjuvant immunotherapy.

A recent phase III clinical trial (CheckMate 816) showed strikingly increased MPR following neoadjuvant chemoimmunotherapy (36.8%) versus chemotherapy alone (8.6%)¹². In this context, our gene profiling analysis showed that NSCLCs treated with neoadjuvant chemoimmunotherapy displayed relatively higher signature scores for various immune cells such as CD8 and CD4 T cells, as well as B-cell subsets. Overall offering a comprehensive overview of immune gene programs that may underlie response to and effects of chemoimmunotherapy in early-stage NSCLC.

Our study is not without limitations. It is important to mention that IHC CD73 expression was evaluated in tissue microarrays of LUAD, with these arrays typically harboring relatively small tissue cores which may bring about increased tumor and, thus, immune marker heterogeneity and under-representation of luminal structures of adenocarcinomas – thus warranting future studies probing CD73 in whole tissue specimens. It is also noteworthy, given our study design and goals, that our cohort was primarily composed of resected early-stage tumors with, thus, under-representation of relatively more advanced (e.g., metastatic) LUADs. In this context, our study is unable to ascertain relative patterns of CD73 expression (and localization), along with features of host anti-tumor immunity and immune evasion, between early-stage and more advanced LUADs. Since mechanisms of host immune evasion by the tumor, along with genomic and mutational complexity, are expectantly more pronounced in advanced-stage tumors, future studies are warranted to fully probe CD73 and other members of the adenosine pathway along the continuum of different stages (e.g., early, local/ oligometastatic to distant metastatic) in LUAD. Additionally, future studies warrant further evaluation of mechanisms involving CD73 expression and its interaction with host immune responses in LUAD. Also, our findings when comparing the three cohorts (treatment-naïve, neoadjuvant chemo and neoadjuvant chemoimmunotherapy) should be interpreted with caution due to the small number of patients in the treated groups, differences in pathologic stage, PD-L1 expression, and disease course among the three cohorts, along with the multicenter nature of the chemoimmunotherapy cohort. These findings warrant validation in future studies that include larger cohorts. Notably, we described TIME phenotypes based on CD8⁺ T cell densities and it cannot be neglected that markers for other immune cells could impact these phenotypes. Nevertheless, we found that TIME phenotypes based on extent and infiltration of CD8⁺ T cells still showed robust differences in their frequencies by pathologic stage, PD-L1 expression, and TMB. Also, our study focused on immune gene profiling

of different cohorts of resected NSCLC. A paucity of adequate tissues from patients treated with chemotherapy and chemoimmunotherapy impeded a more comprehensive examination of TIME phenotypes, for instance by high-plex spatial analysis of immune cells. Future studies are warranted to perform spatial immune profiling of neoadjuvant-treated NSCLCs. Nonetheless, our study provides new and comprehensive information into diverse patterns of CD73 expression and localization, in association with genomic, immune, and clinical features, in early stage LUAD, thus offering a roadmap in the future to interrogate the role of CD73 expression in immunotherapy and/or response to ICI. Additionally, and given the ongoing efforts exploring ICI in early-stage NSCLC our work provides new insights on immune programs that are disparate among early-stage NSCLCs and in the context of neoadjuvant therapy.

In conclusion, our study points to the potential role of CD73, and other members of the adenosine signaling pathway, as potential mechanisms of tumor immune evasion and resistance to ICI, thus providing additional rationale for propagating anti-CD73 antibodies in new combinatorial immunotherapeutic regimens. As mentioned before, we found that differential (e.g., BL vs. L) CD73 localization was associated with distinct clinicopathological and molecular features in LUAD. It is intriguing to propose that in-depth assessment of CD73 expression along with its membrane localization will provide comprehensive assessment of patients who may benefit from agents targeting this immune marker. Additionally, and using targeted gene sequencing analysis, we characterized immune programs across patients that underwent upfront surgery, neoadjuvant chemotherapy, or neoadjuvant chemoimmunotherapy. We identified immune gene programs that are unique to PD-L1 positive and PD-L1 negative NSCLCs as well as those that are shared between both groups. Spatial distribution of CD8⁺ T cells, PD-L1 expression and CD103⁺ immune cells unveiled distinctive TIME phenotypes whose frequencies differed on the basis of major

clinicopathologic and genomic features. Longitudinal analysis of patients following neoadjuvant chemoimmunotherapy showed strong upregulation of immune cells signatures within the TIME. Comparative analysis underscored immune programs and signatures that overall were progressively modulated along the spectrum of treatment-naïve, neoadjuvant chemotherapy-treated, up to those treated with chemoimmunotherapy, pointing to an association between perturbation of an expanded repertoire of immune gene sets with neoadjuvant chemoimmunotherapy. All in all, our study showcases immune gene signatures, programs, and phenotypes that inform the immunopathology of localized NSCLC as well as its response to early immunotherapy.

Chapter 6

CONCLUSIONS

1. CD73 is expressed in 75% of lung adenocarcinomas and defines subgroups with disparate clinicopathological and immune features.
2. High expression of CD73 positively correlates with PD-L1 expression in tumor cells and immune cell infiltration.
3. CD73 expression associates with genomic features (*TP53* and *STK11*) and somatic mutation burden.
4. CD73 expression is associated with other markers (CD38) involved in the non-canonical pathway promoting adenosine generation.
5. Lung adenocarcinomas, PD-L1 positive, and *EGFR* wild-type tumors displayed elevated immune expression programs in treatment-naïve NSCLC.
6. CD8 T cell densities and spatial distribution define tumor immune microenvironment phenotypes – inflamed, cold, and excluded – with distinct gene expression programs.
7. Immune genes linked to innate immune response and B-cell biology positively associated with pathologic response after neoadjuvant chemotherapy.
8. Chemoimmunotherapy elicits pronounced immune-wide expression changes in resectable NSCLC across T, B, and myeloid cells.

Chapter 7

REFERENCES

1. Siegel, R. L., Miller, K. D., Fuchs, H. E. & Jemal, A. Cancer statistics, 2022. *CA. Cancer J. Clin.* 72, 7–33 (2022).
2. SEOM. Las cifras del cáncer en España - 2022.
3. Sung, H. et al. Global Cancer Statistics 2020: GLOBOCAN Estimates of Incidence and Mortality Worldwide for 36 Cancers in 185 Countries. *CA. Cancer J. Clin.* 71, 209–249 (2021).
4. de Koning, H. J. et al. Reduced Lung-Cancer Mortality with Volume CT Screening in a Randomized Trial. *N. Engl. J. Med.* 382, 503–513 (2020).
5. National Lung Screening Trial Research Team. Lung Cancer Incidence and Mortality with Extended Follow-up in the National Lung Screening Trial. *J. Thorac. Oncol.* 14, 1732–1742 (2019).
6. IASLC. IASLC Statement on the Updated United States Preventive Task Force Guidelines on Lung Cancer Screening. (2021). Available at: <https://www.iaslc.org/iaslc-news/press-release/iaslc-statement-updated-united-states-preventive-task-force-guidelines>.
7. Rami-Porta, R., Asamura, H., Travis, W. D. & Rusch, V. W. Lung cancer - major changes in the American Joint Committee on Cancer eighth edition cancer staging manual. *CA. Cancer J. Clin.* 67, 138–155 (2017).
8. Pignon, J.-P. et al. Lung adjuvant cisplatin evaluation: a pooled analysis by the LACE Collaborative Group. *J. Clin. Oncol.* 26, 3552–9 (2008).

9. Strauss, G. M. et al. Adjuvant paclitaxel plus carboplatin compared with observation in stage IB non-small-cell lung cancer: CALGB 9633 with the Cancer and Leukemia Group B, Radiation Therapy Oncology Group, and North Central Cancer Treatment Group Study Groups. *J. Clin. Oncol.* 26, 5043–51 (2008).
10. NSCLC Meta-analysis Collaborative Group. Preoperative chemotherapy for non-small-cell lung cancer: a systematic review and meta-analysis of individual participant data. *Lancet (London, England)* 383, 1561–71 (2014).
11. Felip, E. et al. Adjuvant atezolizumab after adjuvant chemotherapy in resected stage IB-IIIa non-small-cell lung cancer (IMpower010): a randomised, multicentre, open-label, phase 3 trial. *Lancet (London, England)* 398, 1344–1357 (2021).
12. Forde, P. M. et al. Neoadjuvant Nivolumab plus Chemotherapy in Resectable Lung Cancer. *N. Engl. J. Med.* 386, 1973–1985 (2022).
13. Zhong, W.-Z. et al. Gefitinib Versus Vinorelbine Plus Cisplatin as Adjuvant Treatment for Stage II-IIIa (N1-N2) EGFR-Mutant NSCLC: Final Overall Survival Analysis of CTONG1104 Phase III Trial. *J. Clin. Oncol.* 39, 713–722 (2021).
14. Wu, Y.-L. et al. Osimertinib in Resected EGFR-Mutated Non-Small-Cell Lung Cancer. *N. Engl. J. Med.* 383, 1711–1723 (2020).
15. Govindan, R. et al. ALCHEMIST Trials: A Golden Opportunity to Transform Outcomes in Early-Stage Non-Small Cell Lung Cancer. *Clin. Cancer Res.* 21, 5439–44 (2015).
16. Reck, M. et al. Pembrolizumab versus Chemotherapy for PD-L1-Positive Non-Small-Cell Lung Cancer. *N. Engl. J. Med.* 375, 1823–1833 (2016).
17. Reck, M. et al. First-line nivolumab (NIVO) plus ipilimumab (IPI) plus two cycles of chemotherapy (chemo) versus chemo alone (4 cycles) in patients with advanced non-small cell lung cancer (NSCLC): Two-year update from CheckMate 9LA. *J. Clin. Oncol.* 39, 9000–9000 (2021).
18. Paz-Ares, L. G. et al. Nivolumab (NIVO) plus ipilimumab (IPI) versus chemotherapy (chemo) as first-line (1L) treatment for advanced non-small cell lung cancer (NSCLC): 4-year update from CheckMate 227. *J. Clin. Oncol.* 39, 9016–9016 (2021).

19. Paz-Ares, L. et al. Pembrolizumab plus Chemotherapy for Squamous Non–Small-Cell Lung Cancer. *N. Engl. J. Med.* NEJMoa1810865 (2018). doi:10.1056/NEJMoa1810865
20. Paz-Ares, L. et al. VP3-2022: Pembrolizumab (pembro) versus placebo for early-stage non-small cell lung cancer (NSCLC) following complete resection and adjuvant chemotherapy (chemo) when indicated: Randomized, triple-blind, phase III EORTC-1416-LCG/ETOP 8-15 – PEARLS/KEYNOTE. *Ann. Oncol.* 33, 451–453 (2022).
21. Forde, P. M. et al. Neoadjuvant PD-1 Blockade in Resectable Lung Cancer. *N. Engl. J. Med.* (2018). doi:10.1056/NEJMoa1716078
22. Reuss, J. E. et al. Neoadjuvant nivolumab plus ipilimumab in resectable non-small cell lung cancer. *J. Immunother. Cancer* 8, e001282 (2020).
23. Cascone, T. et al. Neoadjuvant nivolumab or nivolumab plus ipilimumab in operable non-small cell lung cancer: the phase 2 randomized NEOSTAR trial. *Nat. Med.* 27, 504–514 (2021).
24. Provencio, M. et al. Neoadjuvant chemotherapy and nivolumab in resectable non-small-cell lung cancer (NADIM): an open-label, multicentre, single-arm, phase 2 trial. *Lancet. Oncol.* 21, 1413–1422 (2020).
25. Shu, C. A. et al. Neoadjuvant atezolizumab and chemotherapy in patients with resectable non-small-cell lung cancer: an open-label, multicentre, single-arm, phase 2 trial. *Lancet Oncol.* 21, 786–795 (2020).
26. Lee, J. et al. PS01.05 Surgical and Clinical Outcomes With Neoadjuvant Atezolizumab in Resectable Stage IB–IIIB NSCLC: LCMC3 Trial Primary Analysis. *J. Thorac. Oncol.* 16, S59–S61 (2021).
27. Kwiatkowski, D. J. et al. Neoadjuvant atezolizumab in resectable non-small cell lung cancer (NSCLC): Interim analysis and biomarker data from a multicenter study (LCMC3). *J. Clin. Oncol.* 37, 8503 (2019).
28. Provencio-Pulla, M. et al. Nivolumab + chemotherapy versus chemotherapy as neoadjuvant treatment for resectable stage IIIA NSCLC: Primary endpoint results of pathological complete response (pCR) from phase II NADIM II trial. *J. Clin. Oncol.* 40, 8501–8501 (2022).

29. Cogdill, A. P., Andrews, M. C. & Wargo, J. A. Hallmarks of response to immune checkpoint blockade. *Br. J. Cancer* 117, 1–7 (2017).
30. Chafft, J. E. et al. Evolution of systemic therapy for stages I–III non-metastatic non-small-cell lung cancer. *Nat. Rev. Clin. Oncol.* (2021). doi:10.1038/s41571-021-00501-4
31. Cottrell, T. R. et al. Pathologic features of response to neoadjuvant anti-PD-1 in resected non-small-cell lung carcinoma: a proposal for quantitative immune-related pathologic response criteria (irPRC). *Ann. Oncol.* 29, 1853–1860 (2018).
32. Liu, J. et al. Improved efficacy of neoadjuvant compared to adjuvant immunotherapy to eradicate metastatic disease. *Cancer Discov.* 6, 1382–1399 (2016).
33. Junker, K., Langner, K., Klinke, F., Bosse, U. & Thomas, M. Grading of tumor regression in non-small cell lung cancer : morphology and prognosis. *Chest* 120, 1584–91 (2001).
34. Betticher, D. C. et al. Mediastinal lymph node clearance after docetaxel-cisplatin neoadjuvant chemotherapy is prognostic of survival in patients with stage IIIA pN2 non-small-cell lung cancer: a multicenter phase II trial. *J. Clin. Oncol.* 21, 1752–9 (2003).
35. Hellmann, M. D. et al. Pathological response after neoadjuvant chemotherapy in resectable non-small-cell lung cancers: proposal for the use of major pathological response as a surrogate endpoint. *Lancet. Oncol.* 15, e42-50 (2014).
36. Pataer, A. et al. Histopathologic response criteria predict survival of patients with resected lung cancer after neoadjuvant chemotherapy. *J. Thorac. Oncol.* 7, 825–32 (2012).
37. Cortazar, P. et al. Pathological complete response and long-term clinical benefit in breast cancer: the CTNeoBC pooled analysis. *Lancet (London, England)* 384, 164–72 (2014).
38. Travis, W. D. et al. IASLC Multidisciplinary Recommendations for Pathologic Assessment of Lung Cancer Resection Specimens After Neoadjuvant Therapy. *J. Thorac. Oncol.* 15, 709–740 (2020).

39. Qu, Y. et al. Pathologic Assessment After Neoadjuvant Chemotherapy for NSCLC: Importance and Implications of Distinguishing Adenocarcinoma From Squamous Cell Carcinoma. *J. Thorac. Oncol.* 14, 482–493 (2019).
40. Chaft, J. E. et al. Phase II trial of neoadjuvant bevacizumab plus chemotherapy and adjuvant bevacizumab in patients with resectable nonsquamous non-small-cell lung cancers. *J. Thorac. Oncol.* 8, 1084–90 (2013).
41. Provencio-Pulla, M. et al. Neoadjuvant nivolumab (NIVO) + platinum-doublet chemotherapy (chemo) versus chemo for resectable (IB–IIIA) non-small cell lung cancer (NSCLC): Association of pathological regression with event-free survival (EFS) in CheckMate 816. *J. Clin. Oncol.* 40, LBA8511–LBA8511 (2022).
42. Rimm, D. L. et al. A Prospective, Multi-institutional, Pathologist-Based Assessment of 4 Immunohistochemistry Assays for PD-L1 Expression in Non–Small Cell Lung Cancer. *JAMA Oncol.* 3, 1051 (2017).
43. Mok, T. S. K. et al. Pembrolizumab versus chemotherapy for previously untreated, PD-L1-expressing, locally advanced or metastatic non-small-cell lung cancer (KEYNOTE-042): a randomised, open-label, controlled, phase 3 trial. *Lancet* 393, 1819–1830 (2019).
44. Doroshov, D. B. et al. PD-L1 as a biomarker of response to immune-checkpoint inhibitors. *Nat. Rev. Clin. Oncol.* 18, 345–362 (2021).
45. Forde, P. M. et al. Neoadjuvant PD-1 Blockade in Resectable Lung Cancer. *N. Engl. J. Med.* 378, 1976–1986 (2018).
46. Carbone, D. et al. OA06.06 Clinical/Biomarker Data for Neoadjuvant Atezolizumab in Resectable Stage IB–IIIB NSCLC: Primary Analysis in the LCMC3 Study. *J. Thorac. Oncol.* 16, S115–S116 (2021).
47. Rojas, F., Parra, E. R., Wistuba, I. I., Haymaker, C. & Solis Soto, L. M. Pathological Response and Immune Biomarker Assessment in Non-Small-Cell Lung Carcinoma Receiving Neoadjuvant Immune Checkpoint Inhibitors. *Cancers (Basel)*. 14, 2775 (2022).
48. Binnewies, M. et al. Understanding the tumor immune microenvironment (TIME) for effective therapy. *Nat. Med.* 24, 541–550 (2018).

49. Ganesan, A.-P. et al. Tissue-resident memory features are linked to the magnitude of cytotoxic T cell responses in human lung cancer. *Nat. Immunol.* 18, 940–950 (2017).
50. Forde, P. M. et al. Neoadjuvant PD-1 Blockade in Resectable Lung Cancer. *N. Engl. J. Med.* 378, 1976–1986 (2018).
51. Helmink, B. A. et al. B cells and tertiary lymphoid structures promote immunotherapy response. *Nature* 577, 549–555 (2020).
52. Cabrita, R. et al. Tertiary lymphoid structures improve immunotherapy and survival in melanoma. *Nature* 577, 561–565 (2020).
53. Ruffin, A. T. et al. B cell signatures and tertiary lymphoid structures contribute to outcome in head and neck squamous cell carcinoma. *Nat. Commun.* 12, 3349 (2021).
54. Vanhersecke, L. et al. Mature tertiary lymphoid structures predict immune checkpoint inhibitor efficacy in solid tumors independently of PD-L1 expression. *Nat. Cancer* 2, 794–802 (2021).
55. Fridman, W. H. et al. B cells and tertiary lymphoid structures as determinants of tumour immune contexture and clinical outcome. *Nat. Rev. Clin. Oncol.* 19, 441–457 (2022).
56. Burnet, F. M. The Concept of Immunological Surveillance. in 1–27 doi:10.1159/000386035
57. Dunn, G. P., Bruce, A. T., Ikeda, H., Old, L. J. & Schreiber, R. D. Cancer immunoediting: from immunosurveillance to tumor escape. *Nat. Immunol.* 3, 991–998 (2002).
58. Schreiber, R. D., Old, L. J. & Smyth, M. J. Cancer Immunoediting: Integrating Immunity's Roles in Cancer Suppression and Promotion. *Science* (80-.). 331, 1565–1570 (2011).
59. Galon, J. & Bruni, D. Approaches to treat immune hot, altered and cold tumours with combination immunotherapies. *Nat. Rev. Drug Discov.* 18, 197–218 (2019).

60. Galon, J. et al. Type, Density, and Location of Immune Cells Within Human Colorectal Tumors Predict Clinical Outcome. *Science* (80-.). 313, 1960–1964 (2006).
61. Kinoshita, T. et al. Prognostic value of tumor-infiltrating lymphocytes differs depending on histological type and smoking habit in completely resected non-small-cell lung cancer. *Ann. Oncol. Off. J. Eur. Soc. Med. Oncol.* 27, 2117–2123 (2016).
62. Mazzaschi, G. et al. Low PD-1 Expression in Cytotoxic CD8+ Tumor-Infiltrating Lymphocytes Confers an Immune-Privileged Tissue Microenvironment in NSCLC with a Prognostic and Predictive Value. *Clin. Cancer Res.* 24, 407–419 (2018).
63. Behrens, C. et al. Female Gender Predicts Augmented Immune Infiltration in Lung Adenocarcinoma. *Clin. Lung Cancer* (2020). doi:10.1016/j.clc.2020.06.003
64. Federico, L. et al. Distinct tumor-infiltrating lymphocyte landscapes are associated with clinical outcomes in localized non-small-cell lung cancer. *Ann. Oncol.* 33, 42–56 (2022).
65. Petersen, R. P. et al. Tumor infiltrating Foxp3+ regulatory T-cells are associated with recurrence in pathologic stage I NSCLC patients. *Cancer* 107, 2866–72 (2006).
66. Schulze, A. B. et al. Tumor infiltrating T cells influence prognosis in stage I-III non-small cell lung cancer. *J. Thorac. Dis.* 12, 1824–1842 (2020).
67. Lavin, Y. et al. Innate Immune Landscape in Early Lung Adenocarcinoma by Paired Single-Cell Analyses. *Cell* 169, 750-765.e17 (2017).
68. Hegde, P. S., Karanikas, V. & Evers, S. The Where, the When, and the How of Immune Monitoring for Cancer Immunotherapies in the Era of Checkpoint Inhibition. *Clin. Cancer Res.* 22, 1865–1874 (2016).
69. Hegde, P. S. & Chen, D. S. Top 10 Challenges in Cancer Immunotherapy. *Immunity* 52, 17–35 (2020).
70. Herbst, R. S. et al. Predictive correlates of response to the anti-PD-L1 antibody MPDL3280A in cancer patients. *Nature* 515, 563–7 (2014).
71. Allard, B., Allard, D., Buisseret, L. & Stagg, J. The adenosine pathway in immuno-oncology. *Nat. Rev. Clin. Oncol.* (2020). doi:10.1038/s41571-020-0382-2
72. Antonioli, L., Blandizzi, C., Pacher, P. & Haskó, G. Immunity, inflammation and cancer: a leading role for adenosine. *Nat. Rev. Cancer* 13, 842–57 (2013).

73. Mittal, D. et al. Antimetastatic effects of blocking PD-1 and the adenosine A2A receptor. *Cancer Res.* 74, 3652–8 (2014).
74. Gourdin, N. et al. Autocrine Adenosine Regulates Tumor Polyfunctional CD73+CD4+ Effector T Cells Devoid of Immune Checkpoints. *Cancer Res.* 78, 3604–3618 (2018).
75. Cekic, C., Day, Y.-J., Sag, D. & Linden, J. Myeloid expression of adenosine A2A receptor suppresses T and NK cell responses in the solid tumor microenvironment. *Cancer Res.* 74, 7250–9 (2014).
76. Beavis, P. A. et al. Adenosine Receptor 2A Blockade Increases the Efficacy of Anti-PD-1 through Enhanced Antitumor T-cell Responses. *Cancer Immunol. Res.* 3, 506–17 (2015).
77. Beavis, P. A. et al. Blockade of A2A receptors potently suppresses the metastasis of CD73+ tumors. *Proc. Natl. Acad. Sci. U. S. A.* 110, 14711–6 (2013).
78. Vijayan, D., Young, A., Teng, M. W. L. & Smyth, M. J. Targeting immunosuppressive adenosine in cancer. *Nat. Rev. Cancer* 17, 709–724 (2017).
79. Wang, R., Zhang, Y., Lin, X., Gao, Y. & Zhu, Y. Prognostic value of CD73-adenosinergic pathway in solid tumor: A meta-analysis and systematic review. *Oncotarget* 8, 57327–57336 (2017).
80. Jiang, T. et al. Comprehensive evaluation of NT5E/CD73 expression and its prognostic significance in distinct types of cancers. *BMC Cancer* 18, 267 (2018).
81. Inoue, Y. et al. Prognostic impact of CD73 and A2A adenosine receptor expression in non-small-cell lung cancer. *Oncotarget* 8, 8738–8751 (2017).
82. Fridman, W. H., Zitvogel, L., Sautès-Fridman, C. & Kroemer, G. The immune contexture in cancer prognosis and treatment. *Nat. Rev. Clin. Oncol.* 14, 717–734 (2017).
83. Sidders, B. et al. Adenosine Signaling Is Prognostic for Cancer Outcome and Has Predictive Utility for Immunotherapeutic Response. *Clin. Cancer Res.* 26, 2176–2187 (2020).

84. Herbst, R. S. et al. COAST: An Open-Label, Phase II, Multidrug Platform Study of Durvalumab Alone or in Combination With Oleclumab or Monalizumab in Patients With Unresectable, Stage III Non–Small-Cell Lung Cancer. *J. Clin. Oncol.* (2022). doi:10.1200/JCO.22.00227
85. Tina Cascone, Rosario García-Campelo, Jonathan Spicer, Walter Weder, Davey Daniel, David Spigel, Maen Hussein, Julien Mazieres, Julio Oliveira, Edwin Yau, Alexander Spira, Raymond Mager, Oday Hamid, Lin-Yang Cheng, Ying Zheng, Jorge Blando, Lara McGrath, P. F. CT011 - NeoCOAST: open-label, randomized, phase 2, multidrug platform study of neoadjuvant durvalumab alone or combined with novel agents in patients (pts) with resectable, early-stage non-small-cell lung cancer (NSCLC). *Annu. Meet. Am. Assoc. Cancer Res.* 2022 April 8-13; New Orleans LA (2022).
86. Gao, Z. W., Dong, K. & Zhang, H. Z. The roles of CD73 in cancer. *Biomed Res. Int.* 2014, (2014).
87. Allard, B., Pommey, S., Smyth, M. J. & Stagg, J. Targeting CD73 enhances the antitumor activity of anti-PD-1 and anti-CTLA-4 mAbs. *Clin. Cancer Res.* 19, 5626–5635 (2013).
88. Horenstein, A. L. et al. A CD38/CD203a/CD73 ectoenzymatic pathway independent of CD39 drives a novel adenosinergic loop in human T lymphocytes. *Oncoimmunology* 2, e26246 (2013).
89. de Andrade Mello, P., Coutinho-Silva, R. & Savio, L. E. B. Multifaceted Effects of Extracellular Adenosine Triphosphate and Adenosine in the Tumor-Host Interaction and Therapeutic Perspectives. *Front. Immunol.* 8, 1526 (2017).
90. Regateiro, F. S., Cobbold, S. P. & Waldmann, H. CD73 and adenosine generation in the creation of regulatory microenvironments. *Clin. Exp. Immunol.* 171, 1–7 (2013).
91. Chen, D. S. & Mellman, I. Elements of cancer immunity and the cancer–immune set point. *Nature* 541, 321–330 (2017).
92. Chen, L. et al. CD38-mediated immunosuppression as a mechanism of tumor cell escape from PD-1/PD-L1 blockade. *Cancer Discov.* 8, 1156–1175 (2018).

93. Pervez, S., Arshad, S. & Abro, B. HER2 Basolateral versus Circumferential IHC Expression Is Dependent on Polarity and Differentiation of Epithelial Cells in Gastric/GE Adenocarcinoma. *Patholog. Res. Int.* 2018, (2018).
94. Minor, M., Alcedo, K. P., Battaglia, R. A. & Snider, N. T. Cell type- and tissue-specific functions of ecto-5'-nucleotidase (CD73). *Am. J. Physiol. Cell Physiol.* (2019). doi:10.1152/ajpcell.00285.2019
95. Vigano, S. et al. Targeting Adenosine in Cancer Immunotherapy to Enhance T-Cell Function. *Front. Immunol.* 10, 925 (2019).
96. Chen, S. et al. CD73 expression on effector T cells sustained by TGF- β facilitates tumor resistance to anti-4-1BB/CD137 therapy. *Nat. Commun.* 10, 150 (2019).
97. Teng, F., Meng, X., Kong, L. & Yu, J. Progress and challenges of predictive biomarkers of anti PD-1/PD-L1 immunotherapy: A systematic review. *Cancer Lett.* 414, 166–173 (2018).
98. Perrot, I. et al. Blocking Antibodies Targeting the CD39/CD73 Immunosuppressive Pathway Unleash Immune Responses in Combination Cancer Therapies. *Cell Rep.* 27, 2411-2425.e9 (2019).
99. Reck, M. et al. Five-Year Outcomes With Pembrolizumab Versus Chemotherapy for Metastatic Non-Small-Cell Lung Cancer With PD-L1 Tumor Proportion Score \geq 50. *J. Clin. Oncol.* 39, 2339–2349 (2021).
100. Grant, M. J., Herbst, R. S. & Goldberg, S. B. Selecting the optimal immunotherapy regimen in driver-negative metastatic NSCLC. *Nat. Rev. Clin. Oncol.* (2021). doi:10.1038/s41571-021-00520-1
101. Tang, H. et al. PD-L1 on host cells is essential for PD-L1 blockade-mediated tumor regression. *J. Clin. Invest.* 128, 580–588 (2018).
102. Lin, H. et al. Host expression of PD-L1 determines efficacy of PD-L1 pathway blockade-mediated tumor regression. *J. Clin. Invest.* 128, 805–815 (2018).
103. Roepman, P. et al. An Immune Response Enriched 72-Gene Prognostic Profile for Early-Stage Non-Small-Cell Lung Cancer. *Clin. Cancer Res.* 15, 284–290 (2009).

104. Prat, A. et al. Immune-Related Gene Expression Profiling After PD-1 Blockade in Non-Small Cell Lung Carcinoma, Head and Neck Squamous Cell Carcinoma, and Melanoma. *Cancer Res.* 77, 3540–3550 (2017).
105. Patel, S. S. et al. The microenvironmental niche in classic Hodgkin lymphoma is enriched for CTLA-4-positive T cells that are PD-1-negative. *Blood* 134, 2059–2069 (2019).
106. Carey, C. D. et al. Topological analysis reveals a PD-L1-associated microenvironmental niche for Reed-Sternberg cells in Hodgkin lymphoma. *Blood* 130, 2420–2430 (2017).
107. Bruni, D., Angell, H. K. & Galon, J. The immune contexture and Immunoscore in cancer prognosis and therapeutic efficacy. *Nat. Rev. Cancer* 20, 662–680 (2020).
108. Litchfield, K. et al. Meta-analysis of tumor- and T cell-intrinsic mechanisms of sensitization to checkpoint inhibition. *Cell* (2021). doi:10.1016/j.cell.2021.01.002
109. AbdulJabbar, K. et al. Geospatial immune variability illuminates differential evolution of lung adenocarcinoma. *Nat. Med.* 26, 1054–1062 (2020).
110. Casanova-Acebes, M. et al. Tissue-resident macrophages provide a pro-tumorigenic niche to early NSCLC cells. *Nature* (2021). doi:10.1038/s41586-021-03651-8
111. Bagaev, A. et al. Conserved pan-cancer microenvironment subtypes predict response to immunotherapy. *Cancer Cell* 39, 845-865.e7 (2021).
112. van Dijk, N. et al. Preoperative ipilimumab plus nivolumab in locoregionally advanced urothelial cancer: the NABUCCO trial. *Nat. Med.* 26, 1839–1844 (2020).
113. Altorki, N. K. et al. Neoadjuvant durvalumab with or without stereotactic body radiotherapy in patients with early-stage non-small-cell lung cancer: a single-centre, randomised phase 2 trial. *Lancet. Oncol.* 22, 824–835 (2021).
114. Rothschild, S. I. et al. SAKK 16/14: Durvalumab in Addition to Neoadjuvant Chemotherapy in Patients With Stage IIIA(N2) Non-Small-Cell Lung Cancer—A Multicenter Single-Arm Phase II Trial. *J. Clin. Oncol.* JCO.21.00276 (2021). doi:10.1200/JCO.21.00276
115. Gao, S. et al. Neoadjuvant PD-1 inhibitor (Sintilimab) in NSCLC. *J. Thorac. Oncol.* 15, 816–826 (2020).

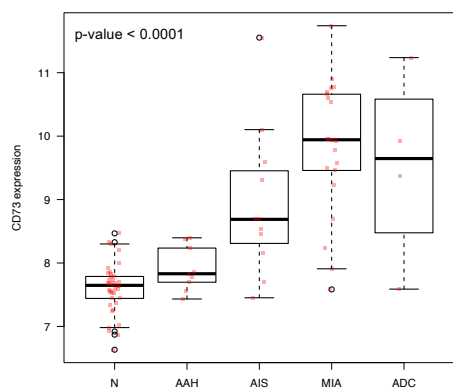
Chapter 8

114

SUPPLEMENTARY MATERIAL

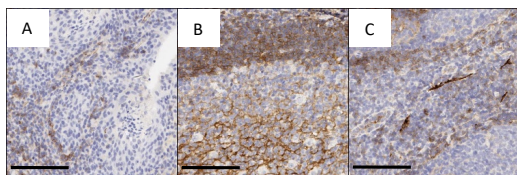
8.1 SUPPLEMENTARY MATERIAL ARTICLE 1.

Supplementary Figure 1

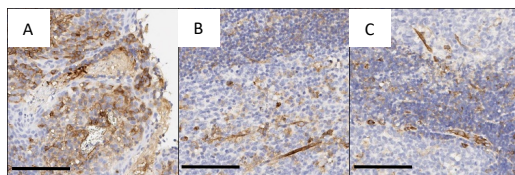


Supplementary Figure 2

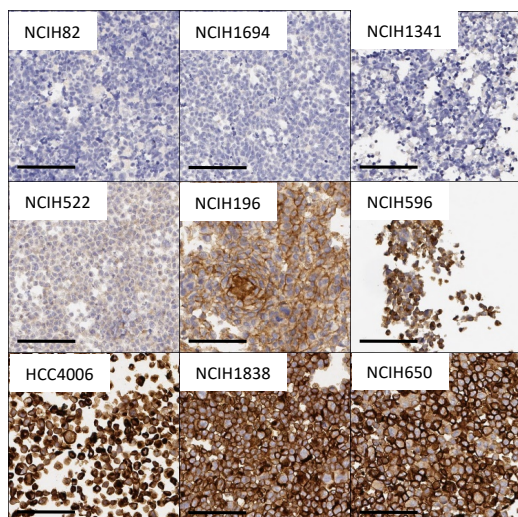
a



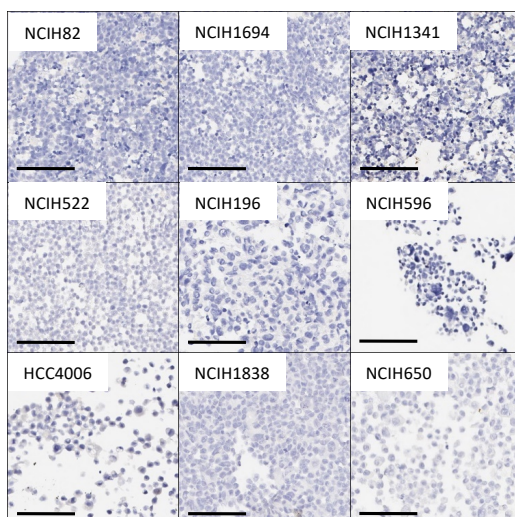
b



c



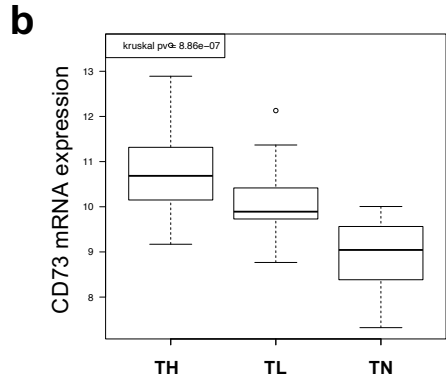
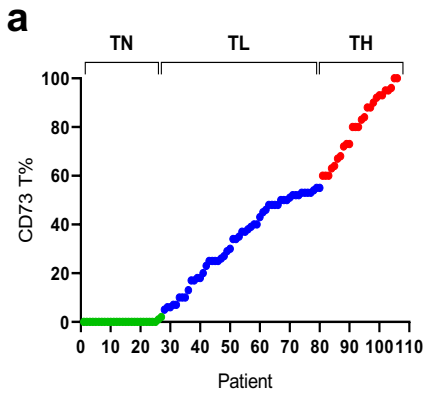
d



e

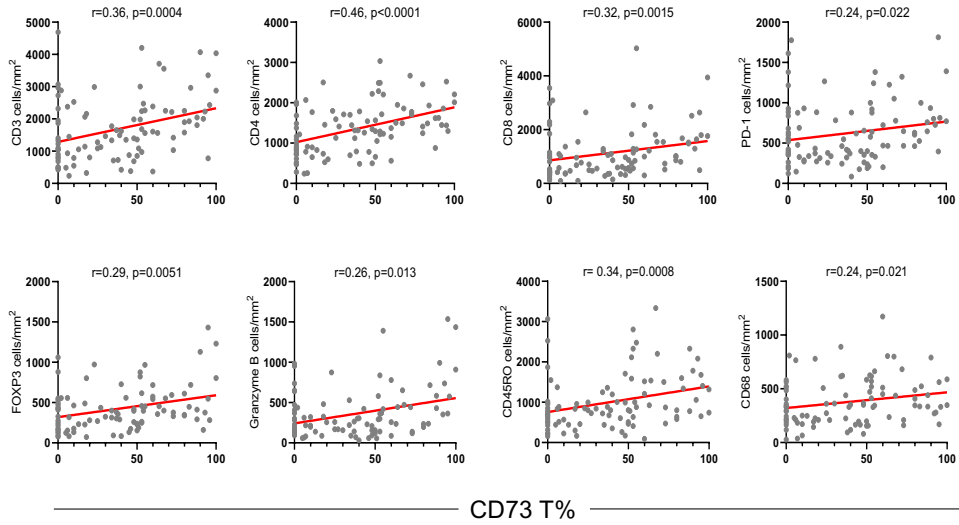
Cell line	<i>CD73</i> mRNA*	<i>CD73</i> IHC Membrane	<i>CD39</i> mRNA*	<i>CD39</i> IHC Membrane
NCIH82	-4.51793	0	2.379744	0
NCIH1694	-3.78588	0	2.788662	0
NCIH1341	-1.9469	0	2.226699	0
NCIH522	-1.16531	0	2.266061	0
NCIH196	3.111517	2+	-0.20666	0
NCIH596	4.066031	2+	-0.55199	0
HCC4006	5.828985	3+	-1.03664	0
NCIH1838	7.296265	3+	1.27548	0
NCIH650	7.760806	3+	1.163237	0

Supplementary Figure 3

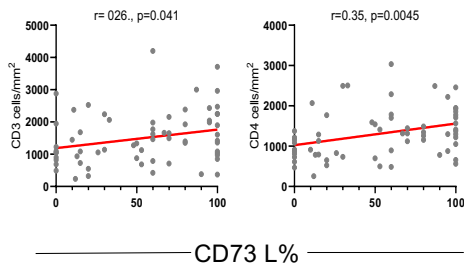


Supplementary Figure 4

a

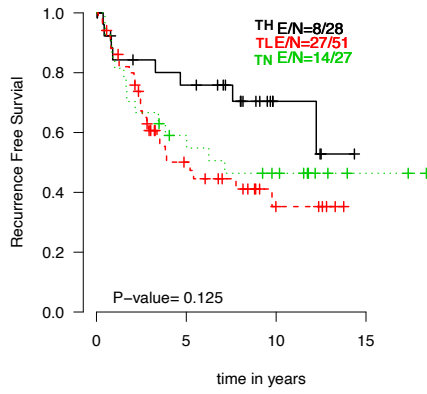


b

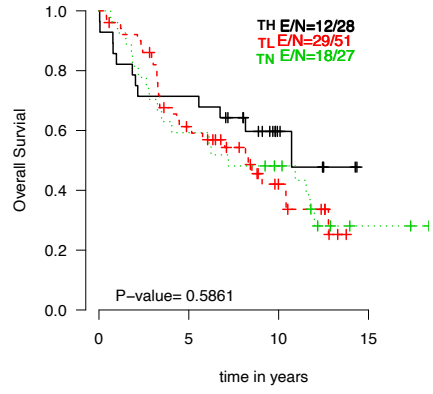


Supplementary Figure 5

a

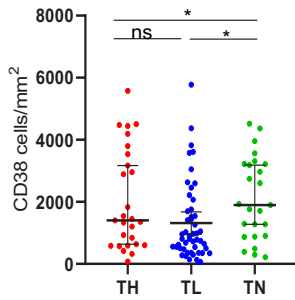


b

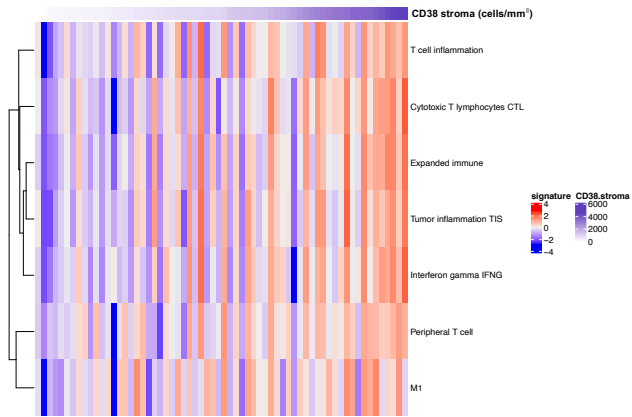


Supplementary Figure 6

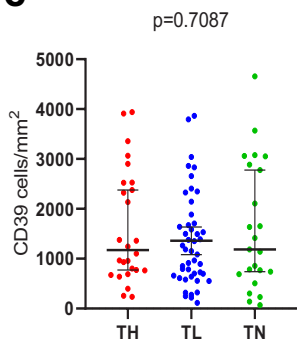
a



b



c



SUPPLEMENTARY TABLES.

Supplementary table 1. Annotated genes included to define the immune gene signatures.

Signature	Reference	Genes included
Adenosine	Sidders et al. ³²	PPARG,CYBB,COL3A1,FOXP3,LAG3,APP,GPI,PTGS2,CASP1,FOS,MAPK1,MAPK3
T cell inflammation	Spranger et al. ²⁹	CD8A,CCL2,CCL3,CCL4,CXCL9,CXCL10,ICOS,GZMK,IRF1,HLA-DMA,HLA-DMB,HLA-DOA,HLA-DOB
Cytotoxic T lymphocytes (CTL)	Jian et al. ³⁰	CD8A,CD8B,GZMA,GZMB,PRF1
Expanded immune	Ayers et al. ²⁸	CD3D,IDO1,CIITA,CD3E,CCL5,GZMK,CD2,CXCL13,NKG7,HLA-E,CXCR6,LAG3,TAGAP,CXCL10,STAT1,GZMB
Tumor inflammation (TIS)	Danaher et al. ³³	PSMB10,HLA-DQA1,HLA-DRB1,HLA-E,NKG7,CD8A,CCL5,CXCL9,CD27,CXCR6,IDO1,S
Interferon-gamma (IFNG)	Ayers et al. ²⁸	TAT1,TIGIT,LAG3,CD274
Peripheral T cell	Hwang et al. ³¹	IFNG,STAT1,CCR5,CXCL9,CXCL10,CXCL11,IDO1,PRF1,GZMA,HLA-DRA
M1	Hwang et al. ³¹	HLA-DOA,GPR18,STAT1
		CCR7,CD27,CD48,FOXO1,HLA-B,HLA-G,IFIH1,IKZF4,LAMP3,NFKBIA,SAMHD1

Supplementary table 2. Information of antibodies used for immunohistochemistry analysis

Biomarker	Clone	Vendor	Catalogue #	Antigen Retrieval	Dilution
PD-L1	E1L3N	Cell Signaling	13684	Epitope Retrieval #1 (Citrate Buffer pH6)	1:100
CD38	SPC32	Leica/Novocastra	NCL-L-CD38-290	Epitope Retrieval #1 (Citrate Buffer pH6)	1:100
CD39	EPR20461	Abcam	ab223843	Epitope Retrieval #1 (Citrate Buffer pH6)	1:500
CD73	D7F9A	Cell Signaling	13160S	Epitope Retrieval #2 (Tris-EDTA Buffer)	1:200

Supplementary table 3. Overview of Luminal (L) and Basolateral (BL) membrane expression of CD73 in LUADs

Basolateral CD73 expression	Luminal CD73 expression			Total
	L CD73+	L CD73-	Non-lumen	
	N (%)	N (%)	N (%)	N (%)
BL CD73+	44 (42)	1 (1)	19 (18)	64 (60)
BL CD73-	16 (15)	11 (10)	15 (14)	42 (40)
Total	60 (57)	12 (11)	34 (32)	106 (100)

Supplementary table 4. Clinicopathological characteristics of patients with lung adenocarcinoma and associations with CD73 IHC expression in different membrane compartments of malignant cells

Characteristic	Total (T) CD73+ (79/106, 75%)				Basolateral (BL) CD73+ (68/106, 64%)			Tumors with evaluable Lumen	Luminal (L) CD73+ (60/72, 86%)		
	N	N	%	p value*	N	%	p value*		N	%	p value*
Age											
≤65	53	38	72%	0,6562	33	62%	0,8397	31	23	74%	0,1094
>65	53	41	77%		35	66%		41	37	90%	
Sex											
Female	52	41	79%	0,3759	39	75%	0,0268	37	31	84%	1
Male	54	38	70%		29	54%		35	29	83%	
Smoking History											
Never	15	15	100%	0,0107	13	87%	0,0788	15	15	100%	0,0598
Current/Former	91	64	70%		55	60%		57	45	79%	
TNM 8 th Edition											
I	58	46	79%	0,2438	41	71%	0,0896	42	36	86%	0,6201
II	26	16	62%		12	46%		16	12	75%	
III	22	17	77%		15	68%		14	12	86%	
Pathological T (8th)											
pT1a - pT2a	70	54	77%	0,4810	47	67%	0,3984	50	43	86%	0,4932
pT2b - T4	36	25	69%		21	58%		22	17	77%	
Pathological N (8th)											
N0	78	59	76%	0,6922	51	65%	0,9400	55	46	84%	0,2996
N1	20	15	75%		12	60%		12	11	92%	
N2	8	5	63%		5	63%		5	3	60%	
Histologic pattern											
Any-Solid	46	29	63%	0,0243	29	63%	0,8412	12	10	83%	1
Non-Solid	60	50	83%		39	65%		60	50	83%	
Molecular characteristics											
<i>EGFR</i> Mutated	15	14	93%	0,1069	12	80%	0,2532	13	12	92%	0,4351
<i>EGFR</i> Wild-type	85	60	71%		54	64%		54	43	80%	
<i>STK11</i> Mutated	7	3	43%	0,0626	3	43%	0,1948	7	3	43%	0,0041
<i>STK11</i> Wild-type	56	44	79%		40	71%		35	33	94%	
<i>KRAS</i> Mutated	26	21	81%	0,6021	20	77%	0,1614	20	17	85%	1
<i>KRAS</i> Wild-type	77	56	73%		47	61%		50	42	84%	
<i>TP53</i> Mutated	27	18	67%	0,2507	16	59%	0,2741	11	9	82%	0,6437
<i>TP53</i> Wild-type	36	29	81%		27	75%		31	27	87%	
Somatic Mutation burden											
Median (range)	63	47	99 (2-955)	0.0400	43	127 (2-955)	0.5401	42	36	75 (2-940)	0.3178

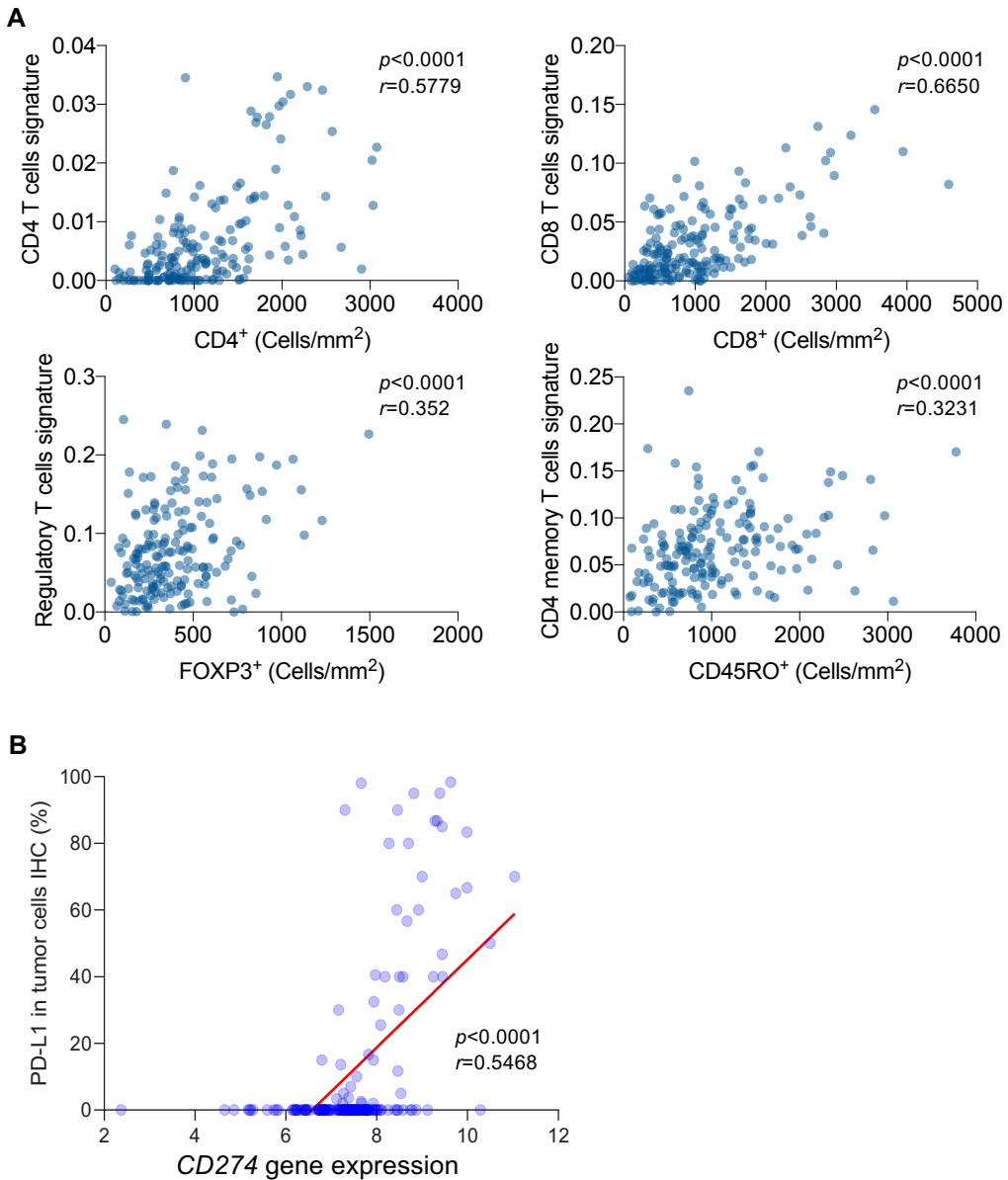
Supplementary table 5. Overview of Luminal (L) and Basolateral (BL) membrane expression of CD73 in CD73 Groups.

Cell compartment CD73 IHC	T High N (%)	T low N (%)	T Negative N (%)	Total N (%)
BL+	28 (26.4)	35 (33.0)	1 (0.9)	64 (60.4)
BL-	0 (0)	16 (15.1)	26 (24.5)	42(39.4)
L+	13 (12.3)	51 (44.3)	0 (0)	60 (56.6)
L-	0 (0)	0(0)	12 (11.3)	12 (11.3)
L NE*	15 (14.2)	4 (3.7)	15 (14.2)	34 (32.8)
Total	28 (26.4)	51 (48.1)	27 (25.2)	106 (100)

*NE: not evaluable (no luminal membrane present)

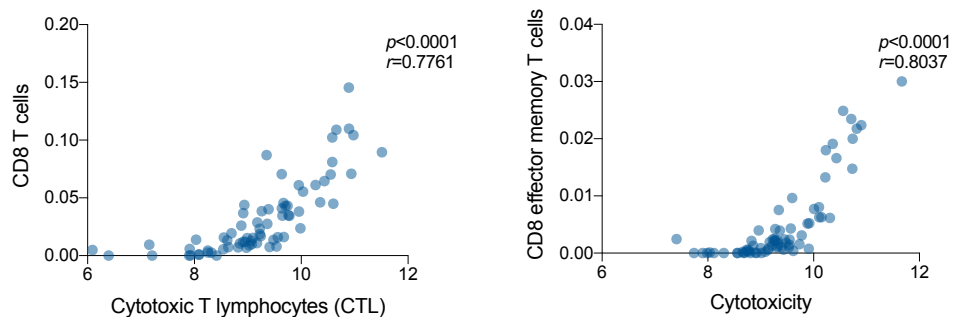
8.2 SUPPLEMENTARY MATERIAL ARTICLE 2.

Supplementary Figure 1



Supplementary Figure 1. Correlation between immune marker expression by immunohistochemistry and targeted RNA sequencing. A) Scatter plots showing statistically positive associations between cell densities for immune markers (CD4, CD8, FOXP3 and CD45RO) that were determined by immunohistochemistry (IHC) analysis and their respective cellular immune scores that were derived by targeted RNA sequencing. **B)** Correlation plot showing statistically positive association between PD-L1 immunohistochemical expression in malignant cells (%) and *CD274* gene expression. Correlations were statistically assessed using Spearman correlation.

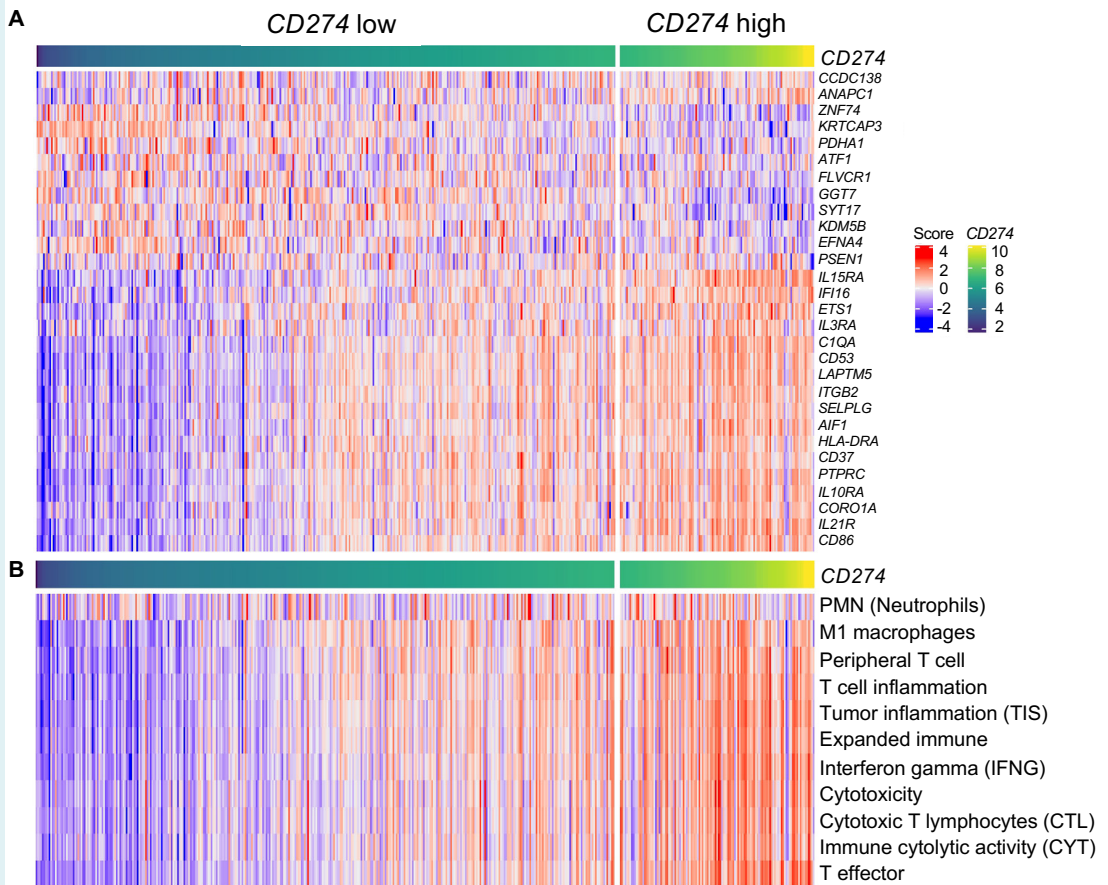
Supplementary Figure 2



126

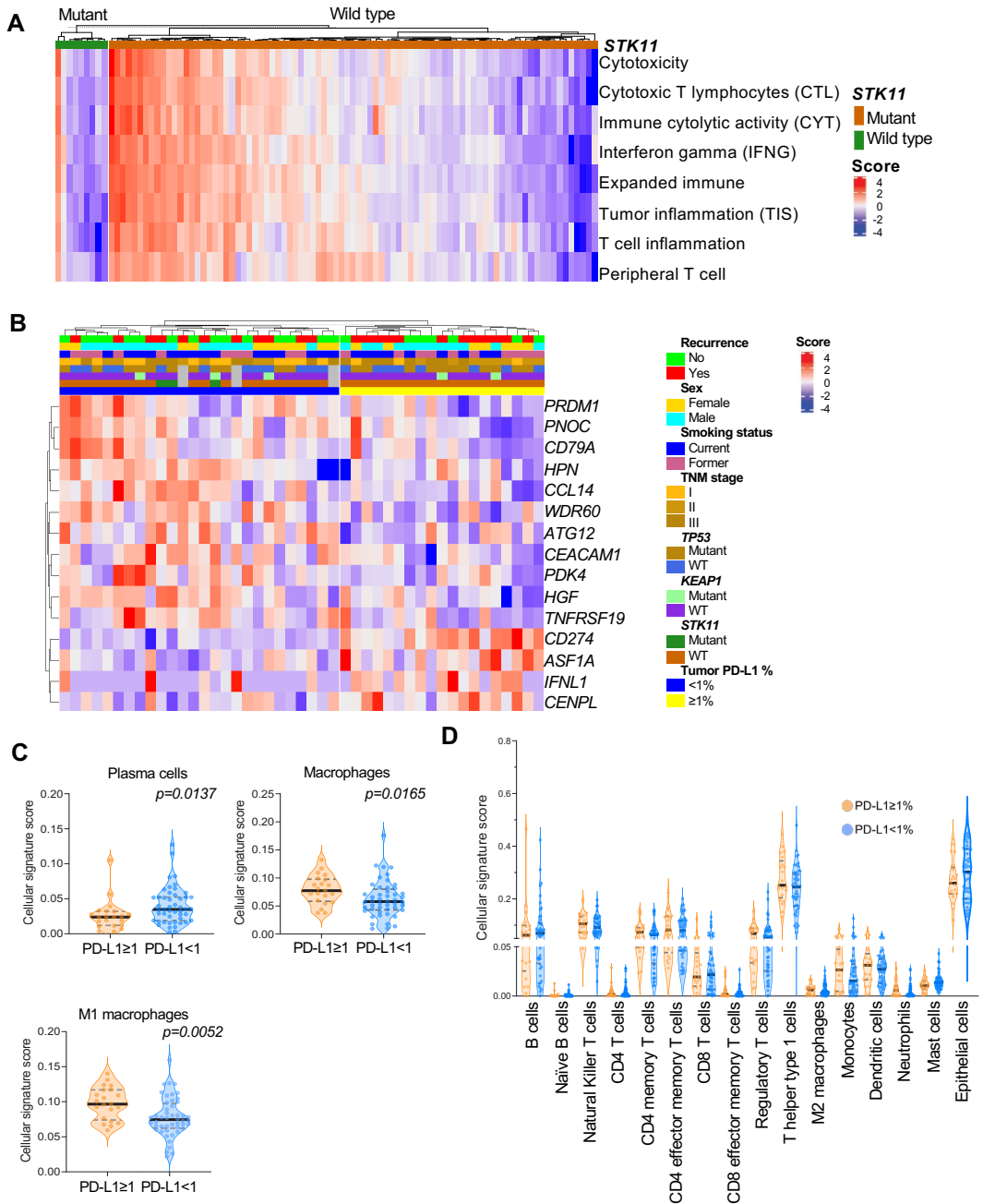
Supplementary Figure 2. Correlation between CD8 T cell scores derived from targeted RNA sequencing with previously published immune signatures. Correlation plots showing statistically positive associations between signatures of CD8 T cells and CD8 effector memory T cells derived in this study following targeted immune profiling with previously reported signatures denoting cytotoxic T lymphocytes (CTLs) (Jian et al, Nature, 2018) and cytotoxicity (Sidders et al, Clinical Cancer Research, 2020) respectively. Correlations were statistically assessed using Spearman correlation.

Supplementary Figure 3



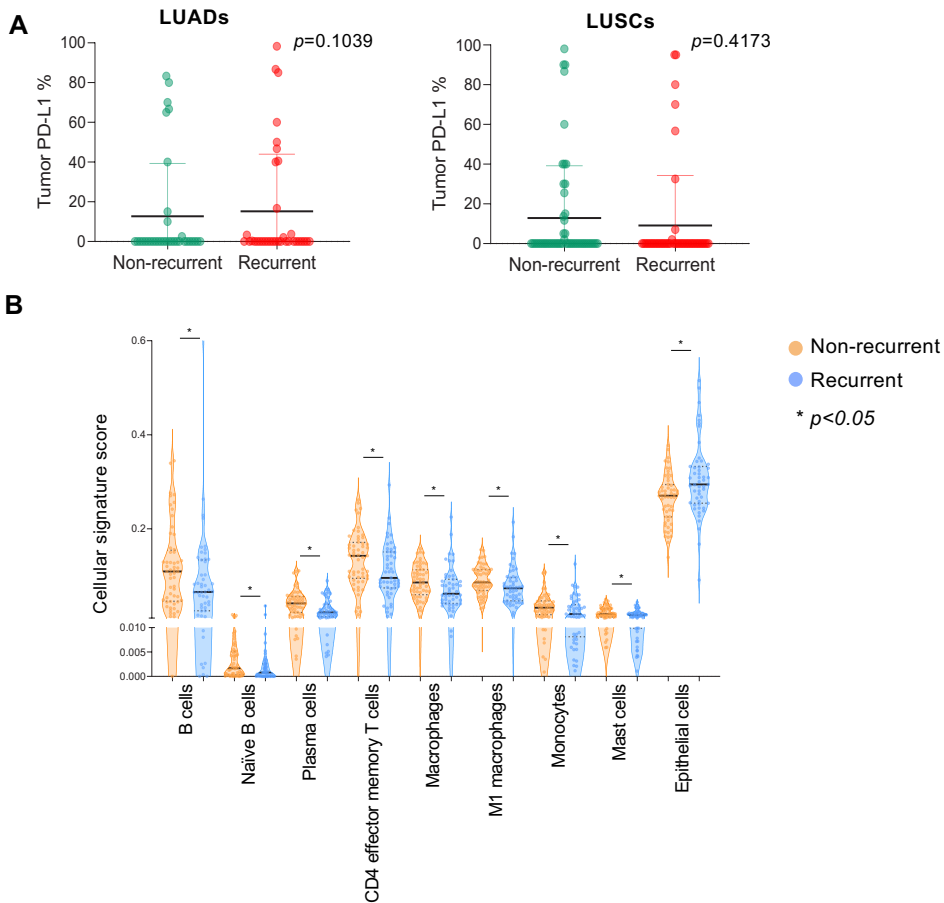
Supplementary Figure 3. Immune expression programs differentially expressed in PD-L1 positive and negative treatment-naïve LUADs from the TCGA cohort. A) Heat map showing differentially expressed genes (DEGs) between PD-L1 positive (upper quartile) and PD-L1 negative (lower three quartiles) treatment-naïve LUADs from TCGA. DEGs were selected based on a statistical threshold of adjusted $p < 0.05$. Columns denote samples and rows represent DEGs (red, relatively higher expression; blue, relatively lower expression). **B)** Differential expression of functional gene signatures (red, higher expression; blue, relatively lower expression; adjusted p -value < 0.05) between PD-L1 positive and negative LUADs from the TCGA cohort.

Supplementary Figure 4



Supplementary Figure 4. Analysis of immune gene programs in NSCLC subsets. A) Heat map showing differently expressed immune gene programs (adjusted $p < 0.05$) between patients with and without *STK11* mutation. Columns denote samples. Rows represent differently expressed immune gene programs (red, relatively higher expression; blue, relatively lower expression). **B)** Heat map showing DEGs (adjusted $p < 0.05$) between PD-L1 positive ($\geq 1\%$) and PD-L1 negative ($< 1\%$) treatment-naive LUSCs. Columns represent samples which were annotated with clinicopathological and molecular features, and rows represent DEGs (red, relatively higher expression; blue, relatively lower expression). **C)** Violin plots for significantly different cellular signature scores in PD-L1 positive ($\geq 1\%$, orange) and negative ($< 1\%$, blue) tumors, **D)** and for non-significant cellular signature scores. P-values were calculated based on the Mann Whitney test, black lines represent median values, and gray lines correspond to 95% CIs.

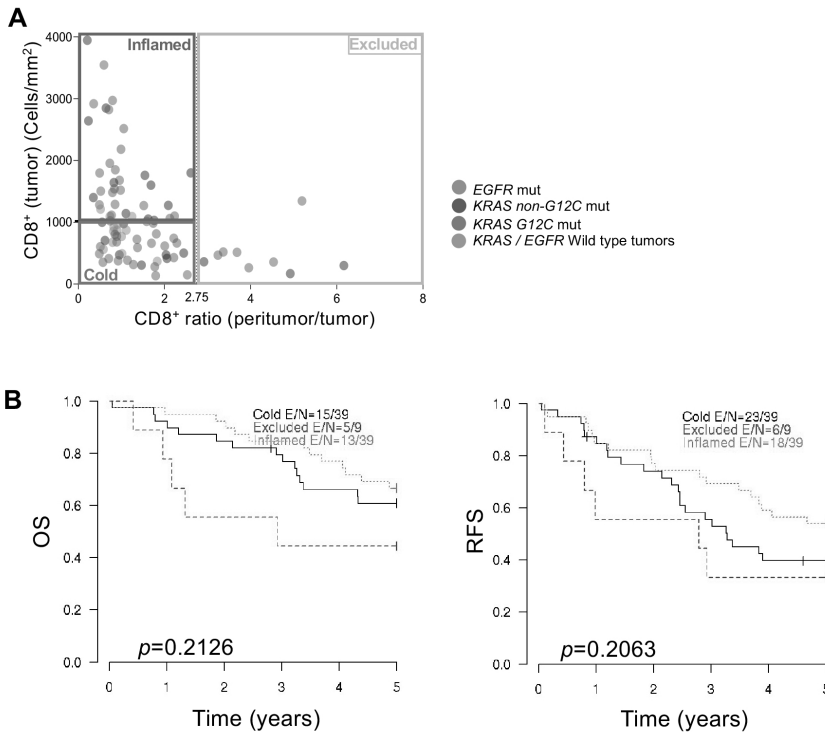
Supplementary Figure 5



Supplementary Figure 5. Association of PD-L1 protein expression and cellular signatures with recurrence.

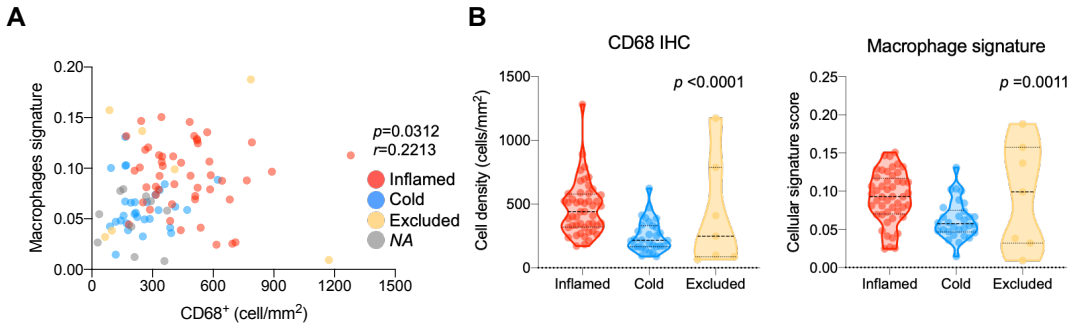
A) Analysis of PD-L1 % protein expression in recurrent and non-recurrent NSCLCs was performed separately in LUADs (right panel) and LUSCs (left panel). **B)** Differences in cellular signature scores between relapsed (orange) and non-recurrent (blue) LUADs. P-values were calculated based on the Mann Whitney test, black lines represent median values, and gray lines correspond to 95% CIs.

Supplementary Figure 6



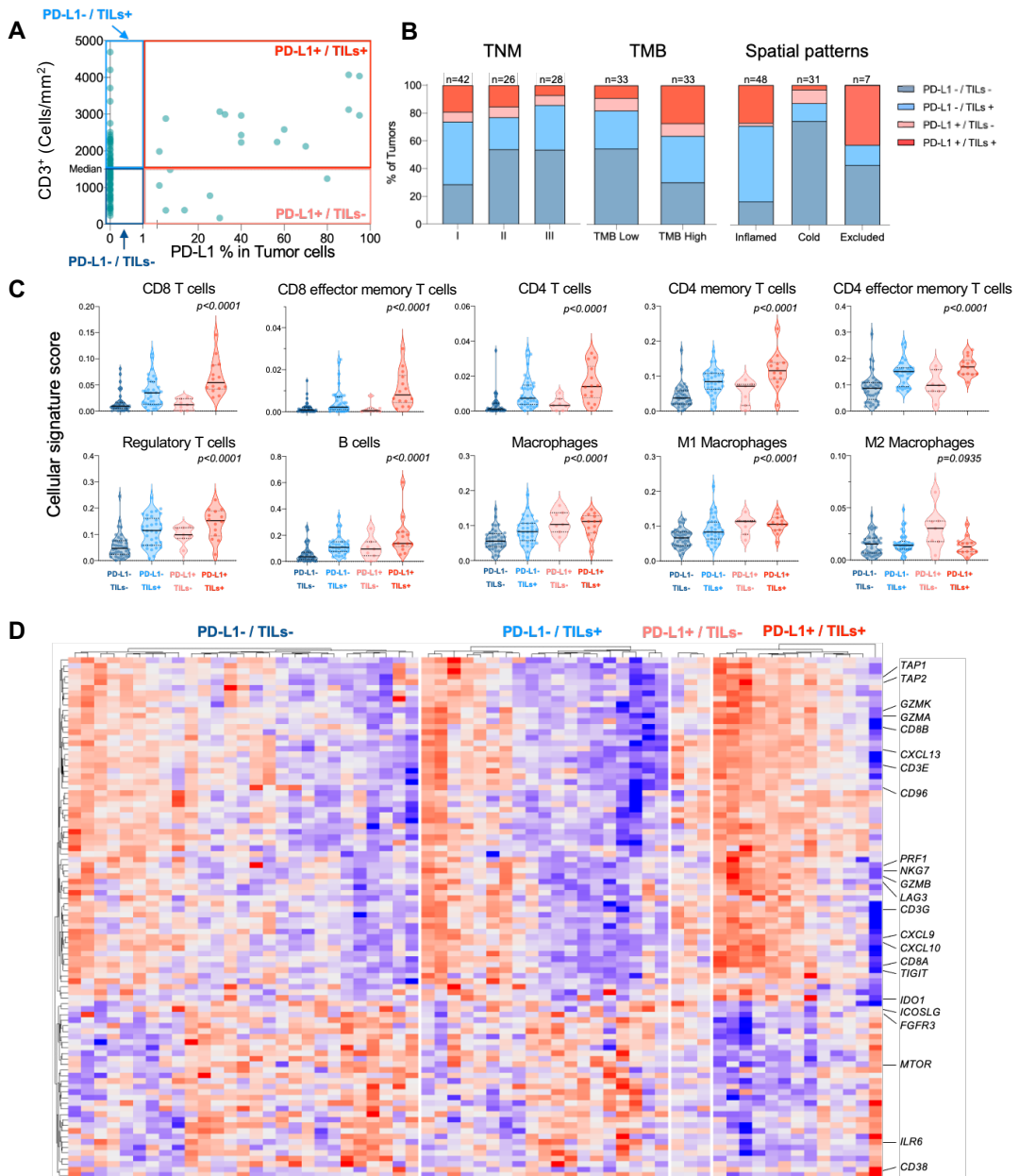
Supplementary Figure 6. Associations between tumor immune microenvironment phenotypes in LUADs with driver mutations and survival outcomes. A) Scatter plot showing the distribution of LUADs with and without driver mutations (*EGFR*, *KRAS*) based on tumoral cell densities of CD8⁺ T cells (y-axis) and peritumoral/tumoral ratios for CD8⁺ T cells. LUADs were classified into inflamed (red rectangle), cold (blue rectangle), and excluded (yellow rectangle) phenotypes, **B)** Analysis of differences in overall survival (OS) and recurrence free survival (RFS) based on tumor immune microenvironment phenotypes.

Supplementary Figure 7



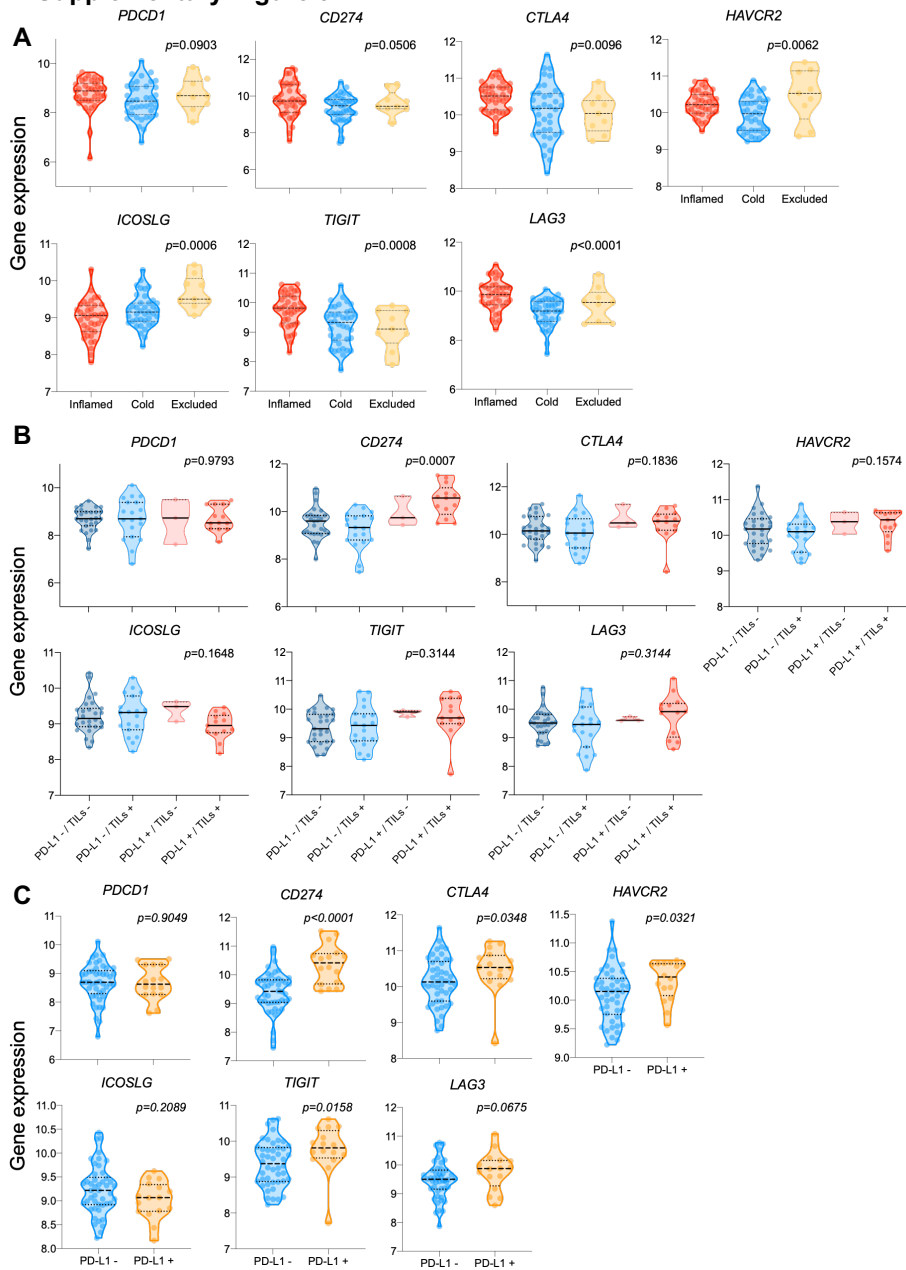
Supplementary Figure 7. Correlation between immune marker expression by immunohistochemistry and targeted RNA sequencing. **A** Scatter plot showing statistically positive association between CD68⁺ cell densities by IHC and the macrophage signature. Violin plots showing differences in CD68⁺ cell densities and macrophage signature across the TIME phenotypes. P-values were calculated based on the Mann Whitney test, black lines represent median values, and gray lines correspond to 95% confidence intervals (CIs). Correlations were statistically assessed using Spearman correlation.

Supplementary Figure 8



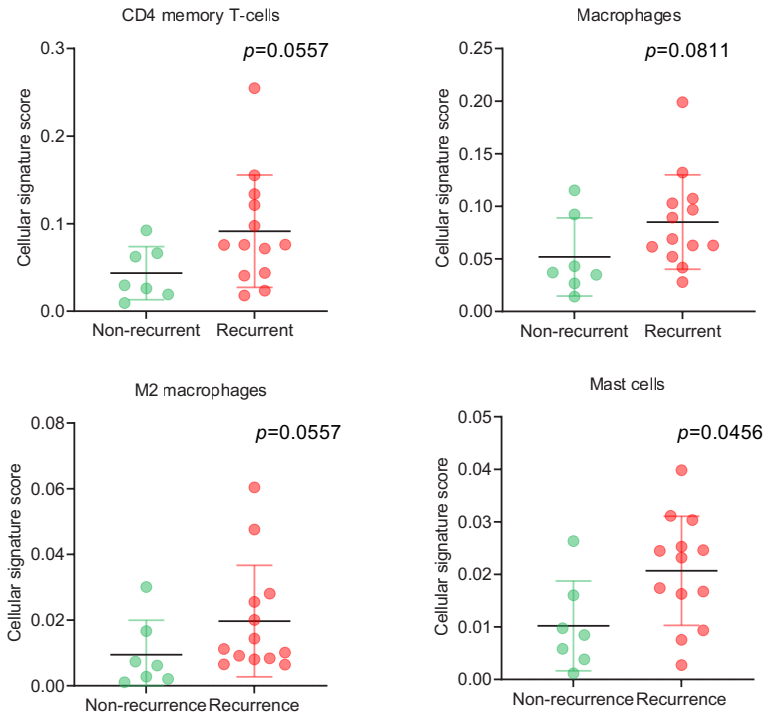
Supplementary Figure 8. Gene expression programs associated with tumoral PD-L1 and TILs in treatment-naïve LUADs. A) Scatter plot showing distribution of LUADs based on tumoral cell densities of CD3⁺ T cells and PD-L1 % in tumor cells. **B)** Frequencies of TIME phenotypes in LUAD by pathological stage, tumoral PD-L1 expression, as well as somatic mutational burden (TMB; TMB high, \geq median; TMB low, $<$ median). **C)** Violin plots depicting cellular signature scores across the three TIME phenotypes. P-values were calculated based on the Kruskal-Wallis test, black lines represent median levels, and gray lines correspond to 95% confidence intervals (CIs). **D)** Heat map showing 94 DEGs (adjusted $p < 0.05$) between the four groups.

Supplementary Figure 9



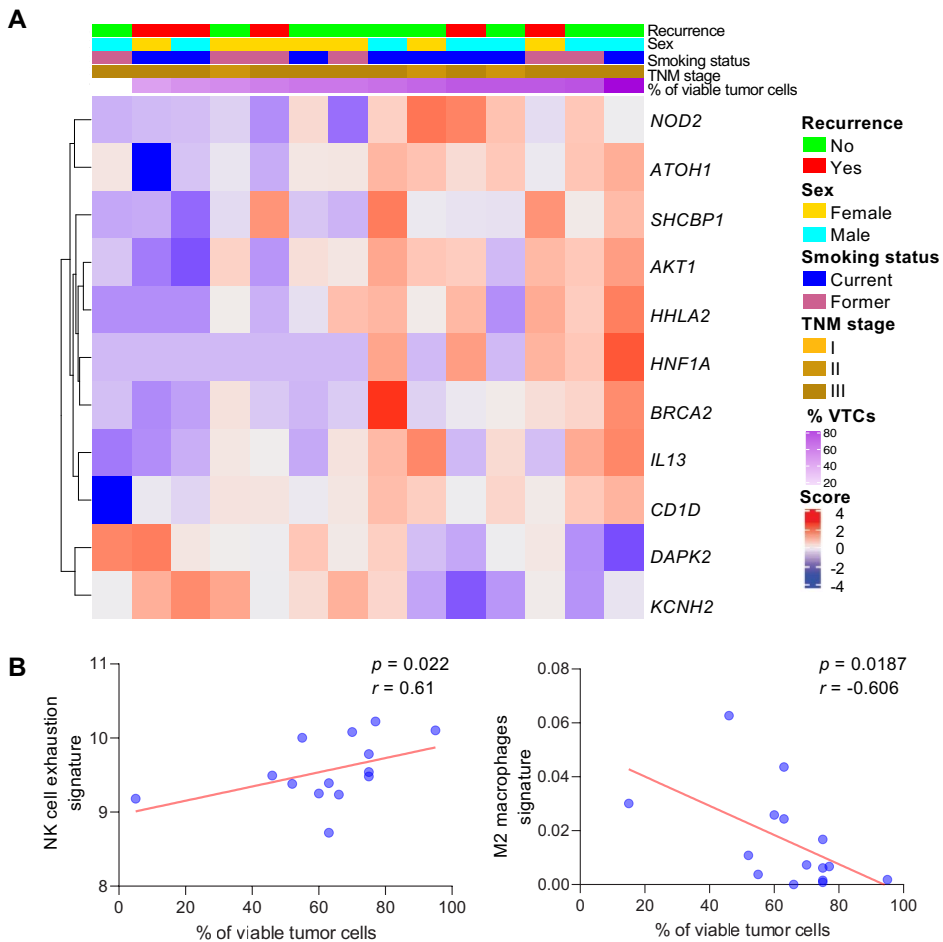
Supplementary Figure 9. Comparison of immune checkpoints across different TIME phenotypes. Violin plots depicting differences in expression levels of the indicated immune checkpoints between the inflamed, excluded, and cold TIME groups (A), among four groups based on the expression of tumoral PD-L1 and presence of TILs (B), as well as between PD-L1 negative (<1%) and positive ($\geq 1\%$) tumors (C). P-values were calculated based on Kruskal-Wallis tests (A and B) and Mann-Whitney tests (C) and bars correspond to median values $\pm 95\%$ CIs.

Supplementary Figure 10



Supplementary Figure 10. Comparative analysis of immune cell signature scores between recurrent and non-recurrent LUADs after neoadjuvant chemotherapy. P-values were calculated based on the Mann Whitney test, black lines represent median values, and bars correspond to 95% CIs.

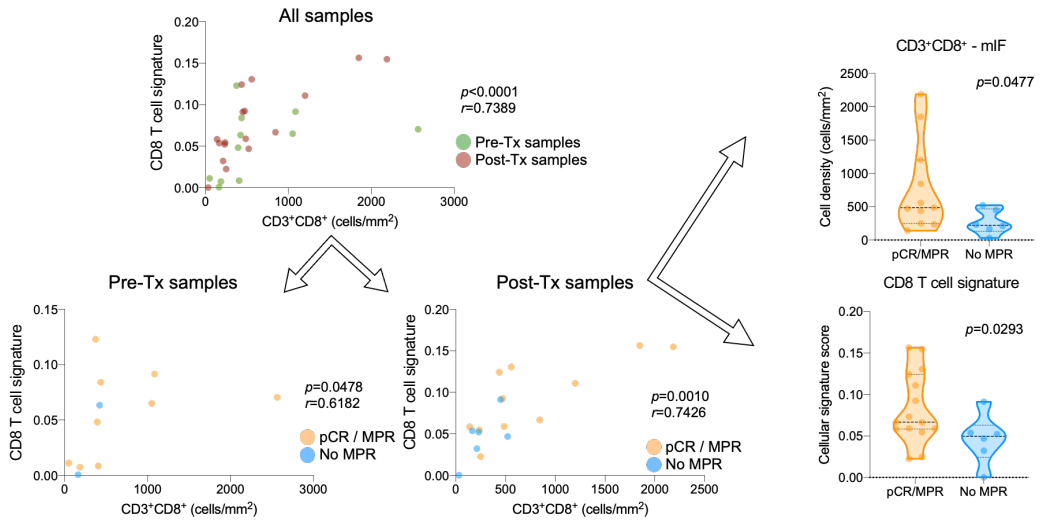
Supplementary Figure 11



Supplementary Figure 11. Immune expression changes after neoadjuvant chemotherapy in LUSCs. A) Heat map showing DEGs (adjusted $p < 0.05$) that were associated with % of viable tumor cells in early-stage LUSCs treated with neoadjuvant chemotherapy. Columns denote LUSCs that are annotated with clinicopathological features and rows represent DEGs (red, relatively higher expression; blue, relatively lower expression). **B)** Correlation plots showing statistically significant correlations of % viable tumor cells with NK cell exhaustion (left) and M2 macrophage (right) signatures. Correlations were statistically examined used Spearman correlation.

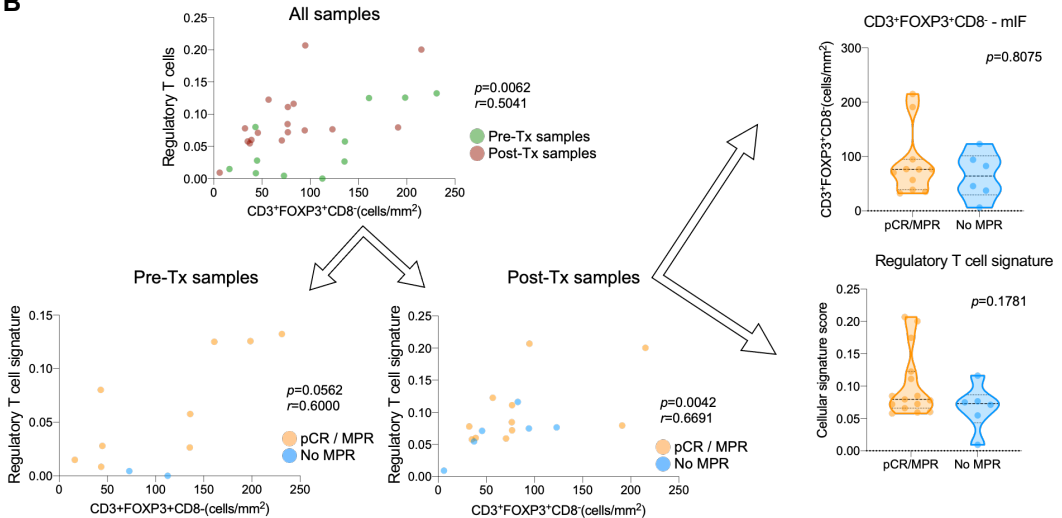
Supplementary Figure 12

A



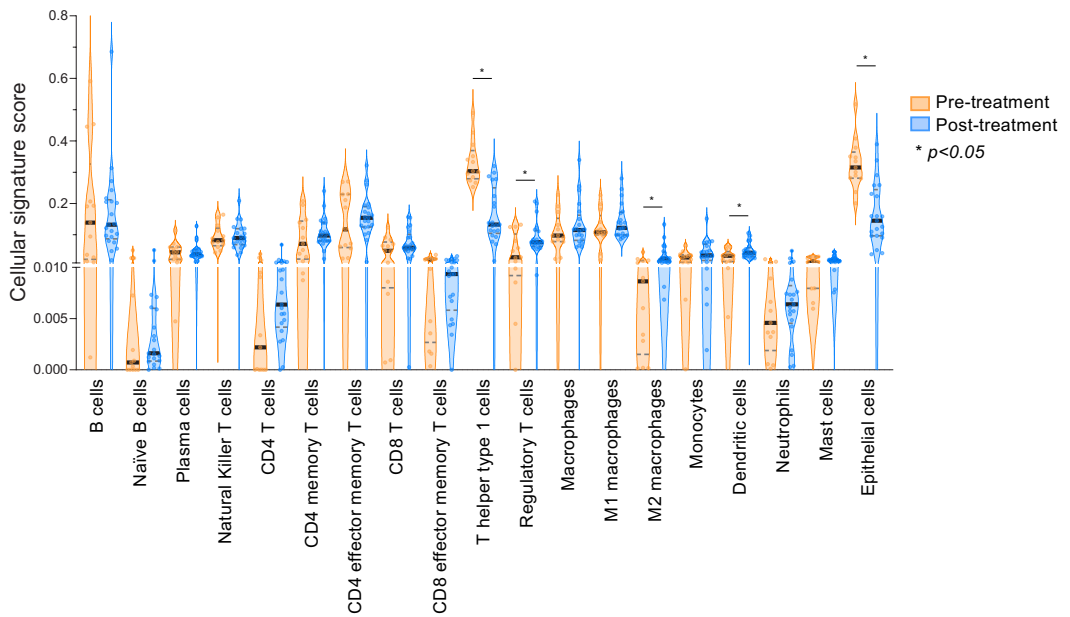
136

B



Supplementary Figure 12. Correlation between expression of immune markers by multiplex immunofluorescence (mIF) and RNA immune signatures. **A.** Scatter plots showing statistically positive association between CD3⁺CD8⁺ cell densities evaluated by mIF (CD3⁺CD8⁺), and a CD8 T cell signature derived by targeted immune profiling (left). Violin plots showing concordantly increased levels of both CD3⁺CD8⁺ T cell densities by mIF and the targeted RNA-seq-derived CD8 T cell signature in chemoimmunotherapy-treated patients with pCR/MPR compared to those without MPR (right). **B.** Scatter plots showing statistically positive association between CD3⁺FOXP3⁺CD8⁻ cell densities evaluated by mIF and a regulatory T cell signature derived by targeted immune profiling (left). Violin plots showing concordantly showing no statistically significant changes in both CD3⁺FOXP3⁺CD8⁻ T cell densities by mIF and the targeted RNA-seq-derived regulatory T cell signature in chemoimmunotherapy-treated patients with pCR/MPR compared to those without MPR (right). Correlations were statistically assessed using Spearman correlation. P-values for pairwise comparisons were obtained using Mann-Whitney tests.

Supplementary Figure 13



Supplementary Figure 13. Comparison of cell signature scores pre- and post-neoadjuvant chemoimmunotherapy. Violin plots for cellular signatures scores comparing pre- (n=13) and post-treatment (n=21) samples. P-values were calculated based on the Mann-Whitney test, black lines represent median values, and gray lines correspond to 95% CIs.

Supplementary Table 1. Antibodies used for immunohistochemical analysis

Immune marker	Clone	Vendor	Antigen Retrieval	Dilution
PD-L1	E1L3N	Cell Signaling	Epitope Retrieval #1 (Citrate Buffer ph6)	0,1111111111
CD4	4B12	Leica Biosystems	Epitope Retrieval #2 (Tris-EDTA Buffer ph9)	0,0972222222
CD8	C8/144B	ThermoFisher	Epitope Retrieval #1 (Citrate Buffer ph6)	01:25
CD45RO	UCHL1	Leica Biosystems	Epitope Retrieval #1 (Citrate Buffer ph6)	RTU
FOXP3	206D	BioLegend	Epitope Retrieval #2 (Tris-EDTA Buffer ph9)	01:50

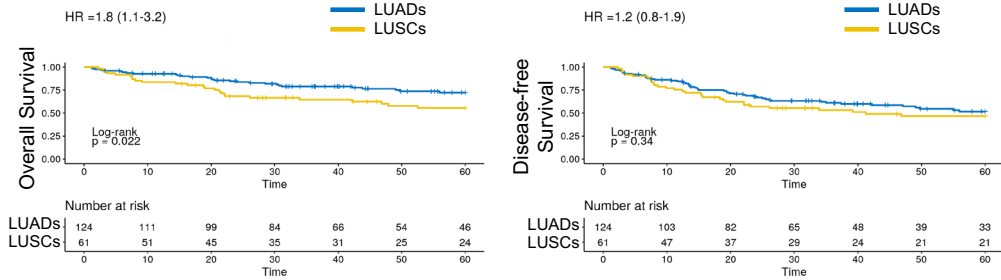
Supplementary Table 3. Previously reported immune signatures interrogated in our study

Previously reported immune cell and program signatures	Reference	Genes
M1 macrophages	Hwang et al., Scientific Reports, 2020	<i>CBLB, CCR7, CD27, CD48, FOXO1, FYB1, HLA-B, HLA-G, IFIH1, IKZF4, LAMP3, NFKBIA, SAMHD1</i>
Peripheral T cells	Hwang et al., Scientific Reports, 2020	<i>HLA-DOA, GPR18, STAT1</i>
T cell inflammation	Spranger et al., Nature, 2015	<i>CD8A, CCL2, CCL3, CCL4, CXCL9, CXCL10, ICOS, GZMK, IRF1, HLA-DMA, HLA-DMB, HLA-DOA, HLA-DOB</i>
Immune cytolytic activity (CYT)	Rooney et al., Cell, 2016	<i>GZMA, PRF1</i>
Tumor inflammation (TIS)	Danaher et al., JITC 2018	<i>PSMB10, HLA-DQA1, HLA-DRB1, CMKLR1, HLA-E, NKG7, CD8A, CCL5, CXCL9, CD27, CXCR6, IDO1, STAT1, TIGIT, LAG3, CD274</i>
Cytotoxic T lymphocytes (CTL)	Jian et al., Nature, 2018	<i>CD8A, CD8B, GZMA, GZMB, PRF1</i>
Interferon gamma (IFNG)	Ayers et al., JCI, 2017	<i>IFNG, STAT1, CCR5, CXCL9, CXCL10, CXCL11, IDO1, PRF1, GZMA, HLA-DRA</i>
Expanded immune	Ayers et al., JCI, 2017	<i>CD3D, IDO1, CIITA, CD3E, CCL5, GZMK, CD2, HLA-DRA, CXCL13, IL2RG, NKG7, HLA-E, CXCR6, LAG3, TAGAP, CXCL10, STAT1, GZMB</i>
Adenosine	Sidders et al., CCR, 2020	<i>PPARG, CYBB, COL3A1, FOXP3, LAG3, APP, CD81, GPI, PTGS2, CASP1, FOS, MAPK1, MAPK3, CREB1</i>
NK cell exhaustion	Sidders et al., CCR, 2020	<i>KIR3DL1, KIR3DL2, IL2RA, IL15RA, HAVCR2, EOMES</i>
Cytotoxicity	Sidders et al., CCR, 2020	<i>NKG7, CST7, PRF1, GZMA, GZMB, IFNG</i>
EMT	Wang et al., Nat Commu 2018	<i>FLNA, EMP3, CALD1, FN1, FOXC2, LOX, FBN1, TNC</i>
PMN (Neutrophils)	Kargl et al., JCI, 2019	<i>S100A8, S100A9, KRT23</i>
T effector signature	McDermott et al., Nat Med, 2018	<i>CD8A, EOMES, PRF1, IFNG, CD274</i>
Myeloid inflammation signature	McDermott et al., Nat Med, 2020	<i>IL6, CXCL1, CXCL2, CXCL3, CXCL8, PTGS2</i>

8.3 SUPPLEMENTARY MATERIAL ARTICLE 3.

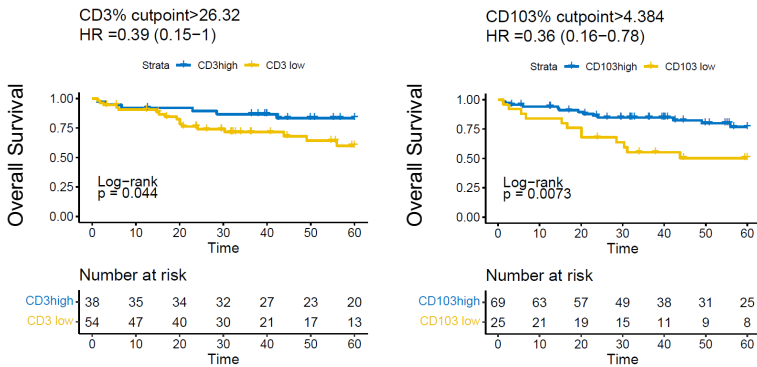
Supplementary Figure 1.

A



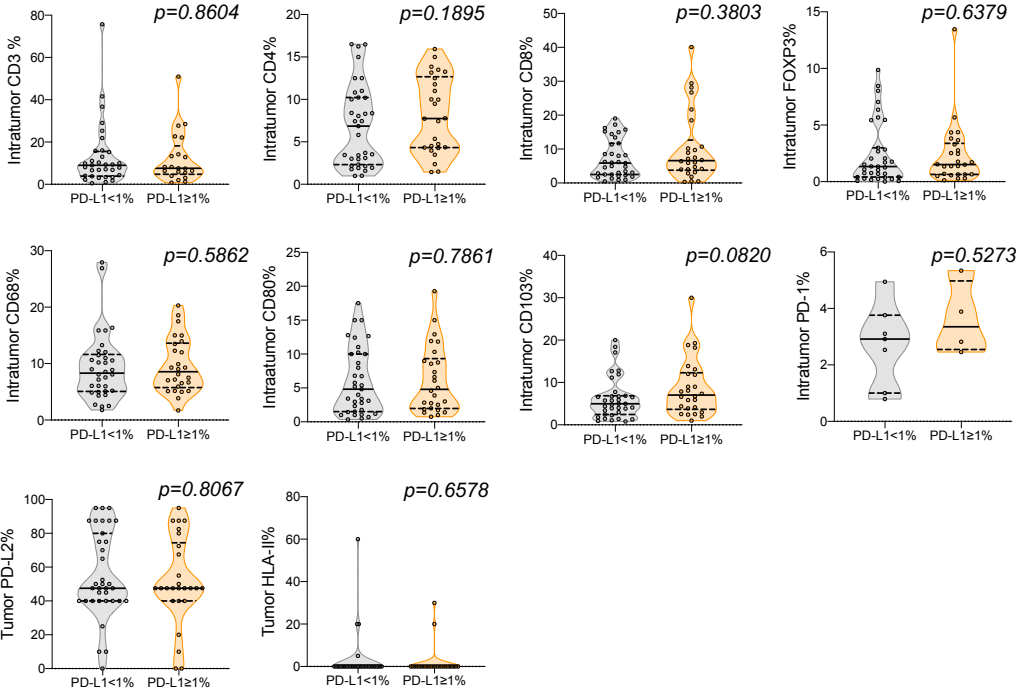
B

Overall survival in LUADs *EGFR* wild-type



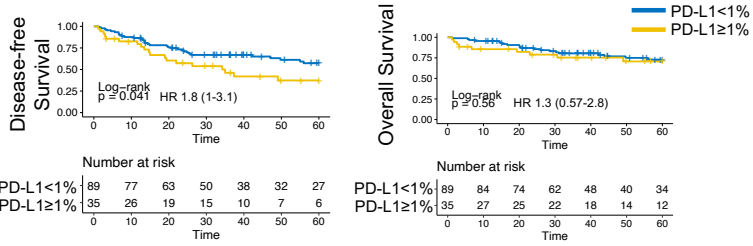
Supplementary Figure 2.

A

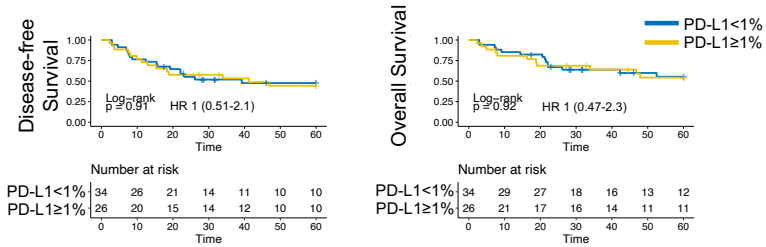


B

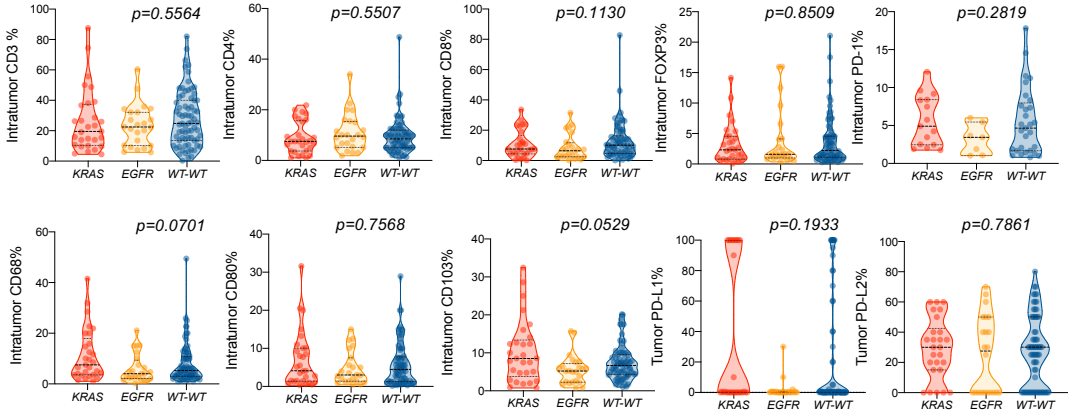
LUADs



LUSCs



Supplementary Figure 3.



Supplementary Table 1. Information of antibodies used for immunohistochemistry analysis.

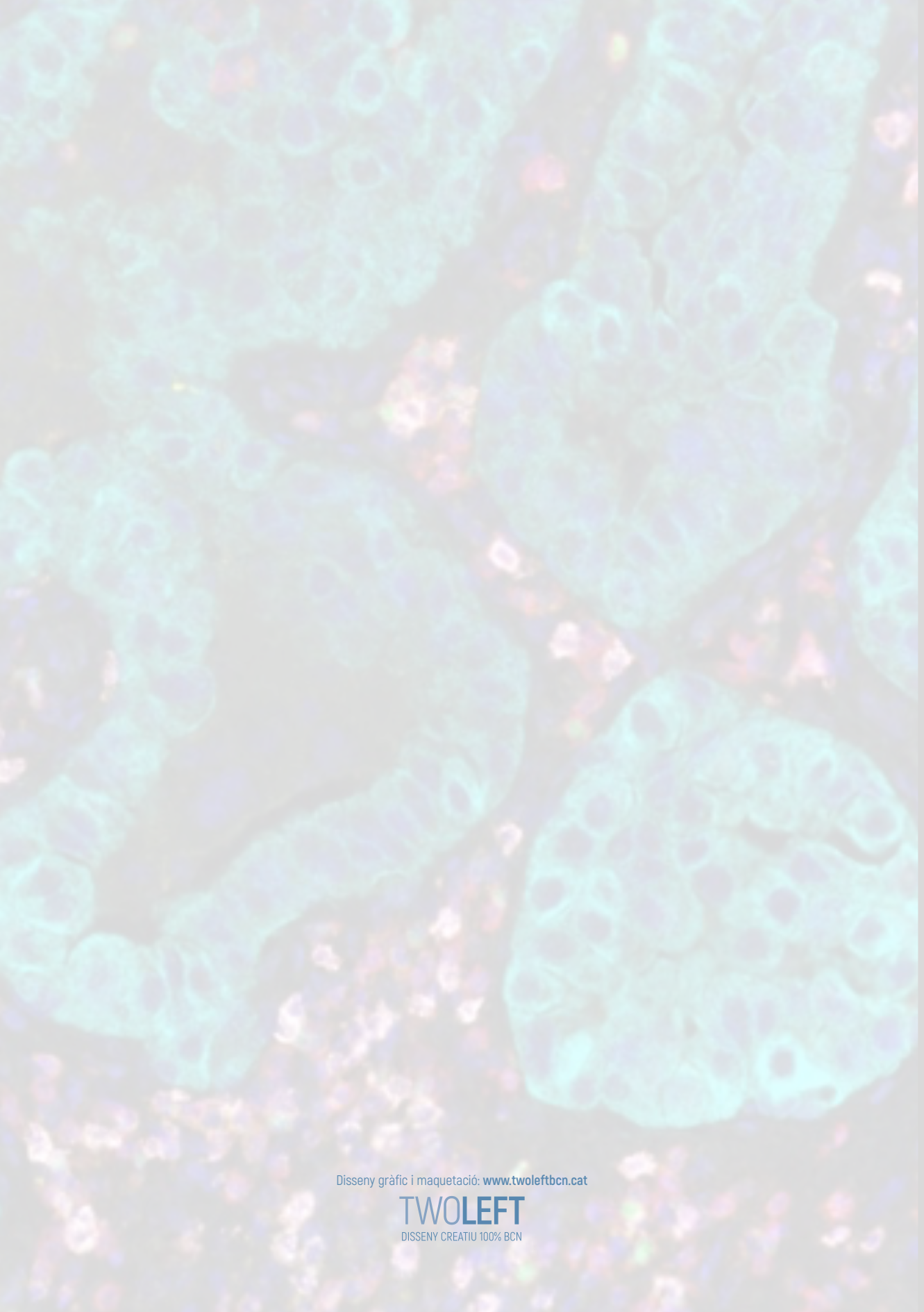
Antibody Clone	Vendor	Catalogue number	Antigen Retrieval	Dilution	Samples analysed	
PD-L1	SP263	ROCHE	07494190001	CC1	RTU	184
CD3	2GV6	ROCHE	05278422001	CC1	RTU	175
CD4	SP35	ROCHE	05552737001	CC1	RTU	185
CD8	SP57	ROCHE	05937248001	CC1	RTU	183
CD68	PGM1	DAKO	M0701	HIGH	1/100	182
CD80	37711	RD SYSTEMS	MAB140-00	HIGH	1/50	183
CD103	EPR4166	ABCAM	129202	HIGH	1/500	184
FOXP3	236A/E7	INVITROGEN	14-4777-82	HIGH	1/100	183
PD-1	NAT105	ROCHE	07099029001	CC1	RTU	63
PD-L2	176611	RD SYSTEMS	MAB1224-100	HIGH	1/600	173
HLA-II	EMR8-5	DAKO	M0775	HIGH	1/800	185
FAP	SP325	ABCAM	227703	HIGH	1/100	182

Supplementary Table 2. Clinicopathological characteristics of patients diagnosed with lung adenocarcinoma.

Characteristic (n=124)	N	%
Age - median (range)	65.5 (42-84)	
Sex		
Female	36	29,0%
Male	88	71,0%
Smoking status		
Never	21	16,9%
Former	49	39,5%
Current	53	42,7%
NA	1	0,8%
TNM 8th Ed.		
I	62	50,0%
II	24	19,4%
III	38	30,6%
Molecular features		
KRAS		
Mut	28	22,6%
WT	93	75,0%
NA	3	2,4%
EGFR		
Mut	23	18,5%
WT	94	75,8%
NA	7	5,6%
Tumor PD-L1		
<1%	89	71,8%
≥1%	35	28,2%
NA	0	0,0%
Recurrence		
Yes	38	30,6%
No	86	69,4%
Survival		
Death	40	32,3%
Alive	84	67,7%

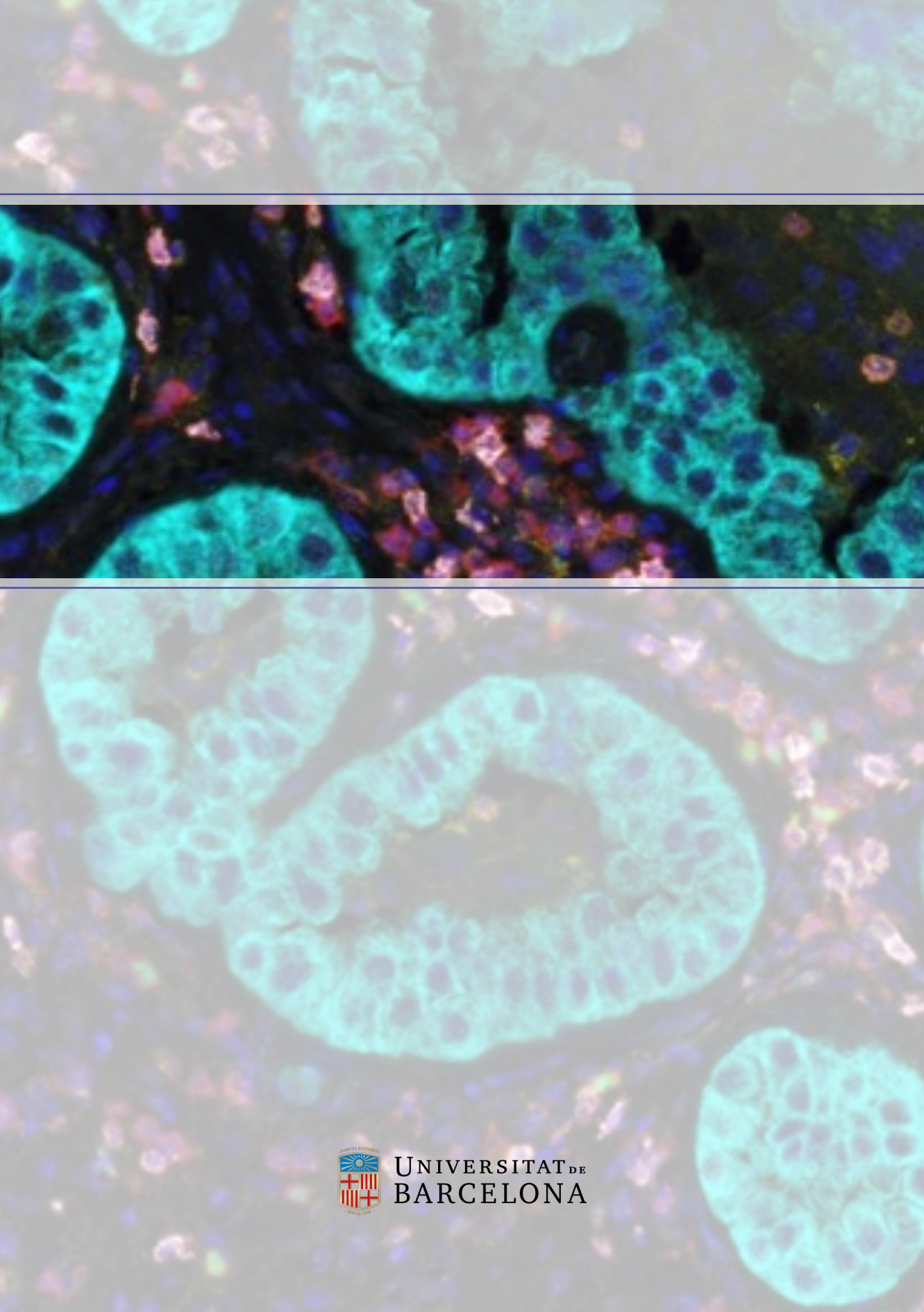
Supplementary Table 3. Clinicopathological characteristics of patients diagnosed with lung squamous carcinoma.

Characteristic (n=61)	N	%
Age - median (range)	66 (45-86)	
Sex		
Female	8	13,1%
Male	53	86,9%
Smoking status		
Never	1	1,6%
Former	27	44,3%
Current	33	54,1%
TNM 8th Ed.		
I	25	41,0%
II	24	39,3%
III	12	19,7%
Tumor PD-L1		
<1%	34	55,7%
≥1%	26	42,6%
NA	1	1,6%
Recurrence		
Yes	19	31,1%
No	42	68,9%
Survival		
Death	34	55,7%
Alive	27	44,3%



Disseny gràfic i maquetació: www.twoleftbcn.cat

TWOLEFT
DISSENY CREATIU 100% BCN



UNIVERSITAT DE
BARCELONA